Foxg1 control of neuronal morphology

Thesis submitted for the degree of *Doctor Philosophiae*

PhD program in Functional and Structural Genomics
Neuroscience Area

CANDIDATE

Simone Chiola

SUPERVISOR

Prof. Antonello Mallamaci

Academic year 2017-2018

TRIESTE

A chi non respira più con me.
Ma continua a vivere al mio fianco.

ABSTRACT

The architecture of neocortical projection neurons is subject of a complex gene control. Here we demonstrated that *Foxg1*, a transcription factor gene which patterns the early rostral brain and sets the pace of telencephalic neuronogenesis, specifically stimulates dendrite elongation. This phenomenon occurs *in vivo* like *in vitro*, and it is detectable even upon moderate changes of *Foxg1* expression levels.

We found that Foxg1 acts by (a) stimulating *Hes1*, which in turn upregulates the well-known pro-dendritogenic effector pCreb1, and (b) downregulating *Syt* and *Ndr1*, namely two established antagonizers of dendrite elongation. *Foxg1* impact on *Hes1* turned out to stem from direct transactivation and indirect derepression. The latter was mediated by knock-down of *Nfia* and *Sirt1*, which normally antagonize *Hes1* transcription. Next, *Foxg1*-driven pCreb1 upregulation required PKA and AKT, and correlated with reduced PP1 and PP2A phosphatase activity. Finally, *Foxg1/Hes1* circuitry mastering dendritogenesis included two key homeostatic branches, i.e. *Hes1*-dependent *Foxg1* downregulation and *Syt* upregulation.

These findings contribute to clarify normal neurodevelopmental and activity-related regulation of neuritogenesis. They further suggest that an abnormal sizing of the dendritic tree of neocortical projection neurons may occur in West and Rett syndrome patients with anomalous *FOXG1* allele dosages and contribute to their neuropathological profiles.

INDEX

INTRODUCTION

A key master regulator of developing telencephalon: Foxg1

Human behavior largely originates form the activity of neuronal circuits located in the forebrain, the most complex part of the mammalian brain. The most anterior part of the forebrain is called telencephalon and it is formed by a wide number of neurons with different morphologies and electrical properties; these neuronal cells comprise the inhibitory interneurons (INs) produced in rodents by the ventral telencephalon and the excitatory projection neurons (PNs) generated by the dorsal telencephalon. These cellular species originally come from a “horse-shoe” shaped structure located at the most anterior border of the neural plate during gastrulation (Fig.1) that undergoes progressive morphological and area-specific partitions in which complex neuronal organization arises.

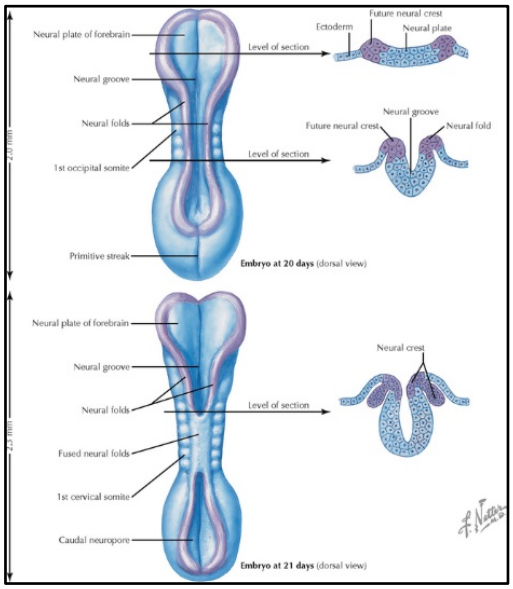

Figure 1. Formation of the neural plate, neural tube and neural crest in the human embryonic development (adapted from *Netter’s Atlas of Neuroscience, Developmental Neuroscience*)

The organization of the neural territories relies on the restricted expression of transcription factors (TFs) that define the specific regions inside the telencephalon. In vertebrates the forkhead box G1 (Foxg1) transcription factor is one of the first TFs expressed in the telencephalic territory (Danesin and Houart 2012). Its expression in the embryonic telencephalon indicates its roles in brain development (first named Brain-Factor-1; BF1) and the severe microcephaly that was observed in the *Foxg1* knockout mice (Xuan et al. 1995), led to a rapid increase in the number of studies devoted to this TF.

Human *FOXG1* is located on the long (q) arm of chromosome 14 at position 12 (14q12), whereas mouse *Foxg1* is located on chromosome 12qB3. Foxg1 is a winged helix TF that contains a single open reading frame surrounding the forkhead binding domain (FBD) (Sugahara et al. 2016). The amino acid sequence from FBD to the C-terminal domain is highly conserved (96%) among species (Bredenkamp et al. 2007), whereas the N-terminal domain is quite variable. Although the first 32 amino acids and successive histidine (H) repeats are well-conserved, mammals have acquired small insertions (six amino acids) and successive proline (P)-glutamine (Q) repeats (HPQ rich domain, Fig.2). The proline-rich repeat was selectively expanded in the primate species (Bredenkamp et al. 2007). These changes in *Foxg1* sequences are important not only for the canonical transcription factor function, but also for acquisition of novel regulatory interactions with other proteins that are responsible for transmitting diverse downstream events (Fig.2).

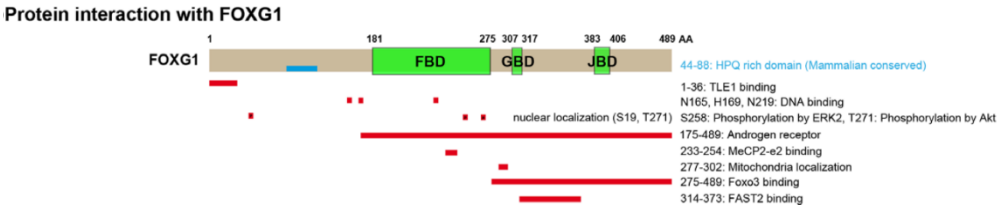

Figure 2. Protein interaction with Foxg1(adapted from Kumamoto and Hanashima 2017)

Foxg1 gene induction and its role in Rostro-Caudal specification

Starting from E7 in mice, the primitive node or organizer and the anterior visceral endoderm (AVE) send signals for neural induction and maintenance to organize the early rostro-caudal patterning. The AVE is characterized by the expression of a specific set of molecular markers (such as *Hex*, *Lhx1*, *Cer1* and *Lefty1*) and is required for the correct specification of anterior neural identity (Beddington and Robertson 1999). Then, *Foxg1* is induced in the future telencephalon at E8.0-8.5 in mouse. The anterior neural ridge (ANR) plays an essential role in triggering *Foxg1* expression via Fgf8 release. The ANR formation itself requires signaling coming from the anterior neural border (ANB) during mid-gastrulation. The ANB activity is at least partly carried by the secreted frizzled-related proteins (sFRP). These molecules work as Wnt antagonists, counteracting Wnt signals released by the midbrain/hidbrain boundary (MHB). The ANB activity is responsible for Fgf8 induction in the ANR, which in turn induces and/or maintains *Foxg1* expression. Hedgehog (Hh) signaling also contributes to *Foxg1* induction: blockade of Hh activity just before telencephalon specification reduced the initial levels of *Foxg1* expression.

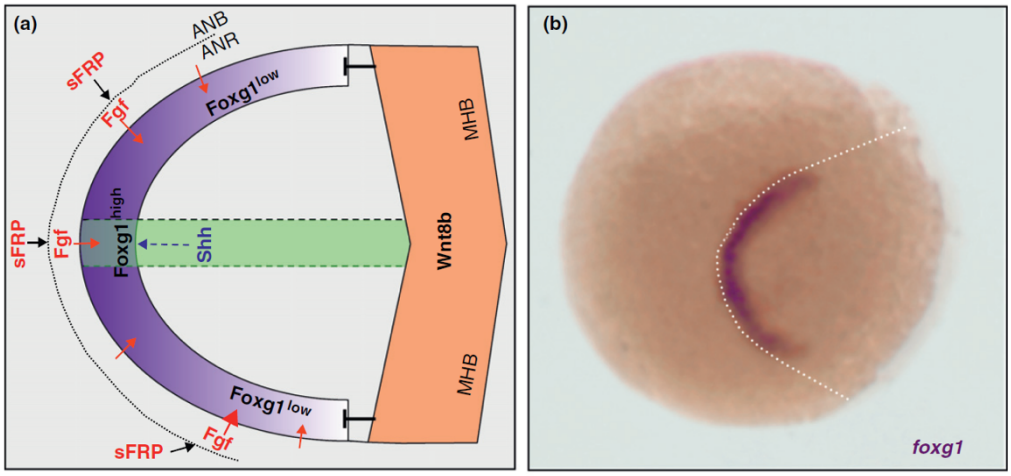

Figure 3. (a) Schematics of the neural plate, anterior to the left. (b) Dorsal view, anterior to the left, of a zebrafish embryo at early neurula stage (10hpf) showing *foxg1* expression in the telencephalic anlage (adapted from Danesin and Houart 2012)

The coordinated activation of *Foxg1* expression by Fgf8 and Shh implies that more inductive signals are secreted at the midline, opening the possibility of a graded *Foxg1* expression from the start, high in the prospective ventral/subpallial telencephalon, and lower in the future dorsal/pallial regions, exposed to Fgf ligands but too far from the midline source of Shh (Fig.3a). At the end of neurulation, *Foxg1* is expressed in a graded fashion (high ventral/anterior to low dorsal/posterior) and excluded from the dorsal most embryonic telencephalon roof. This region is a source of ligands of the Bmp and Wnt family that may participate to *Foxg1* dorso-ventral graded expression by promoting its transcription inhibition.

Foxg1 transcriptional regulation during telencephalic induction

Foxg1 expression during the establishment of the telencephalon in vertebrates is coordinated by the levels of other TFs. These are *Six3* and *Anf/Hesx1*, which are responsible for suppressing *Otx2* expression in the presumptive telencephalic induction domain. Knockdown of *Anf* (*Xenopus laevis Anf*, homologue of the mammalian *Hesx1*) results in the expansion of two homeobox regulators, *Otx2* and *Pax6* in the rostral sector of the anterior neural plate. This indicates that the establishment of the rostral forebrain in vertebrates requires *Anf* expression (Ermakova et al. 2007). *Six3* is one of the earliest TFs to be expressed in the anterior forebrain, and is responsible for determining the competence domain of *Foxg1* induction by Fgf8 (Lagutin 2003). Forced expression of *Six3* in the more caudal regions of the neural plate, was able to induce *Foxg1* surrounding the isthmic organizer (mid-hindbrain junction), where Fgf8 is normally expressed and serves as the caudal signaling center

(Kobayashi et al. 2002). This indicates that the presence of both of *Six3* and Fgf8 is necessary and sufficient to induce *Foxg1*, and that *Six3* restricts the limit of *Foxg1* induction in the most anterior region of the developing neural tube. The transcriptional regulation of *Foxg1* is mediated by the binding of Six3 to the *Foxg1* upstream region, where ChIP analysis in E8.5-9 mouse embryos identified putative *Six3* binding site 1.5 kbs upstream of the 5' UTR of *Foxg1*, in a domain that is highly conserved in vertebrates (Geng et al. 2016). The establishment of the *Foxg1*-expressing telencephalic compartment is also mediated through interactions between multiple signaling molecules that are expressed across the telencephalic-diencephalic territory, in which Smad1 acts as signaling transducer of Fgf8 to regulate downstream *Dkk1* and *Gremlin/Noggin*, *Cerberus* expression. This signaling cascade further secures the rostral *Foxg1* expression in the anterior territory (Aguiar et al. 2014; Fig. 4). Whereas Fgf8 is required for the induction of *Foxg1* in the anterior neural tube, *Foxg1* is necessary for the maintenance of Fgf8 expression. In mouse embryos that lack *Foxg1*, there is a significant reduction of Fgf8 expression in the anterior telencephalon. This is mediated in part by the expanded BMP signaling in the *Foxg1* mutants (Hanashima et al. 2007; Martynoga et al. 2005), which is responsible for *Fgf8* repression in the dorsomedial telencephalon (Ohkubo et al. 2002). Taken together, the acquisition of positive regulators of *Foxg1* and mutual interactions with Fgf8-mediated pathway increases and stabilizes *Foxg1* expression in the anterior neural ectoderm, which leads to the prolonged proliferation of telencephalic progenitor cells that are necessary for cerebral expansion in the vertebrate lineage.

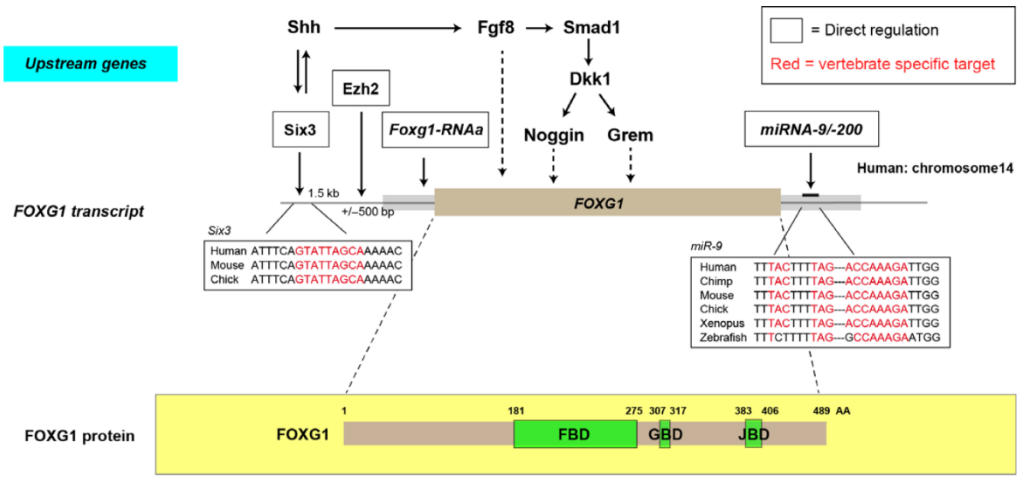

Figure 4. Molecular interactors of *FOXG1* expression (adapted from Kumamoto and Hanashima 2017)

Foxg1 role in Dorso-Ventral specification

Although induction of the telencephalon is the primary function of *Foxg1* in forebrain development, this TF continues to play critical roles in establishing the spatial subdivisions within the telencephalic dorsoventral (DV) and mediolateral compartments. These events require the interplay between *Foxg1* and the surrounding signaling centers. This signaling involves direct suppression of Wnt ligands by *Foxg1* to restrict the dorsal telencephalic identity, whereas *Foxg1* acts as a downstream effector of Shh signaling to induce ventral telencephalic fate (Pottin et al. 2011). After telencephalon induction, expression of Hh and Fgf ligands is detected within ventral region and both factors are required to maintain each other's expression. Since *Foxg1* expression depends on Fgf and Shh activity, a simple model would be that *Foxg1* lies downstream of these signaling pathways in inducing telencephalon identity. However, expression of Shh and Fgf ligands in the ventral telencephalon is itself dependent on *Foxg1*, making the precise relationship complex to assess (Manuel et al. 2011). Although expression of *Fgf8* fails to be maintained in *Foxg1* deficient embryos, both Fgf ligands and pathway targets are first unaltered in these embryos, while subpallial defects are already visible (Manuel et al. 2010; Martynoga et al. 2005). *In vitro* experiments showed that telencephalic progenitors depleted of *Foxg1* can respond to Fgf signaling. Therefore, the early patterning activity of *Foxg1* is likely to be Fgf-independent. As with Fgf ligands, *Shh* expression is altered in ventral telencephalon of *Foxg1*$^{-/-}$ mice (Hu et al. 1999). However, *Foxg1*-depleted telencephalic progenitors are able to receive Shh and initiate a primary response, shown by expression of Hh transcriptional targets, *Patched* and *Gli1* (Danesin et al. 2009), indicating that *Foxg1* is not required for initial Hh activity in the ventral telencephalon. Despite this response to Hh and Fgf, *Foxg1*$^{-/-}$ telencephalic progenitors are incapable to turn on the ventral program. Finally, *Foxg1* gain-of-function is sufficient to induce ventral program in the telencephalon in complete absence of Hh activity, showing that *Foxg1* is an effector of Hh signaling in this process. High levels of *Foxg1*, induced by Fgf and Shh signaling in the presumptive ventral telencephalon, could trigger the subpallial program downstream of these two signals, while low *Foxg1* is required for correct dorsal neuronal differentiation (Fig.5). Consistent with this, *Foxg1* expression is dispensable for *Pax6* expression, a marker gene for dorsal telencephalic progenitors (Manuel et al. 2011). In contrast, the ventral telencephalic domain requires *Foxg1* expression from its onset (Manuel et al. 2010), and knockout cells of *Foxg1* cannot contribute to ventral telencephalic cells that express *Nkx2.1*, *Mash1*, or *Gsh2* (Martynoga et al. 2005).

In addition to its key role in determining ventral character in the telencephalon, *Foxg1* is also required to restrict dorsal fates and limit expression of Bmp and Wnt ligands to the roof plate (Hanashima et al. 2007). BMPs are required for the formation of the cortical hem (Hébert et al. 2002), which in turn regulates

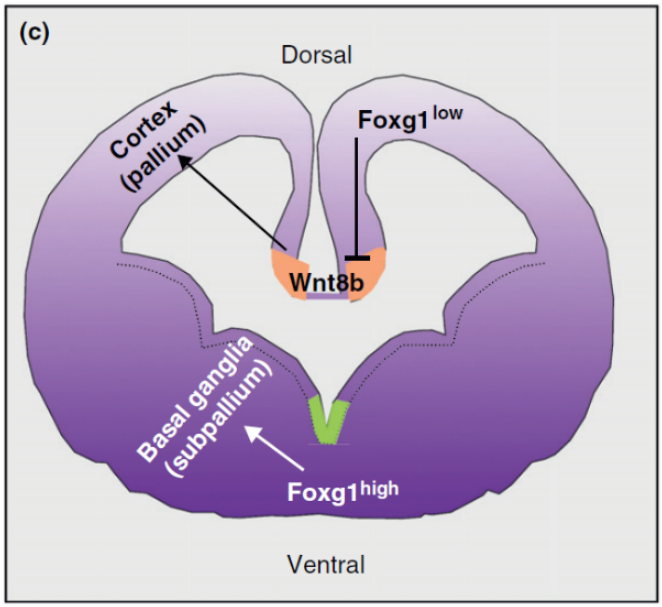

Figure 5. Schematics of *Foxg1* expression domains in a transverse section through the mouse embryonic telencephalon (adapted from Danesin and Houart 2012)

the development of the neighboring hippocampus via the secretion of Wnt ligands (Muzio and Mallamaci 2005). The early telencephalic roof plate is therefore a critical signaling center for pallial differentiation. The size of this signaling center (the expression domain of *Wnt8b*) is restricted to the roof plate by *Foxg1*. Foxg1 binds to *Wnt8b* promoter and represses its transcriptional activity, preventing expansion of the Wnt-secreted population. Thus, isolated dorsal telencephalic progenitors lacking *Foxg1* induce expression of Wnt8b and "dorsalise" neighboring cells by activating the Wnt pathway (Danesin et al. 2009). This unearths the role of *Foxg1* in limiting the formation of a dorsal telencephalic organizer, thereby restricting the induction of pallial cell fates. The DV graded expression of *Foxg1* prevents excessive dorsalisation of the telencephalon by the roof plate signaling center. However, absence of ventral/subpallial fates in *Foxg1*$^{-/-}$ embryos is not simply owing to dorsal/pallial transformation driven by increased Wnt activity but also to a direct requirement of *Foxg1* for ventral identity as shown by zebrafish and mouse mosaic embryos in which *Foxg1*-depleted cells in the ventral half of a wildtype telencephalon cell-autonomously fail to adopt ventral identity although both ventral (Hh) and dorsal (Wnt) signaling centers are normal (Danesin et al. 2009). In parallel to the dorsoventral patterning of the telencephalon, the establishment of pallial subdivisions also involves the expression of *Foxg1* across multiple compartments. In *Foxg1*$^{-/-}$ mice, progenitors fail to contribute to the dorsal pallium (which give rise to the neocortex). Instead, the medial and ventral pallium is expanded (Hanashima et al. 2007). This specification of the dorsal pallium is further achieved by combined action with the LIM domain TF *Lhx2* (Mangale et al. 2008; Muzio and Mallamaci 2005). Together, they suppress the caudomedial pallial territory, which includes the septum, thalamic eminence,

and the cortical hem, all of which contribute to the production of early-born Cajal-Retzius cells in the mammalian neocortex. Whereas the septum and thalamic eminences appear earlier in the vertebrate lineage, the cortical hem is acquired in amniotes, including reptiles and birds, and further expands during mammalian evolution (Roy et al. 2014). Consequently, humans have much larger cortical hem than mice with a concomitant increase in the number of Cajal-Retzius cells that are produced.

Foxg1 function in neocortical histogenesis and neuronal differentiation

The evolution of the mammalian brain consists of a huge neocortical expansion from the dorsal telencephalon characterized by a laminar organization in which neurons gather following a precise inside-out gradient, based on their birth date. Neocortex development in mice starts at around E9.5 when apical neuroepithelial progenitors begin to undergo self-renewal and proliferate through continual symmetry divisions, providing the ventricular zone (VZ) with thickness. Starting from E10.5, dividing progenitors vary in morphology and this shape rearrangement gives rise to radial glial cells (RGCs) with their cell bodies located in the VZ. From the VZ, RGCs emanate their long radial marginal processes toward the pial surface and undergo their first asymmetric division, giving rise to immature post-mitotic neurons and basal progenitors, also named intermediate progenitors (IPCs). In mice, neural progenitor cells that lack *Foxg1* exit the cell cycle prematurely and differentiate into neurons (Hanashima et al. 2002). In humans, the levels of *FOXG1* expression correlates positively to brain size, ranging from microcephaly to macrocephaly (Kortum et al. 2011; Mariani et al. 2015). Starting from E13.5 in mice, basal progenitors occupy the subventricular zone (SVZ) and will either self-renew and produce other two basal progenitors or will symmetrically divide and generate two neurons. The SVZ has further expanded in primates giving rise to an inner and an outer SVZ, whose progenitors are distinct. Inner SVZ (iSVZ) progenitors resemble rodent SVZ intermediate progenitors, while primate outer SVZ (oSVZ) progenitors are more similar to radial glial cells, both in morphology and molecular identity. Moreover, the radial glia-like progenitors of the oSVZ are able to undergo symmetric, as well as asymmetric divisions, thus generating progenitors that can further proliferate (Fig.6). This latter capacity of oSVZ progenitors enhances neuronal output and represents an important evolutionary step in the expansion of the neocortex (Fietz and Huttner 2011; Hansen et al. 2010). New-born neurons start their migration following radial processes emanating from RGCs, that act in this way as migratory scaffolding (Molyneaux et al. 2007) and are fundamental in neuron's guidance towards the cortical plate (CP). New-born neurons migrate outside the VZ and the SVZ into the CP, where they differentiate, establish synaptic connections and allocate in their final cortical residence (Fig.7).

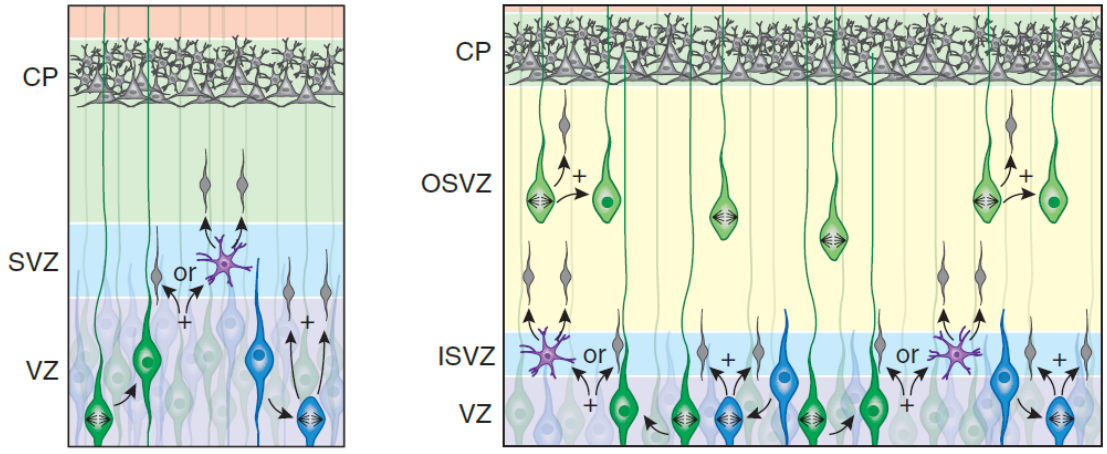

Figure 6. Comparison of germinal zones in rodent (~E13.5) and primates (~8.5 GW) embryonic neocortex (adapted from Tyler and Haydar 2010)

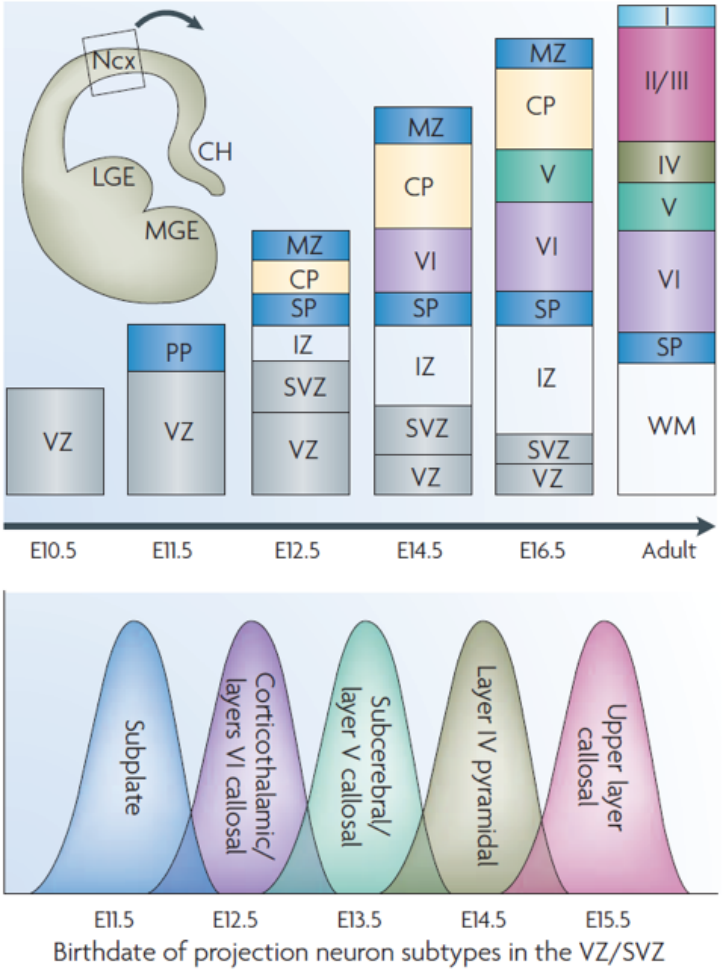

Figure 7. Timing of cortical neurogenesis in mice (adapted from Molyneaux et al. 2007)

Foxg1 control of the cell cycle in basal progenitor cells

During neurogenesis, there is a progressive lengthening of the cell cycle duration that can be largely attributed to a lengthening of the G1 phase. Besides, lengthening of the cycle is accompanied by an increase in the fraction of cells exiting from the cell cycle (Takahashi et al. 1995). As the G1 phase length increases, cell division switches from a symmetrical self-renewing to asymmetrical neurogenic differentiating pattern and, lastly, to an asymmetrical differentiative one (Calegari 2003; Götz and Huttner 2005). Therefore, the transition through the G1 phase is particularly crucial for proliferative or differentiative fate choice. The molecular mechanism that underlie the augmented cell proliferation involves the suppression of multiple cell cycle related pathways by *Foxg1*. Foxg1 interacts with FOXO/SMAD (Vezzali et al. 2016), a complex that activates TGFβ and PI3K/Akt signaling, which is involved in controlling proliferation of neuroepithelial cells by the p21Cip1 promoter (Seoane et al. 2004). Furthermore, haploinsufficiency of *Foxg1* exhibit decreased Tbr2-positive basal progenitor population that coincides with increased expression of this cell-cycle inhibitor p21 in the progenitor cells (Siegenthaler et al. 2008). In this cascade, the phosphorylation of Ser19 at the N-terminus of Foxg1 promotes nuclear import. This blocks TGFβ mediated p21Cip1 induction in mouse cortical progenitor cells, glioblastoma (Seoane et al. 2004) and ovarian cancer cell lines (Chan et al. 2009; Fig.8). This *Foxg1*-mediated suppression of p21 is also regulated by Sfn2l, a mammalian ISWI chromatin remodeling protein, which binds to the *Foxg1* locus at the mid-neurogenesis stage. *Sfn2l* mutant mice exhibit reduced expression of cell cycle inhibitors *Cdnk1b* and *Cdnk2a*, a phenotype that is rescued by decreasing the *Foxg1* dosage, which reveals that *Sfn2l* and *Foxg1* function antagonistically to regulated cell cycle and brain expansion (Yip et al. 2012).

DL and UL competence: a close transcriptional network regulated by *Foxg1*

Mammalian neocortex has a six-layer structure that consists of distinct neuronal subtypes that have common molecular ad hodological properties. In mice, these layer neurons are generated from progenitors through 9 to 11 asymmetric cell divisions within a 6-day period, whereas the neurogenesis period extends up to 20 weeks in humans (Takahashi et al. 1999; Kang et al. 2011; Gao et al. 2014; Toma et al. 2014). Due to the time differences in the developmental schedule of mammals, the mechanisms that control neuronal subtype generation in the neocortex should accommodate temporal scaling mechanisms to adjust the neuronal number during the course of neuronal production. In this regard, *Foxg1* is one of the key TFs that switch temporal competence from earliest-born Cajal-Retzius cells to the subsequent

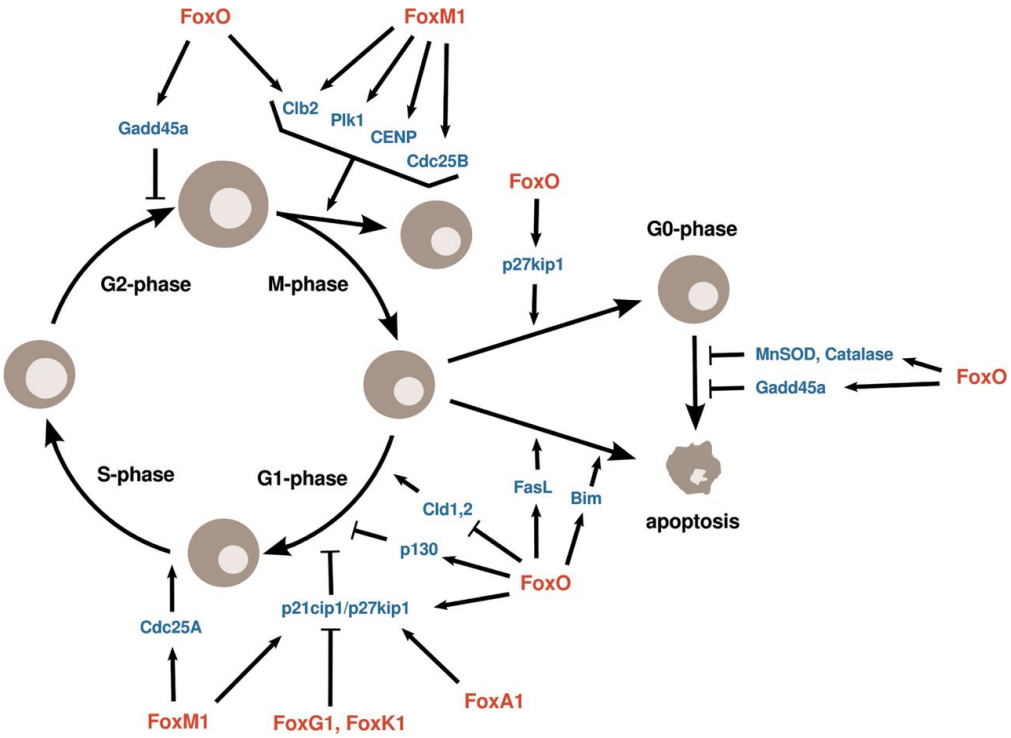

Figure 8. Forkhead TFs in cell cycle and survival (adapted from Wijchers et al. 2006)

production of deep-layer neurons in the neocortex (Hanashima et al. 2007; Shen et al. 2006; Kumamoto et al. 2013; Toma et al. 2014). This is achived by direct repression of *Foxg1* on multiple TFs (including *Dmrt* genes, *Ebf2/3*, *Tbr1*; Kumamoto et al. 2013), resulting in an expanded repertoire of genes that are expressed uniquely in Cajal-Retzius cells. The Cajal-Retzius cells serve as potential signaling cells for radial progenitors and neurons, in which the contact with their basal and leading processes regulates multiple steps from proliferation, migration, and differentiation (Pilaz et al. 2016). Progenitor cells, after successive rounds of asymmetric cell division, progressively restrict their competence producing at first deep layer (DL) neurons and then upper layer (UL) neurons (Frantz and McConnell 1996; Desai and McConnell 2000). Franco and colleagues discovered UL fate-committed early progenitors, which raise an alternative view regarding the lineage relation between DL and UL neurons (Franco et al. 2012). Besides, genetic studies have shown that a closed transcriptional network is responsible to establish segregation among the principal layer subtypes of the cerebral cortex. In particular, the cross-repression among four TFs-*Fezf2*, *Ctip2*, *Satb2* and *Tbr1*-is sufficient to establish the subcerebral, intracortical and cortico-thalamic projection identities within the postmitotic neurons (Alcamo et al. 2008; Britanova et al. 2008; Chen et al. 2008; Han et al. 2011; McKenna et al. 2011; Srinivasan et al. 2012). UL competence is tightly linked to DL neurogenesis and this sequence of layer neurogenesis is determined through *Tbr1* repression. A continued repression of *Tbr1*, expressed in the majority of early-born neurons including preplate

Cajal-Retzius cells and subplate neurons (Hevner et al. 2001), favors the acquisition of *Fezf2* DL neurons identity. Moreover, the subsequent transition from DL to UL competence requires the repression of DL determinants to terminate DL competence. The onset of UL competence is achived thanks to negative feedback propagated from postimitotic DL neurons (Toma et al. 2014). The triggering of a neurogenetic sequence arises from the break of the eliquilibrium established in the *Tbr1-Fezf2-Satb2-Ctip2* negative feedback loop, occurring through a derepression of one of the genes in the transcriptional loop. The onset of *Foxg1* switches the transcriptional program to acquire PN identity and, concomitantly, to confer the sequence of DL and UL neurogenesis (Toma et al. 2014; Fig. 9). Within the newly formed PNs subpopulations, *Fezf2* alone can cell-autonomously instruct the acquisition of subtype specific features related to corticospinal motor neurons (CSMNs). In particular, *Fezf2* directly instruct the expression of *EphB1*, a neuronal subtype-specific axon guidance receptor expressed in CSMNs, which in turn executes crucial ipsilateral axon guidance decisions of the corticospinal tract (Lodato et al. 2014).

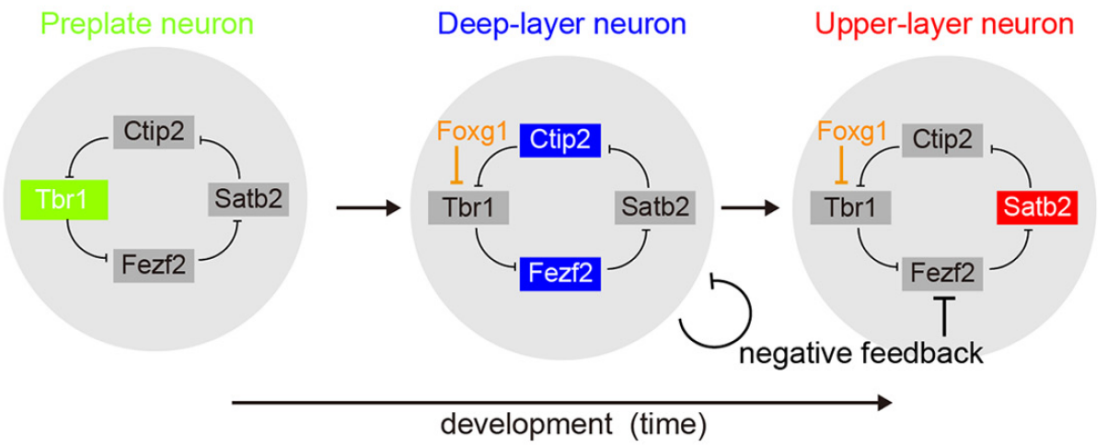

Figure 9. Schematic model of identified genetic interactions between the layer TFs (adapted from Toma et al. 2014)

Dynamic expression of *Foxg1* during PNs differentiation

Within the cerebral cortex, the expression of *Foxg1* is dynamically regulated during the transition period from precursors state to neuronal differentiation. In particular, *Foxg1* is transiently downregulated at the onset of neuronal migration. In turn, neuronal precursors acquire multipolar shape morphology and express *Unc5D*, a receptor for fibronectin and leucin-rich transmembrane proteins (FLRT) (Yamagishi et al. 2011; Fig.10). This change in *Foxg1* expression during the migration and cortical plate entry is critical for control of the timing of neuronal integration and recruiting pyramidal neurons into the

cortical network (Miyoshi and Fishell 2012). Interestingly, this early step of neuronal migration is affected by somatic mutation of *Akt3*, which mediates phosphorylation and cytoplasmic sequestration of Foxg1, leading to de-repression of Reelin expression in post-mitotic neurons (Baek et al. 2015). While *Foxg1* plays fundamental roles in the growth and patterning of the progenitor cells, it is expressed at high levels in postmitotic neurons. This expression persists into adulthood, where it continues to play important roles in promoting neuronal survival and maintenance of neuronal circuits. Studies using cultured rat cortical neurons and cerebellar granule neurons have shown that *Foxg1* is a downstream mediator of IGF-1/AKT signaling to promote neuronal survival, and that this signaling is mediated through the first 36 amino acid residues of Foxg1 (Dastidar et al. 2011). The survival promoting effect of Foxg1 is mediated by direct interaction with methyl-CpG binding protein 2 (MeCP2)-e2 isoform by 20 amino acids region (234-256) of Foxg1 protein. MeCP2 is a widely expressed protein which is known to promote apoptosis and is responsible for Rett syndrome. High *Foxg1* expression levels sustain cell surivial by inhibiting MeCP2-e2-promoted neuronal cell death and toxicity in cortical and cerebellar granule neurons (Dastidar et al. 2011).

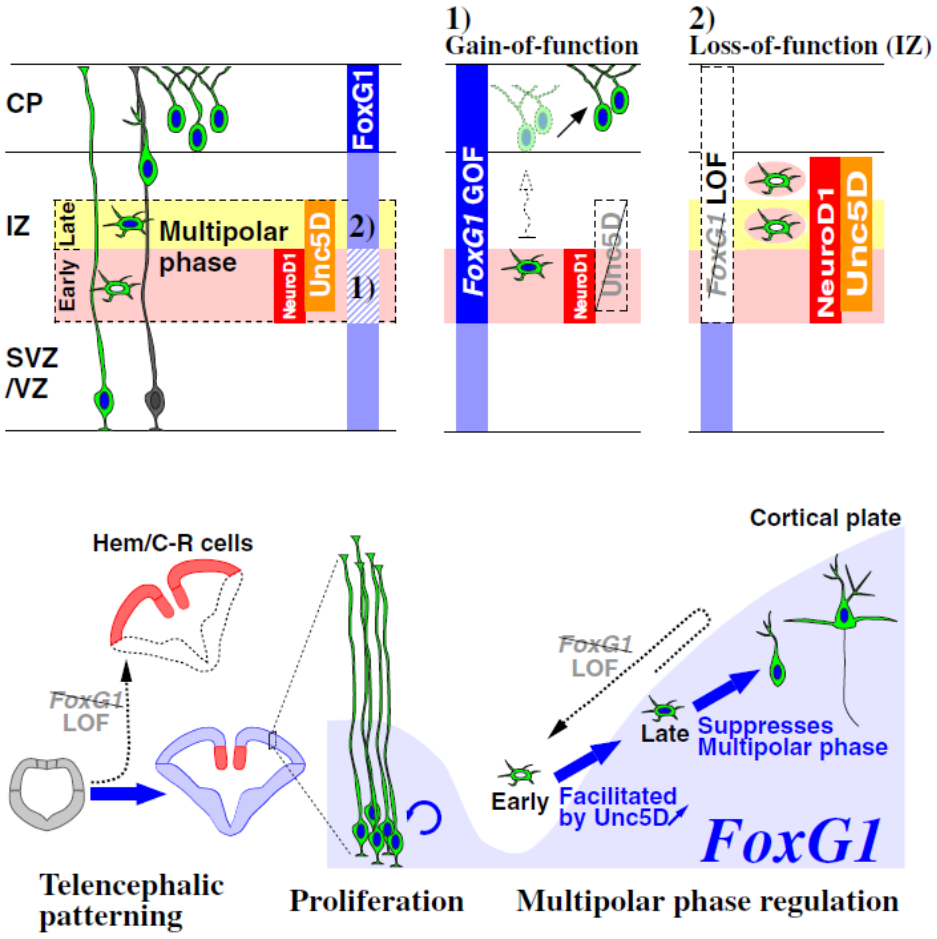

Figure 10. Dynamic *Foxg1* expression during the postmitotic multipolar phase (adapted from Miyoshi and Fishell 2012)

Foxg1 is crucial in INs differentiation and migration

In contrast to the development of glutamatergic neurons in the forebrain, the progenitor cells that lack *Foxg1* cannot contribute to the ventral telencephalic progenitors and GABAergic interneurons that arise from the progenitors (Martynoga et al. 2005). Suppression of *Foxg1* expression soon after cell cycle exit compromises gene expression of GABAergic interneurons and their tangential cell migration into the dorsal telencephalon. This implies the continous need for *Foxg1* in the telencephalic GABAergic population (Miyoshi and Fishell 2012). An attempt to identify the molucues that are responsible for this migration defect in cortical interneuros by using interneuron-specific (*Dlx5/6*-Cre) deletion of *Foxg1*, revealed that *Foxg1* acts as an upstream regulator of *Dlx1/2*, *Mash1*, and *Prox1* that are required for interneuron differentiation. In these mutant mice, expression of multiple receptor molecules, such as *Robo1*, *Eph4*, and *Cxcr4/7*, are also significanlty decreased. These *Foxg1* mutant cells show shorter neurites, fewer branches and severe migration defects when cultured *in vitro*. This indicates that *Foxg1* plays multiple steps of interneuron development in mammalian neocortex (Yang et al. 2017).

Post-transcriptional regulation of *Foxg1* expression

In addition to the mechanism of Fgf8-Six3 mediated induction, a post-trascriptional regulation of *Foxg1* expression in the developing telencephalon is present. Among miRNAs, *miR-9* is highly expressed in the developing vertebrate brain to regulate multiple gene expression in cellular functions and brain development (Lagos-Quintana et al. 2002; Kapsimali et al. 2007; Shibata et al. 2011). The seed sequences for *miR-9* in the 3' UTR of *Foxg1* mRNA is conserved among vertebrates (Shibata et al. 2008; Garaffo et al. 2015). Attenuating *miR-9* expression by *miR9-2/miR9-3* double knockout in mice results in increased Foxg1 protein levels and reduced Cajal-Retzius cells in the cerebral cortex. Interestingly in mouse cortex at later stages, Elavl2 (an AU-rich RNA-binding protein) attenuates *miR-9* mediated *Foxg1* suppression by binding to the U-rich region that is located upstream of the *miR-9* responsive element (Shibata et al. 2008). These studies indicate that the fine-tuning of *Foxg1* levels is regulated by miRNAs, which are critical for control of neuronal differentiation. In parallel, the post-translational regulation of Foxg1 is also mediated by controlling their nuclear-cytosolic shuttling within the cell. In mouse embryos, the subcellular localization of Foxg1 is differentially regulated by casein kinase I and FGF signaling, whereas the phosphorylation of Ser19 and Thr226 promotes nuclear import and export of Foxg1, respectively (Regad et al. 2007). Although this shuttling of Foxg1 between the nucleus and cytoplasm may regulate the progenitor and differentiation state of neural cells, a more

recent study using primary culture and mouse cortex reported that a fraction of Foxg1 can specifically target the mitochondrial matrix in an energy-dependent manner by interaction of its amino acids 277-302. The mitochondrial control in neuron development has been correlated with differentiation of neurons and can modulate the cellular and mitochondial function to regulate cell proliferation, axon and dendritic growth, mitochondrial membrane potential, formation and reorganization of synapses. Collectively, the dynamic subcellular shuttling of Foxg1 in the nucleus, cytosol, and mitochondrial matrix provides a novel link between gene expression with metabolism and mitochondrial bioenergetics (Pancrazi et al. 2015).

FOXG1-linked West and Rett syndromes

CNS morphogenesis requires a proper regulation of Foxg1 expression levels. Excessive or insufficient levels of *FOXG1* levels cause opposite alterations of telencephalic growth, with a major cognitive disability outcome. Rett syndrome, West syndrome and autism spectrum disorders (ASD) have been reported in the literature (Philippe et al. 2010; Striano et al. 2011; Mariani et al. 2015). Rett syndrome and West syndrome are linked with deletion and duplication of *FOXG1* gene respectively.

FOXG1-gain of function-associated West syndrome

West syndrome (WS, named after the English physician William James West and also known as “Generalized Flexion Epilepsy”, “Infantile Epileptic Encephalopathy”, “Infantile Myoclonic Encephalopathy” and “Salaam spasms”), is a rare epileptic disorder in infants and children, with an incidence about 1.0-1.6/100,000 live births (www.orpha.net, ORPHA: 3451). Boys are more often affected than girls. The onset occurs between 3 and 7 months of age in 50-70% and before 12 months in 90% of cases (Kellaway et al. 1979). However, there are cases with later occurrence, up to 4 years old, so that it may cause delay in treatments.

West syndrome consists of symptomatic triad: infantile spasms, diffuse paroxysmal EEG abnormalities and mental retardation.

The spasm is usually sudden, symmetrical, bilateral, and affects the axial muscle group (Hrachovy and Frost 1989). A behavioral arrest may also occur as a seizure without associated spasms. Alteration in respiration is also a common associated phenomenon, whereas change in heart rate is rare (Kellaway et al. 1979). Spasms do not show a prediction for either day or night. Conversely, they tend to occur soon after awakening or on falling asleep. They may be triggered by sudden loud noises or tactile stimulation, but no photic

stimulation. Most of the spasms occur in clusters (the interval between successive spasms is less than 60 seconds). Usually the intensity of spasms in a given cluster will peak gradually and then decline (Hrachovy and Frost 1989). Crying may frequently follow a spasm. The frequency of spasms varies from only a few times a day to several hundred a day (Kellaway et al. 1979).

The usual EEG abnormalities consist of diffuse, high amplitude, non-synchronous paroxysmal and slow wave theta and delta activity with loss of background features that is continuous when awake and fragmented in sleep (Fig.11). Such “chaotic” pattern becomes more organized with time (Hrachovy et al. 1981; Watanabe et al. 1993) and, between 2 years and 4 years of age, may evolve into the generalized slow sharp and slow-wave pattern of Lennox-Gastaut syndrome. Infantile spasms are associated with several different ictal EEG patterns (Kellaway et al. 1979). The duration of each ictal episode ranges from 0.5 seconds to almost 2 minutes. The longer ones are associated with behavioral arrest.

Because the onset of West syndrome is early (3-7 months old), the psychomotor impairment and mental retardation signs and symptoms are quite poor and elusive, including: (1) loss of hand grasping and simple muscular movements; (2) axial hypotonia and dysphonia; (3) no visual attention and abnormal ocular movement; (4) no social response. Among these symptoms, loss of eye contact has a negative prognostic significance. Overall, only about 5% to 12% of patients have normal mental and motor development. Approximately one-half are left with motor impairment and 70% to 78% are mentally retarded (Jeavons et al. 1973; Matsumoto et al. 1981; Riikonen 1982; Glaze et al. 1988). Within specific clinical subgroups, mortality may arise up to 25% in the absence of pharmacological treatment (Glaze et al. 1988).

Specific histological and neurocircuital anomalies occurring in WS patients have been suggested to contribute to the syndrome itself. In particular, an overexpression of axonal collaterals and excitatory synapses that play a major role in the development of cortical functions could determine major hyperexcitability of the developing brain cortex and could be responsible of continuous spiking activity. Lack of myelin at that age would account for the absence of interhemispheric synchrony, thus producing the hypsarrhythmic pattern (Dulac et al. 1994). Continuous, paroxysmal activity would account for the cognitive decline. It would also determine subcortical disinhibition, with paroxysmal discharges in the basal ganglia (Chugani et al. 1990). Thus, a loop including the cortex and basal ganglia would be involved in the genesis of WS (Desguerre et al. 2013).

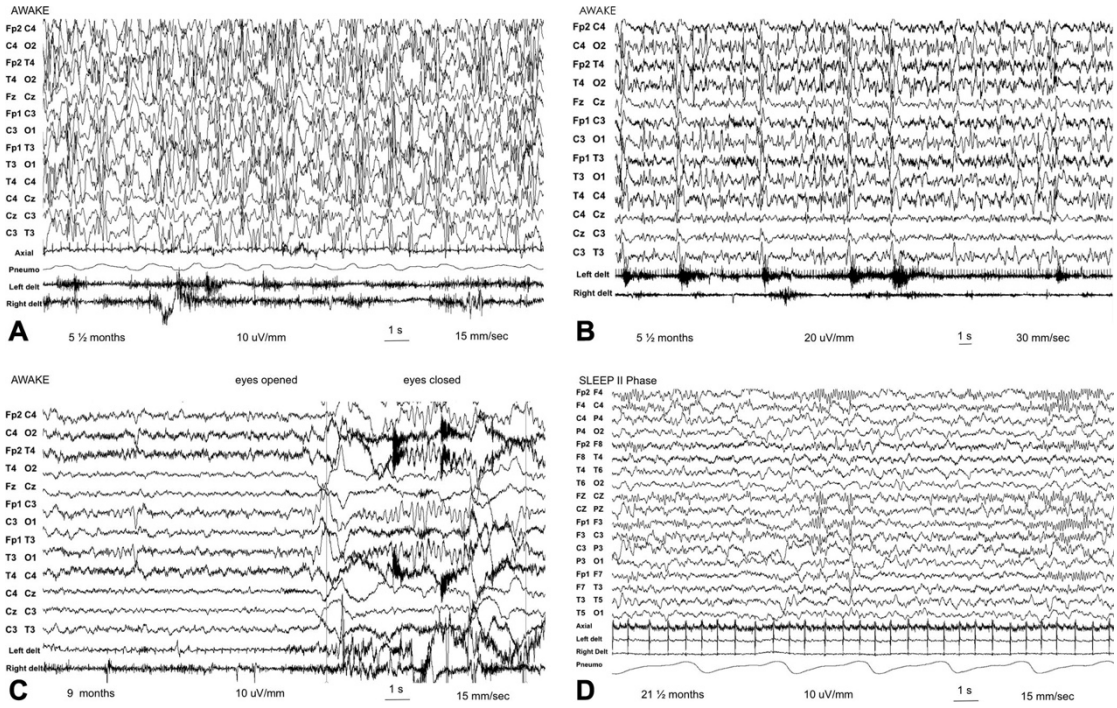

Figure 11. EEG recording in a patient. (A) EEG and polygraphic recordings during wakefulness at the age of 5½ months: slow waves of large amplitude mixed with almost continuous, independent and multifocal, high amplitude spikes, sharp-waves, and spike and slow-wave complexes, variable in amplitude and topography, with a slight tendency to become synchronous, configuring a modified hypsarrhythmia. (B) clusters of asymmetrical epileptic spasms at the age of 5½ months. (C) EEG and polygraphic recordings during wakefulness at the age of 9 months showing a normal background activity, with a posterior dominant rhythm, reactive to eye opening and closure. (D) EEG and polygraphic recording during sleep at the age of 21½ months, showing an almost normal activity during a second phase of spontaneous sleep.

WS etiopathogenesis is highly heterogeneous and still largely obscure. WS has been associated with several prenatal, perinatal, and postnatal pathogenic factors, including prenatal (CMV fetopathy) or perinatal (herpes virus or bacterial meninigitis) infection, neonatal ischemia following term (focal or diffuse) or premature delivery, or post-natal ischemia, various brain dysgenesis (lissencephaly, hemimegalencephaly, focal cortical dysplasia, septal dysplasia or callosal agenesis), involvement, neurocutaneous syndrome (tuberous sclerosis, incontinentia pigmenti or Ito syndrome, neurofibromatosis). Moreover, WS can occur in patients harboring specific genetic anomalies, both chromosomal (including Down syndrome, del1p36) and single gene (e.g. *ARX* mutations, *FOXG1* duplication).

Specifically, it has been reported that a number of microduplications of chromosome 14q12 sharing the *FOXG1* locus are associated with developmental delay, delayed/absent speech, and infantile epilepsies (Bertossi et al. 2014; Pontrelli et al. 2014). In particular, in 14dup(14) patients, the size of duplication varied from 88kb to 84Mb and 9/14 of patients developed seizures in the first month of life. Moreover, most of them (8/9) presented infantile spasms and hypsarrhythmia/modified hypsarrhythmia EEG patterns (Bertossi et al. 2014). This observation, together with the notion of the essential role of

Foxg1 in neurogenesis and cortical neural differentiation, has led to the hypothesis that duplication of *FOXG1* may be the main cause of WS phenotype. There were a few reports of single individuals with 14q12 duplication, including *FOXG1*, with normal phenotype, normal intellect and no epilepsy (Shaikh et al. 2009; Amor et al. 2012). However, it is commonly accepted that these phenotypic variabilities might be explained by an incomplete penetrance of *FOXG1* duplication, the variable involvement of its regulatory elements, other genes in the duplicated region and genetic mosaicism (Brunetti-Pierri et al. 2011; Tohyama et al. 2011; Falace et al. 2013; Fig.12).

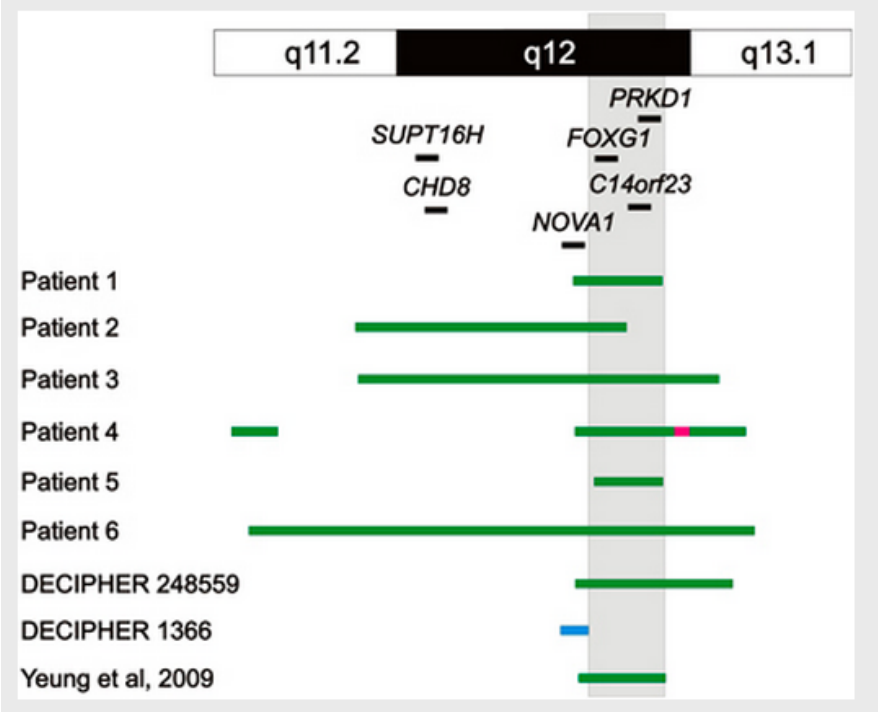

Figure 12. Schematic representation of chromosome 14q11.2q13 duplications and the minimally duplicated region (gray shadow) in cases of developmental epilepsy (adapted from Brunetti-Pierri et al. 2011).

FOXG1-loss of function-associated Rett-like syndrome

In 2005, Shoichet et al. reported a 7-year-old girl with pronounced cognitive disability associated to lateral ventricles enlargement, frontal and parietal hypomyelination, agenesis of the corpus callosum, seizures, tetraplegia and microcephaly with a balanced de novo translocation t(2;14)(p22;q12) and a neighboring 720-kb inversion in chromosome 14q12 that disrupts *FOXG1* (Shoichet et al. 2005).

Later, 14q12 interstitial deletions (3.1 Mb, 2.9 Mb, and 3.6 Mb) including *FOXG1* (MIM 164874) were identified in a number of young patients, characterized by severe mental retardation with a normal perinatal period

followed by a phase of developmental regression at the age of 3–6 months (Bisgaard et al. 2006; Papa et al. 2008; Mencarelli et al. 2009). The phenotype includes postnatal microcephaly, postnatal growth retardation, hypotonia, and stereotypic movements, and mild facial dysmorphisms such as bulbous nasal tip and prognathism (Fig. 13).

Finally, *FOXG1*-null mutations were reported in 2 unrelated girls affected by the congenital variant of Rett syndrome (RTT) (Ariani et al. 2008). This is 1 of the 5 clinical subgroups of atypical RTT, caused in up to 50% of cases by mutations in the methyl-CpG-binding protein 2 (MECP2) gene, the same gene associated to up to 95% of classical RTT (Huppke et al. 2000; Monros et al. 2001; Smeets et al. 2003; Rajaei et al. 2011). Initially described by Rolando, the affected girls showed clinical features observed in classic RTT (microcephaly, either of congenital onset or secondary to early postnatal deceleration of head growth, hand stereotypies, neurogenic scoliosis, and some autonomic features including hypotrophic feet, bloating, and impaired nociperception), but in addition they were described as atonic and mentally retarded from the very first months of life (Rolando 1985). As RTT affects almost exclusively females, large molecular screening of *FOXG1* were initially carried out in female individuals suffering from typical and atypical forms of RTT. That may explain why only few *FOXG1* mutant, male patients were reported (Le Guen et al. 2011).

	Bisgaard et al. [2006]	Papa et al. [2008]	Mencarelli et al. [2009]	Jacob et al. [2009]
Case number	1 (3.1 Mb)	1 (3.12 Mb)	1 (3.6 Mb)	1 (2.59 Mb)
Sex	female	female	male	female
Age	11 months	7 years	10 months	3 years
Normal OFC at birth	33 cm (−1 SD)	32 cm (−1 SD)	33 cm (−1 SD)	32.5 cm (−1 SD)
Deceleration of head growth from birth (microcephaly)	yes	yes	yes	yes
Regression	no	yes (<6 months)	yes (<3 months)	no
Severe intellectual disability	present	present	present	present
Hypotonia	yes	yes	yes	yes
Poor to absent voluntary hand use	no	yes	no	N/A
Facial abnormalities	prominent metopic suture, apparently large ears, bilateral epicanthal folds, bulbous nasal tip, depressed nasal bridge, tented upper lip, and everted lower lip	prominent metopic suture, large ears, bilateral epicanthal folds, bulbous nasal tip, depressed nasal bridge, thick upper lip, everted lower lip, prognathism, and hypermetropia	apparently large ears, bilateral downslanting palpebral fissures, bulbous nasal tip, depressed nasal bridge, thin upper lip, and lower lip, prognathism	low ears, synophrys, depressed nasal bridge, bulbous nasal tip, thin lips, and pointed chin
Seizures	present	present (6 months)	no	present
Stereotypic movements	dyskinetic movements	constant of hands and tongue	yes	yes (face, limb)
Jerky movement of the upper limbs	no	yes	yes	N/A
Bruxism	no	yes	no	yes
Speech	no	no	no	N/A
Delayed myelination or hypomyelination	N/A	N/A	N/A	no
Hypoplastic corpus callosum	no	agenesis	agenesis	N/A
Frontal and temporal atrophy with gyral simplification	no	no	absence of gyrus anguli	no

N/A = Not available.

Three other cases have been described, but clinical data were insufficient to be included in this table (a de novo 0.64-Mb deletion [unpublished data] and two 0.14–1.8-Mb deletions (DECIPHER database) [Mencarelli et al., 2009]).

Figure 13. Clinical summary of the patients with interstitial deletions of the long arm of chromosome 14 including *FOXG1*

Pyramidal neuronal network development and function

The mammalian cortex neuronal network formation depends on GABAerigc and glutamatergic pyramidal neurons' development (Molyneaux et al. 2007; Miyoshi and Fishell 2012). A proper modelling of axon, dendrites and synapses morphogenesis during development is required for the formation of a functional network circuitry in the cortex, underlying synaptic communication and information processing. Neurons receive and send information within the cerebral cortex network via dendrites and axons engaging in numerous specialized cell-to-cell connections. The complexity and degree of both extension and branching of the dendritic arbor is related to the number of synaptic inputs, which is specific to different neuronal types. Different cytoarchitectonics may reflect a different ability in receiving and transmitting information via cell-to-cell interaction. The more developed the neuronal architecture, including the dendritic branching, the higher the communicative potential within a network. How a pyramidal neuron responds to synaptic inputs and generates a postsynaptic action potential appears to be critical for network excitability investigation (Parekh and Ascoli 2013). The number of synapses per neuron and the turnover dynamics are tightly linked to functional changes. Therefore, an analysis comparing normal and abnormal morphometric conditions may provide insight into pathogenic mechanisms underlying infantile spasms syndromes.

Cortical neuritogenesis in pyramidal neurons

The dendritic tree of cortical pyramidal neurons is characterized by basal and apical dendrites. The apical dendrite usually bifurcates at a variable distance from the cell body, it connects the soma to the apical cluster of dendrites that eventually bifurcate again (De Felipe and Fariñas 1992). Pyramidal neurons' key features vary within the cortex at a layer and cortical region level (Spruston 2008). Dendrites may develop from a growth cone-like tip or branch from interstitial sprouts on already formed dendrites, then a series of retracting and extension events take place in a dynamic remodeling fashion (Jan and Jan 2003). The cortical pyramidal neurons' dendritogenesis mechanism is an extremely dynamic process, tightly controlled, both temporally and spatially (Rakic 2002). Dendritic growth, retraction, branching and guidance are basic morphogenic processes that take place during development and peak in the human brain at around the 16th-30th month. These morphogenic processes are controlled by both extrinsic and intrinsic cues (Cline 2001; McAllister and Kimberley 2000). Neurotrophic factors are among the many factors tightly controlling dendritic outgrowth: these extrinsic factors are involved in molecular cascades regulating dendritic growth of pyramidal neurons in the developing

neocortex (McAllister et al. 1995). Neurotrophin-3 (NT-3), brain-derived neurotrophic factor (BDNF) and nerve growth factor (NGF) act as extrinsic factors in monitoring and ruling dendritic growth and branching/arborization, via extension or retracting promotion. Endogenous neurotrophins thus contribute to the regulating of pyramidal neurons' development within neocortex. Moreover, it has been reported that endogenous neurotrophins act as mediators of activity-dependent structural plasticity (McAllister et al. 1999). In addition to neurotrophins, there are many others extrinsic factors involved in dendritic outgrowth during development. These factors include Ephrins and Semaphorins which are large families of chemorepellant and chemoattractive signalling molecules; members of bone morphogenetic protein factors (BMPs); cell-adhesion molecules; glia; hormones and molecules such as Notch1 and Slits (Polleux and Snider 2010; Gould et al. 1990; Gao 1998; McAllister et al. 1995). As regards intrinsic factors involved in dendritic shaping and development, calcium calmodulin dependent protein kinase II (CamKII), microtubule-associated proteins (MAPs), GTPases, dendritic mRNAs and neuronal activity itself (de la Torre-Ubieta et al. 2010; Cline 2001) are among the most important factors modelling dendrites' shape within the developing network (Nguyen et al. 1994; Wu and Cline 1998; Luo et al. 1994).

Normal and pathological dendritogenesis

The structure and development of dendritic arbors is critical for synaptic input processing; thus, circuitry communication seems to be affected by the same factors that are involved in dendritic modelling. Dendritic arbors are highly plastic structures, branching, extending and retracting in response to the environment's variable signals. In the same way that communication is basic and dynamic at a macroscopic scale, so it is at a microscopic level; abnormality in a highly-orchestrated process of dendritic shaping and cell-on-cell adhesion contacts formation, will eventually reflect irregularities at a macroscopic level. Changes in dendrite shaping during development include dendrite retraction or elongation, dendrite fragmentation, loss or increase in branching, as well as dendritic spine density and morphology variation. Neural network development aberrations are related to diverse neurological defects, including autism and epilepsy (Mironov et al. 2014). Specifically, variations in dendrite shaping are associated with several neurodevelopmental and neurological disorders (Kaufmann and Moser 2000; Kulkarni and Firestein 2012; Fig.14), as a matter of cortical circuitry alteration, due to an aberrant synaptic signaling mechanism moving far away from physiology. Previous literature reports various examples of dendritic shaping variations: cortical dendritic arborization is significantly reduced in Rett Syndrome (Armstrong et al. 1995), and CA1-CA4 hippocampal

dendritic arborization is impaired in patients suffering from autism (Raymond et al. 1995).

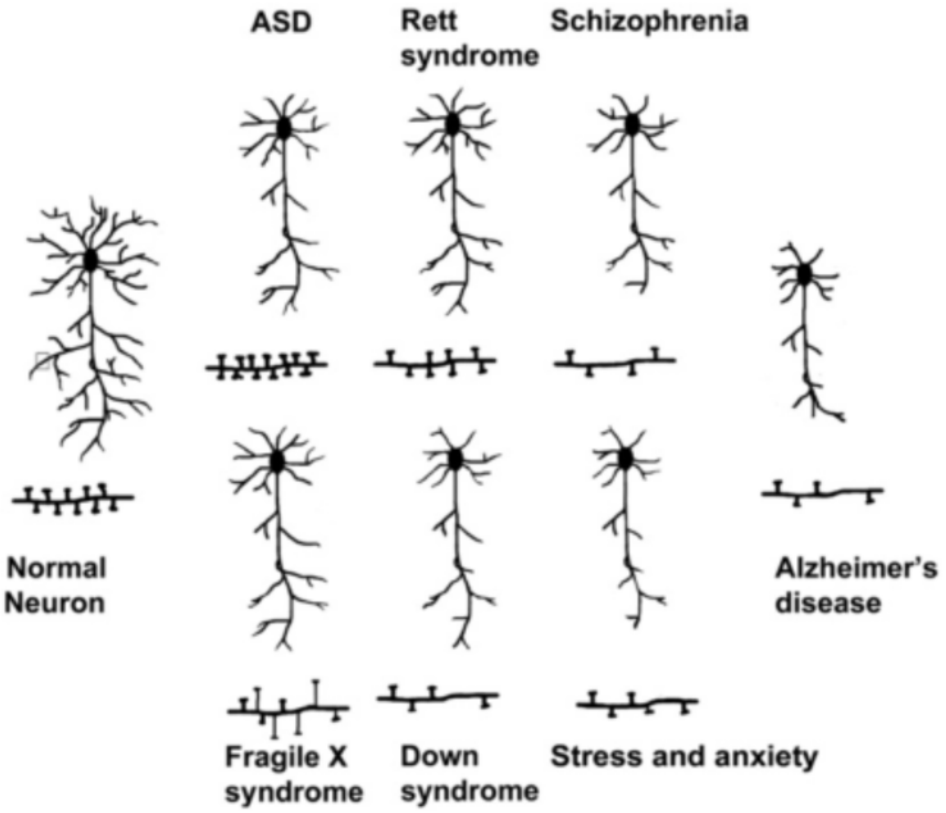

Figure 14. Schematic representation of neurons affected by atrophy and dendritic spines variations in brains of patients with ASD, Rett syndrome, Fragile X syndrome, Down syndrome, AD, Schizophrenia and Stress and anxiety (adapted from Kulkarni et al. 2012)

Molecular mediators of neuritogenesis

To integrate into neuronal circuits, newly generated neurons engage in a series of stereotypical developmental events. After exit from the cell-cycle, postmitotic neurons first undergo axodendritic polarization, a process that encompasses the initial specification of axons and dendrites and their coordinate growth giving rise to the unique neuronal shape. Concurrently, many neurons undergo extensive migration to reach their final destinations in the brain. Axons grow to their appropriate targets, dendrites arborize and prune to cover the demands of their receptive field, and synapses form and are refined to ensure proper connectivity. A large body of work has established that these fundamental events are regulated by extrinsic cues including secreted growth factors, adhesion molecules, extracellular matrix components, and neuronal activity (Katz and Shatz 1996; Tessier-Lavigne and Goodman 1996; Markus and

Snider 2002; McAllister 2002; Huber et al. 2003; Dijkhuizen and Ghosh 2005). Accumulating evidence also supports the concept that cell intrinsic mechanisms have major roles in neuronal morphogenesis and connectivity. These mechanisms comprise developmentally inherited pathways that operate largely independently of cellular environments, orchestrate neuronal responses to extrinsic cues and in turn may be influenced by these cues. This intrinsic identity may also influence how neurons respond to extrinsic cues. Application of the same neurotrophic factor to neurons located in distinct cerebral cortical layers elicits differential effects on dendrite morphology (McAllister et al. 1995, 1997), suggesting that neurons inherit distinct developmental programs that dictate their responses to extrinsic signals. Purified rat embryonic retinal ganglion neurons cultured in a variety of conditions grow axons much faster than ganglion neurons from postnatal animals (Goldberg et al. 2002). In addition, with maturation retinal granule neurons undergo a switch from preferential axon growth to preferential dendrite growth (Goldberg et al. 2002). Collectively, these observations suggest that neurons harbor developmentally inherited cell-intrinsic mechanisms that determine in large part neuronal morphogenesis. Transcriptional control of gene expression represents a major mode of cell-intrinsic regulation of neuronal development. TFs can govern entire developmental programs, directing distinct stages of neuronal development as well as altering the competency and response of cells to extrinsic cues. Accordingly, often the expression of one or a set of TFs is sufficient to direct the subtype specification of distinct neuronal populations and thus their morphology and projection patterns (Arlotta et al. 2005; Chen et al. 2005; Hand et al. 2005; Lai et al. 2008; Liodis et al. 2007). Studies of the mammalian cerebellar cortex have highlighted the importance of TFs in distinct aspects of neuronal morphogenesis and connectivity (Fig.15).

Transcriptional control of axonogenesis

Axon growth in cerebellar granule neurons is controlled by the transcriptional regulators *SnoN* and *Id2*, both of which are subject to degradation by the ubiquitin proteasome system (Konishi et al. 2004; Lasorella et al. 2006; Stegmuller et al. 2008). Cdh1-anaphase promoting complex (Cdh1-APC), an E3 ubiquitin ligase, targets SnoN and Id2 for degradation and in turn restricts axon growth (Konishi et al. 2004; Lasorella et al. 2006; Stegmüller et al. 2006). Interestingly, a recent study has revealed that *SnoN* also regulates in an isoform-specific manner granule neuron migration and positioning by controlling the expression of the microtubule-binding protein doublecortin (*Dcx*) (Huynh et al. 2011). Following parallel fiber axon growth, establishment of synaptic connections in the molecular layer occurs through complex interactions between pre-synaptic sites in parallel fiber axons and dendritic

spines in Purkinje neurons. Parallel fiber presynaptic sites are under transcriptional control as well, with the basic helix-loop-helix (bHLH) family member *NeuroD2* which inhibits presynaptic sites formation in newborn granule neurons (Yang et al. 2009). Similarly to SnoN-and Id2-control of axon growth, NeuroD2 is also regulated by the ubiquitin-proteasome pathway where the Cdh1-APC-related ligase Cdc20-APC triggers NeuroD2 degradation in mature neurons and thereby promotes presynaptic differentiation (Yang et al. 2009). Thus, different aspects of axon development, growth and presynaptic development are regulated by the APC acting on different TFs.

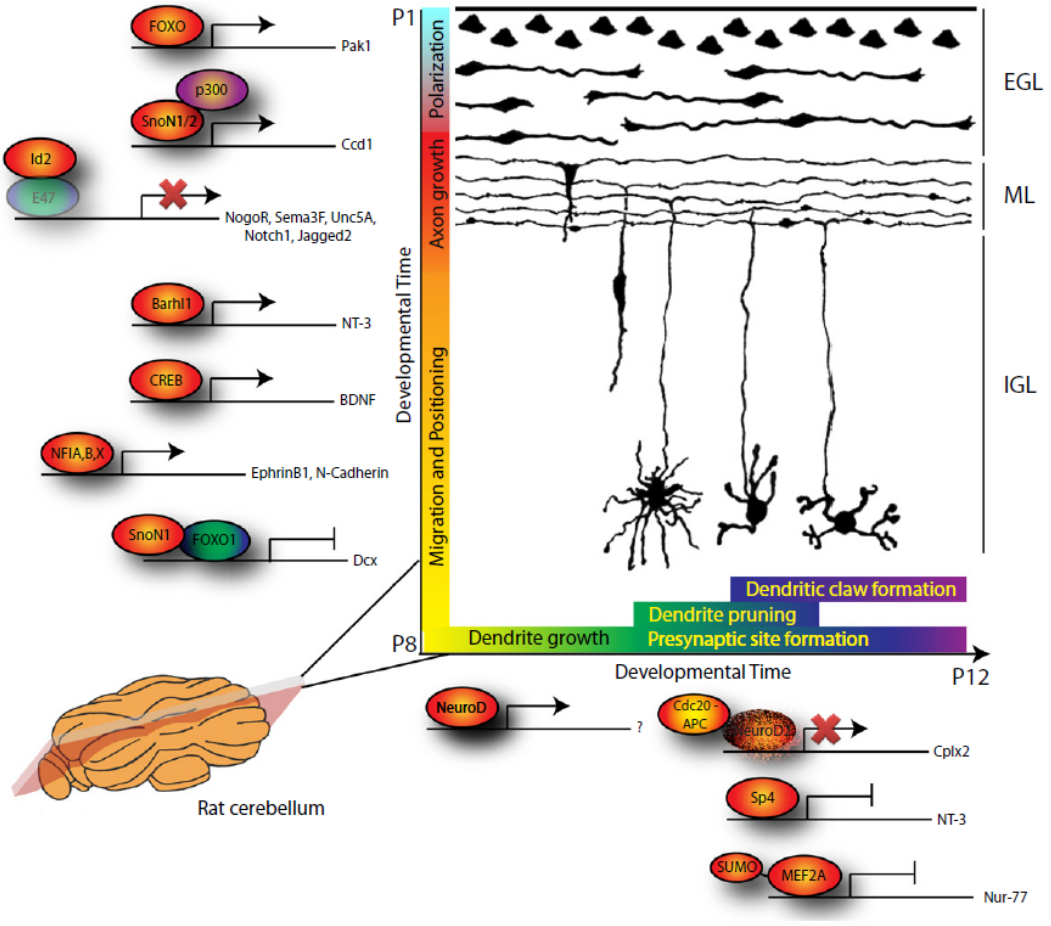

Figure 15. TFs orchestrate distinct stages of neuronal morphogenesis in the cerebellar cortex (adapted from de la Torre-Ubieta and Bonni 2011)

Transcriptional control of dendritogenesis

Dendrites display a greater variety of morphologies in different populations of mammalian neurons. In recent years, a number of TFs have been discovered to regulate distinct stages of dendrite development. *Foxo* TFs, including the brain-enriched *Foxo6*, inhibit dendrite growth while promoting axon growth (de la Torre-Ubieta et al. 2010). Thus, while neurons migrate and their axons grow, transcriptional mechanisms inhibit the formation of dendrites. Subsequently, the bHLH protein NeuroD plays a critical role in the initiation of dendrite growth as well as the branching of neuron dendrite arbors in the cerebellar cortex (Gaudilliére et al. 2004). Later, *Sp4* promotes the pruning of the granule neuron dendrite arbor (Ramos et al. 2007, 2009), and *Mef2a* triggers the morphogenesis of the postsynaptic dendritic claws (Shalizi et al. 2006, 2007).

Although studies in the cerebellar cortex have provided compelling evidence for cell-intrinsic regulation of stage-dependent dendrite morphogenesis that is widely relevant to diverse populations of neurons in the brain, TFs can also shape the development of dendritic arbors characteristic of a particular neuronal subtype. Temporally specific or layer-specific expression of TFs in the cerebral cortex may contribute to define the morphological identity of neurons (Arlotta et al. 2005; Molyneaux et al. 2007, 2009). The zinc finger TF *Fezf2* is required for dendritic arbor complexity in layer V/VI neurons specifically (Chen et al. 2005). The mammalian homologs of the Drosophila TF *Cut*, *Cux1* and *Cux2*, have been implicated in layer II/III pyramidal neuron dendrite development though with seemingly conflicting conclusions (Cubelos et al. 2010; Li et al. 2010). Using a combination of knockout mice and *in vivo* RNAi to generate *Cux1*-and *Cux2*-deficient cortical neurons in the intact cerebral cortex, Cubelos and colleagues have found that *Cux1* and *Cux2* additively promote dendrite growth and branching as well as dendritic spine formation. Cux1 and Cux2 directly repress the putative chromatin modifying proteins *Xlr3b* and *Xlr4b*, which couple *Cux1* and *Cux2* to regulation of dendritic spine morphogenesis, while the transcriptional targets involved in dendrite arbor formation remain to be identified (Cubelos et al. 2010). In contrast, using cortical cultures Li and colleagues have found that overexpression of *Cux1*, but not *Cux2*, decreases dendrite complexity, and conversely that knockdown of *Cux1* leads to excessive dendritic arbor size in cortical neurons. Li and colleagues have also reported that Cux1 directly represses the cell-cycle regulator *p27kip1* and thereby inhibits dendrite growth through RhoA (Li et al. 2010). The findings from Cubelos and colleagues that *Cux1* promotes dendritic complexity are consistent with the function of the fly homolog *Cut*, suggesting functional evolutionary conservation of this TF.

Neuronal activity shapes dendrite morphology

Just as in the cerebellar cortex, studies of dendrite morphogenesis in the cerebral cortex and hippocampus have highlighted the regulation of TFs by neuronal activity and calcium influx (Fig.16). Prominent among these is the transcription factor cAMP-responsive element binding protein (CREB), which is modulated by a variety of extrinsic cues and regulates neuronal survival, dendrite growth, and synaptic function (Flavell and Greenberg 2008; Lonze and Ginty 2002; Shaywitz and Greenberg 1999). Neuronal activity stimulates CaMKIV-driven phosphorylation and activation of CREB in cortical neurons and thus induces dendrite growth and arborization (Redmond et al. 2002). More recently, CaMKIγ has been shown to drive activity-dependent phosphorylation and activation of CREB in hippocampal neurons, resulting into increased dendritic arborization (Wayman et al. 2006). The CREB coactivator CBP also contributes to neuronal activity-induced dendrite morphogenesis (Redmond et al. 2002). Another calcium-regulated transcriptional coactivator termed CREST, is also required for activity-dependent dendrite growth in the cerebral cortex (Aizawa et al. 2004). Further CREB binding partners required for CREB-dependent dendrite growth include TORC1 (transducer of regulated CREB activity) and CRTC1 (CREB-regulated transcription co-activator), which act downstream of activity-dependent signaling and BDNF, respectively (Li et al. 2009; Finsterwald et al. 2010). BDNF represents a potentially relevant target of CREB and associated proteins in the control of dendrite development and branching (McAllister et al. 1997; Tao et al. 1998; Horch and Katz 2002; Dijkhuizen and Ghosh 2005; Cheung et al. 2007). The secreted signaling protein *Wnt-2*, which promotes dendritic arborization, is also induced by CREB downstream of neuronal activity (Wayman et al. 2006). Interestingly, the microRNA *miR-132* is also induced by CREB in an activity-dependent manner and promotes the elaboration of dendrite arbors in hippocampal neurons (Wayman et al. 2008; Magill et al. 2010).

Last but not least, nBAF chromatin remodeling complex is required for dendrite development (Wu et al. 2007; Fig.16). The multimeric BAF complex is assembled from several homologous proteins in a developmental-specific manner. The neuron-specific BAF53b subunit (Lessard et al. 2007) is crucial to both basal and activity-dependent dendrite growth. The BAF53b-containing nBAF complex associates with CREST and modulates the expression of a large number of genes involved in neurite growth (Wu et al. 2007). This is of particular interest in light of the observation that at least two other epigenetic regulators, the histone demethylase SMCX and the DNA methyl-binding transcriptional repressor Mecp2, which are mutated in cases of X-linked mental retardation (XLMR) and Rett syndrome, also control dendrite growth (Ballas et al. 2009; Iwase et al. 2007; Zhou et al. 2006). All that suggests that epigenetic

mechanisms can drive long-lasting transcriptional changes, providing a further key contribution to dendrite development.

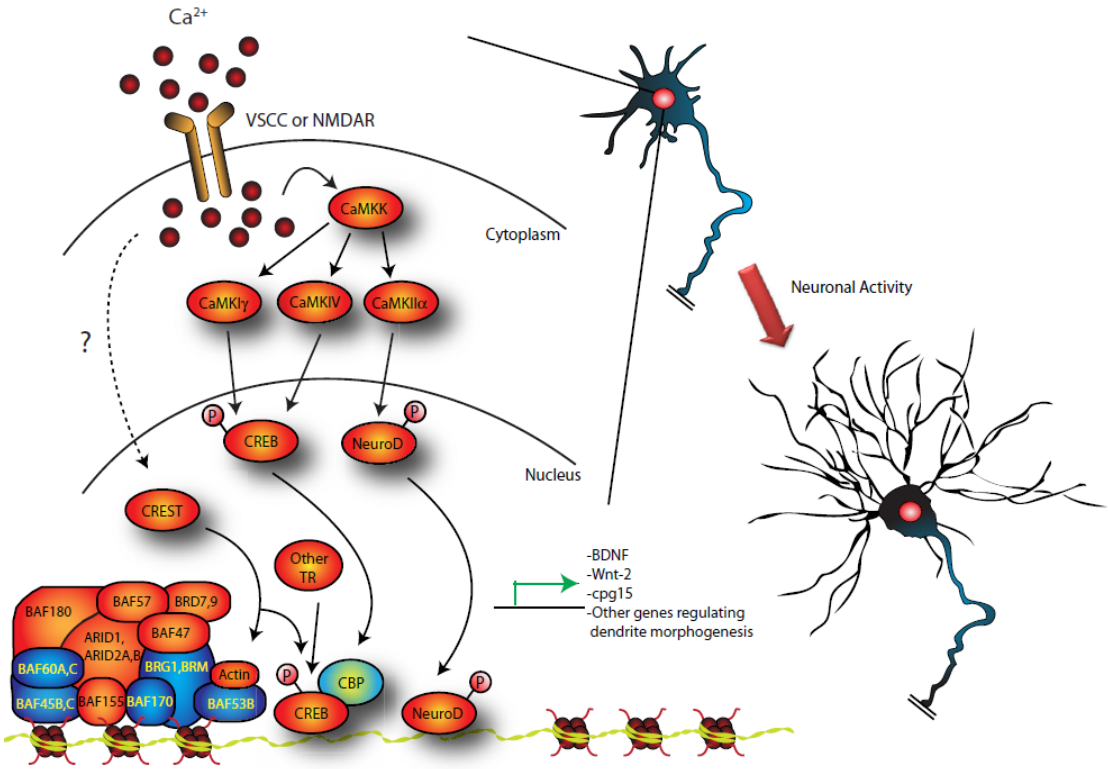

Figure 16. Neuronal activity regulates transcription-dependent dendrite growth (adapted from de la Torre-Ubieta and Bonni 2011)

AIM

Neocortical dendritogenesis is a complex and articulated process. Dendritic trees are primarily shaped according to patterns peculiar to distinctive neuron types and subsequently refined on the basis of spatio-temporal articulation of neuronal activity. Specific dendrite dismorphologies have been associated to a number of human neurological abnormalities (autism, mental retardation, epilepsy) and have been suggested to contribute to their etiopathogenesis.

Physiological sculpting of pyramidal dendrites is driven by a sophisticated molecular machinery ruled by intrinsic and extrinsic factors. *Foxg1* is a key transcription factor gene mastering multiple aspects of rostral brain development and its proper allelic dosage is crucial to neurological health.

Aim of this thesis was to investigate *Foxg1* impact on neocortical dendritogenesis, in physiological conditions as well as upon *Foxg1* misregulation, as a model of patients with abnormal allele dosage.

MATHERIALS AND METHODS

Mice and embryo dissection

Animal handling and subsequent procedures were in accordance with European and Italian laws [European Parliament and Council Directive of 22 September 2010 (2010/63/EU); Italian Government Decree of 4 March 2014, n° 26]. Experimental protocols were approved by SISSA OpBA (Institutional SISSA Committee for Animal Care). *Mtapt*$^{EGFP/+}$ (Tucker et al. 2001), *Foxg1*$^{+/-}$ (Hebert and McConnell 2000) and wild type CD1 males were mated to wild type CD1 females (purchased from Envigo Laboratories, Italy) and maintained at the SISSA mouse facility. E12.5 embryos were staged by timed breeding and vaginal plug inspection. *Mtapt*$^{EGFP/+}$ E12.5 embryos were distinguished from their wild type littermates by inspection under fluorescence microscope. *Foxg1*$^{+/-}$ E12.5 embryos were distinguished from their wild type littermates by PCR genotyping as previously described (Muzio and Mallamaci 2005). Pregnant females were killed by cervical dislocation. Embryonic cortices were dissected out in cold PBS, under sterile conditions.

Neuronal cultures from primary cortical precursors

Depending on the assay in order (neurite morphometry, pCreb1 densitometry, luciferase reporter assays, ChIP and RNA profiling, phosphatase activity assays, *in vivo* transplantations) and as detailed in the corresponding figure panels, neural cultures were set starting from E12.5, E14.5 or E16.5 neocortical precursors. E12.5 precursors were obtained dissecting neocortices from *Mtapt*$^{EGFP/+}$ or wild type embryos and dissociating them to single cells by gentle pipetting. Just in case of Fig. 26 we obtained *Mtapt*$^{EGFP/+}$; *Foxg1*$^{+/-}$ E12.5 precursors by mating *Mtapt*$^{EGFP/+}$ female mice with *Foxg1*$^{+/-}$ male founders (Hebert and McConnell 2000). We obtained ¼ of embryos *Mtapt*$^{EGFP/+}$; *Foxg1*$^{+/-}$ and we discriminate them by both visual genotyping under a blue light lamp and PCR genotyping (Muzio and Mallamaci 2005). Precursors were acutely infected by specific lentivector mixes, as detailed in figure protocol panels. Each lentivector was delivered at a multiplicity of infection (m.o.i.) = 8, which was previously shown to be sufficient to transduce almost the totality of neural cells in such experimental conditions (Brancaccio et al. 2010). Just in case of Fig. 27, miR.αFoxg1.1694 and miR.NC were delivered at m.o.i. = 20, as previously described and tested (Fimiani et al. 2016). The dissection/infection day was referred to as “day in vitro 0” (DIV0) or “post-dissection day 0” (PDD0). Neural cells were cultured for 2 days in uncoated 12 multiwell plates (DB Falcon). $6*10^5$ cortical precursors were plated in each well with 600 µL of serum-free

"DMEM/F12-GFs" pro-proliferative medium [DMEM-F12 (Gibco), 1X Glutamax (Gibco), 1X N2 (Invitrogen), 1 mg/mL BSA, 0.6% glucose, 2 µg/mL heparin (Stem Cell Technologies), 20 ng/mL bFGF (Invitrogen), 20 ng/mL EGF (Invitrogen), 1× Pen-Strept (Gibco), 10 pg/mL Fungizone (Gibco)], and grown as floating neurospheres (Brancaccio et al. 2010).

In case of *in vitro* neurite morphometry and pCreb1 densitometry, DIV2 "green" *Mtapt*$^{EGFP/+}$/*Mtapt*$^{EGFP/+}$;*Foxg1*$^{+/-}$ and "black" wild type/*Foxg1*$^{+/-}$ neurosphere derivatives were mixed at a 1:500 ratio (that was intended to allow a better morphological profiling of single neurons, albeit belonging to a dense ensemble). In particular, 10^5 premixed neurosphere-derivative cells were transferred to 2 cm^2-coverslips pretreated with 200 µg/mL poly-L-lysine, under 300 µL of "Neurobasal A" pro- differentiative medium/well [1× Neurobasal A, 1X Glutamax (Gibco), 1X B27 supplement (Invitrogen), 0.5 mM glutamine, 25 µM β-Mercaptoethanol, 1× Pen/Strep (Gibco), 10 pg/mL fungizone (Gibco)]. Cells were cultured up to DIV12, replacing one-third of pro-differentiative medium with fresh medium every 3.5 days.

Limited to luciferase reporter assays, acute E14.5 neocortical precursors, dissociated to single cells by gentle pipetting, were employed in place of neurosphere derivatives. These precursors were plated at $2*10^5$ cells/2 cm^2, in 24-multiwell plates pretreated with 200 µg/mL poly-L-lysine, under "Neurobasal A" pro-differentiative medium, and employed as detailed below.

Concerning RNA and ChIP profiling as well as phosphatase activity assays we used two different neuronal preparations, as detailed in figure panels. On the one hand, DIV2 neurosphere derivatives were transferred to 12-multiwell plates pretreated with 200 µg/mL poly-L-lysine, at $8*10^5$ cells/4 cm^2 under 600 µL of "Neurobasal A" pro-differentiative medium/well. On the other hand, E14.5 or E16.5 neocortical precursors were dissociated and plated in 12-multiwell plates pretreated with 200 µg/mL poly-L-lysine, at $8*10^5$ cells/4 cm^2 under 600 µL of "Neurobasal A" pro-differentiative medium/well. Cells were cultured up to DIV12, replacing one-third of pro-differentiative medium with fresh medium every 3.5 days.

In case of RNA, ChIP, phosphatase and luciferase assays, 10µM cytarabine was included in the medium to reduce glial contamination as much as possible.

In general, TetON-modulated transgenes were controlled by timed addition of doxycycline (Sigma#D9891-10G) (final concentration was from 62 to 2000 ng/mL, as detailed in the corresponding figure panels). Upon every medium change, doxycycline was partially replaced by the antibiotic included in fresh medium at the above concentrations.

In case of *in vitro*/*in vivo* experiments, DIV2-7 lentivirus-engineered *Mtapt*$^{EGFP/+}$ neurospheres were dissociated by trypsin to single cells and passaged at the initial culturing density reported in figures. Just prior to transplantation, two

different aliquots of these cells, overexpressing *Foxg1* or a control, were mixed 1:1 and adjusted to total $5*10^4$–10^5 cells/µL in "DMEM/F12-GFs" medium.

Human Neural Precursors (hNPs) cultures and differentiation

We used for our experiments hNPs provided by Dr. Stefano Pluchino (Cambridge University, UK). These cells were cultured as floating neurospheres at clonal density (130,000 cells/cm^2) in NS-A Proliferation medium [Neurocult^{TM} NS-A Proliferation Kit (#05751, StemCell Technologies), 0.2% human Heparin (StemCell Technologies), 10ng/mL bFGF (Gibco), 20 ng/mL EGF (Gibco)]. The growth factors were added every two days and cells were passaged by Accutase (Sigma) every two weeks. In order to differentiate them, hNPs were dissociated at single cells and plated at 60,000 cells/cm^2 on multiwell plates pre-coated with Matrigel (Corning) in NS-A Differentiation medium [Neurocult^{TM} NS-A Differentiation kit (#05752, StemCell Technologies) without any growth factors]. The medium was changed by half every four days. They were acutely infected by specific lentivector mixes, as detailed in figure protocol panels. Each lentivector was delivered at a m.o.i. = 20.

Lentiviral vector packaging and titration

Third generation SIN lentiviruses used for this study are listed below. All lentiviruses were generated and titrated as previously described (Brancaccio et al. 2010).

Third generation SIN lentiviruses used for this study were:

- TREt-Foxg1 (Raciti et al. 2013);

- TREt-PLAP (Falcone et al. 2016);

- pTα1-rtTA (Brancaccio et al. 2010);

- pPgk1-luc [constructed by transferring the NotI-BamHI 1.57 kb fragment from the lentivirus pPgk1-EGFP to NotI-BamHI digested TREt-luciferase (Raciti et al. 2013)];

- pPgk1-mCherry (Falcone et al. 2016);

- pU6-shFoxg1 (Sigma SHCLND-NM_008241, TRCN0000081746);

- pU6-shCtrl [constructed by eliminating the NotI/EcoRI fragment containing CMV-EGFP from the pLL3.7 vector (Rubinson et al. 2003), corresponding to the plasmid #11795 of the Addgene collection];

- pU6-shHES1 (Sigma [SHCLND-NM_005524, TRCN0000018991]);

- TREt-Hes1 (also known as TetO-FUW-Hes1 (Cassady et al. 2014), corresponding to the plasmid #61534 of the Addgene collection);

- TetO-FUW-Nfia (Caiazzo et al. 2015), [purchased from Addgene (#64901)];

- TREt-MAML1-DN [constructed by replacing the AgeI-SalI fragment of TREt-EGFP (Brancaccio et al. 2010) with an AgeI-SalI fragment including the MAML1-DN cds (adapted from (Weng et al. 2003))];

- pCAGGS-LacZ (Pfeifer et al. 2001), [purchased from Addgene (#12108)];

- pLenti6.2/V5-SS18 [purchased from DNASU (clone HsCD00330181)];

- TREt-NDR1 [built starting from TREt-EGFP (Brancaccio et al. 2010), by removing the SalI/SalI Ires-EGFP-cds fragment and replacing the AgeI-PmeI polylinker fragment by the AgeI-ZraI hsa-Ndr1-cds fragment, taken from pFLAG-NDR1 (Devroe et al. 2004) [purchased from Addgene (#8927)]];

- TREt-CREB-DN [constructed by replacing the AgeI-SalI fragment of TREt-EGFP (Brancaccio et al. 2010) with an AgeI-XhoI fragment including the CREB-DN cds (adapted from (Ahn et al. 1998))];

- TREt-Hes6 [constructed by replacing the AgeI-SalI fragment of TREt-EGFP (Brancaccio et al. 2010) with an AgeI-SalI fragment including the mmu-Hes6-001 cds (adapted from (Weng et al. 2003))];

- UbiCp-PSD95-mCherry [obtained via *in vitro* Cre/loxP-mediated FlEx-ing of FU-dio-PSD95-mCherry-W (Villa et al. 2016), purchased from Addgene (#73919)];

-TREt-CrebM1 [built starting from TREt-EGFP (Brancaccio et al. 2010), by removing the SalI/SalI Ires-EGFP-cds fragment and replacing the AgeI-PmeI polylinker fragment by the AgeI-SwaI CREB-M1 fragment, taken from pCF-CREB-M1 (Du et al. 2000) [purchased from Addgene (#22969)]];

- pU6-shSYT (Sigma TRCN0000337696);

-LTR-pPgk1-eGFP-pri-miR.anti-*Foxg1*.1694-Wpre-LTR (Fimiani et al. 2016);

-LTR-pPgk1-eGFP-pri-miR.NC-Wpre-LTR (Fimiani et al. 2016).

RNA profiling

Total RNA was extracted from cells using TRIzol Reagent (Invitrogen) according to the manufacturer's instructions. Agarose gel electrophoresis and spectrophotometric measurements (NanoDrop ND-1000) were employed to estimate its concentration, quality and purity. Prior to retrotranscription, RNA

preparations were treated by TURBO DNA-freeTM Kit (ThermoFisher Scientific). At least 0.5 µg of total purified RNA from each sample was retro-transcribed (RT) by SuperScriptIIITM (Invitrogen) in the presence of random hexamers, according to the manufacturer's instructions. 1/100 of the resulting cDNA was used as substrate of any subsequent qPCR reaction. Negative control PCRs were run on RT (-) cDNA preparations. In general, PCR reactions were performed by the SsoAdvanced SYBR Green SupermixTM platform (Biorad), according to the manufacturer's instructions. For each transcript under examination and each sample, cDNA was PCR-analyzed in technical triplicate, against absolute standards, and average results calculated. Averages were normalized against *Gapdh* and further normalized against controls. Experiments were performed at least in biological triplicate. Results were evaluated by Student's t-test, via Excel software. Oligonucleotides are listed below in the Table 1.

Table 1. RT-qPCR oligos

name	*sequence (5'->3')*
mmuNeurod2Fw	CCTGAACCCACGTTGGCTGAGGTCA
mmuNeurod2Rev	CCAGACGCGCCTTGGTCATCTTGC
mmuHes1Fw	GGCCTCTGAGCACAGAAAGTCATCAAAGCCTATCATGG
mmuHes1Rev	CCGGCGCGGTATTTCCCCAACAC
mmuHes5Fw	GCTCAGTCCCAAGGAGAAAAACCGACTGCG
mmuHes5Rev	CGCGGCGAAGGCTTTGCTGTGTTTCAG
mmuId2Fw	CACTATCGTCAGCCTGCATCACCAGAGA
mmuId2Rev	CACAGAGTACTTTGCTATCATTCGACATAAGCT
mmuSytFw	CAGGCCAGGAAGACTATTATGGGGACCAAT
mmuSytRev	CCTCATAAGGCCTATCGTAGCCTTGTTCAG
mmuRnd2Fw	GCCATAGGCAGCTACGTCGTACTGACT
mmuRnd2Rev	GAGGTTACAGCTCTTGGCTCGATCCTTATG
mmuNdr2Fw	CTATGGAAGAAGAAGGATTGGCAGATGAG
mmuNdr2Rev	AGCTCCTCTTCCTATAACCTTCAGAGACTC
mmuGapdh5Fw	ATCTTCTTGTGCAGTGCCAGCCTCGTC
mmuGapdh5Rev	GAACATGTAGACCATGTAGTTGAGGTCAATGAAGG
mmuCcd1Fw	CCGCTGCTGCTCTGGCTGATGTG
mmuCcd1Rev	GCTGCACAAGAGCCCGCACACTC
mmuCrestFw	ACGTGTCCATGCAGCAGACGGCTCA
mmuCrestRev	GTGCTGAGTTGTAGTGGGACGTGGCT

mmuDab1Fw	CAACCGTCCCAGGCACGAATGACTC
mmuDab1Rev	GGAAATCCTTGAACGACTCCTTCCCCATT
mmuFezf2Fw	CCTGCGAAGTGTGCGGCAAGGTGTT
mmuFezf2Rev	GAGAGTGCTGGCCTGGCGGAAGC
mmuId1Fw	CGGAGTCTGAAGTCGGGACCACC
mmuId1Rev	GGCTGGAACACATGCCGCCTCG
mmuNdr1Fw	AGGAACCTGAACCACAGCCTGCCC
mmuNdr1Rev	ACATGATTACCCCGAGCGACCACCAAT
mmuNeurod1Fw	AGGCTCCAGGGTTATGAGATCGTCAC
mmuNeurod1Rev	CTGCCTCGTGTTCCTCGTCCTGAGAA
mmuFoxg1Fw	CGACCCTGCCCTGTGAGTCTTTAAG
mmuFoxg1Rev	GGGTTGGAAGAAGACCCCTGATTTTGATG
mmuHes1_3UTRFw	CACTGCTACCCGTAAAGTCCCTAGCC
mmuHes1_3UTRRev	TGGTCAGTCACTTAATACAGCTCTCTAC
mmuCreb1Fw	CTGAAGAAGCAGCACGGAAGAGAGAG
mmuCreb1Rev	TTAATCTGATTTGTGGCAGTAAAGGTCCTTA
mmuNfiaFw	TTGGACCTCGTCATGGTGATC
mmuNfiaRev	TGGACACAGAGCCCTGGATTA
mmuSirt1Fw	TACCAGAAACAATTCCTCCACCTGAGC
mmuSirt1Rev	AATACTCAATATCAAACATGGCTTGAGGGT

ChIP-qPCR

The chromatin immunoprecipitation quantitative polymerase chain reaction assays (ChIP-qPCRs) were performed on chromatin extracted from neural cell cultures engineered as shown in Fig. 22B. For each ChIP assay, chromatin from 10^6 cells was fixed by 1% formaldehyde for 10 min at RT. After cell lysis, fixed chromatin was sonicated by a Soniprep 150 apparatus (on ice; 5 s ON, 55 s OFF; oscillation amplitude 5 µm; 5 cycles), giving rise to ~1000 bp fragments. ChIP analysis was performed according to the MAGnifyTM Chromatin Immunoprecipitation System protocol (Invitrogen), with minor modifications. Sonicated chromatin was immunoprecipitated for 2h at 4°C, by 5 µg of an α-Foxg1 antibody (rabbit polyclonal, ab18259, Abcam), in a final volume of 100 µL, keeping the tubes in a rotating device. Next, immunoprecipitated DNA was purified according to the manufacturer's instructions. Last, 1/30 of each immunoprecipitated (IP) DNA sample was amplified by qPCR. For each sample, qPCRs were performed in technical triplicate. Averages were normalized against input chromatin and further

normalized against controls. Experiments were performed at least in biological triplicate. Results were evaluated by Student's t-test, via Excel software. Oligonucleotides are listed below in Table 2.

Table 2. ChIP-qPCR oligos

name	*sequence (5'->3')*
mTbr1_3_Fw	GCATGGGTTCTTTTTCTCTCCCTCTGGAT
mTbr1_3_Rev	CAATGCGATGATCTTACTGACTGGTGTGGT
mTbr1_4_Fw	CTTCAGATGATCTGCAACCAAGTTGGCTGAT
mTbr1_4_Rev	CATAAGCTGTCGCGCTGAAGTGCTTTAATGT
mTbr1_5_Fw	CTTCTCCTCTCTTAACGCTGTGGCTTTC
mTbr1_5_Rev	GTCCTTGCCGCCCCCTCCCC
mHes1_J1_Fw	TAAAAAGGGAGACTGACATTTTCAAGTTGTACACAC
mHes1_J1_Rev	CTGAGCCATCTCTCTATCCCTGCATAAACAA
mHes1_J2_Fw	CGGTTAGAGGTCAGGAGGAGGCTC
mHes1_J2_Rev	GGAAGGGGCTTGCTGAGACCCTAAA
mHes1_J3_Fw	TTTCCGGTCAAAGCACTTGGCATGTTTGG
mHes1_J3_Rev	ATTTAGGAATCACAGGTGTTTACCCTGAGA
mHes1_J4_Fw	CCTTAACTGCCCATACAACTGATCTCCTTAAA
mHes1_J4_Rev	TAACCTCCTGCAGAGTAGACACTCTGATAT
mHes1_J5_Fw	CCCATCTGTTTAGGACATGAAAGGAGTGCCC
mHes1_J5_Rev	GTTTGAAGAAATGATAAACAATGCCTTCTTTGTTAC
mHes1_J6_Fw	TCCTATTTGCCTTATTTTCTGCCCAAGAAAGGT
mHes1_J6_Rev	AAACAGAGGACTTTAATATCTAAATTTGGGATGTGTC
mHes1_J7_fw	AAGAAGTCAAAAGTATTGCTATTCACAGGTGACATA
mHes1_J7_Rev	TTTGTATCCAGACACTTTGCTGAAGGTGTTTATTA
mHes1_J8_Fw	GAGCAGGTAAACACGGCTCTGGTTTTATTATTT
mHes1_J8_Rev	GAAGCCTTGTCATTAATTTCAATTACAAGTATTTACTTG

In vivo transplantation

Neural cell suspension of 3 µL (at 50.000–100.000 cells/µL) prepared as in "Neuronal cultures from primary cortical precursors" was injected by a pulled borosilicate pipette, into the fronto-parietal parenchyma/intraventricular cavity of P0 CD1 wild type mouse pups, pre-anesthetized by hypothermia. Fast green FCF (Sigma) of 0.1% was used to trace the transplanted cells. In case of intraventricular injection, 20 mM EGTA (pH 7) was included in the cellular

preparation just before the transplantation. Operated recipients were returned to mothers and allowed to develop up to P7 or P10.

Immunofluorescence assays

Sample prepararation

Brains dissected from operated animals were fixed by 4% paraformaldehyde overnight, cryoprotected in 30% sucrose, and sliced at 30 or 60µm, according to standard procedures. Neuronal cultures were fixed by 4% PFA for 20 min at 4 °C and washed 3 times in 1X PBS.

Immunofluorescence

Immunofluorescence was performed as previously described (Diodato et al. 2013). A list including all primary and secondary antibodies employed is attached here below.

Antibodies

The following *primary antibodies* were used:

- anti-GFP, chicken polyclonal (Abcam, ab13970), 1:500;

- anti-mCherry, rabbit polyclonal (MBL, PM005), 1:500;

- anti-RFP, rat monoclonal (Antibodies online, ABIN334653), 1:500;

- anti-Smi312, mouse monoclonal (Abcam, ab24574), 1:1000;

- anti-Tubb3, mouse monoclonal (clone Tuj1, Covance, MMS-435P), 1:1000;

- anti-MAP2, rabbit polyclonal (Abcam, ab32454), 1:500;

- anti-NF, mouse monoclonal (Abcam, ab7795), 1:400;

- anti-Cux1, rabbit polyclonal (Santa Cruz, M222), 1:50;

- anti-Ctip2, rat monoclonal (Abcam, ab18465), 1:200;

- anti-neuN, mouse monoclonal, clone A60 (Millipore, MAB377), 1:100;

- anti-CREB [pSer133], rabbit monoclonal (Novus Biologicals, NB110-55727), 1:250;

- anti-Psd95, mouse monoclonal (Abcam, ab2723), 1:1000;

- anti-Gephyrin, rabbit monoclonal, clone RbmAb7 (Synaptic Systems, 147018).

The following *secondary antibodies* were used:

- Alexa Fluor 488 and 594-conjugated anti-mouse, rat, rabbit, chicken Abs (Invitrogen), 1:600;

- biotin-conjugated anti-rabbit Ab (Sigma B7389), 1:600.

- biotin-conjugated anti-rat Ab (SAB3700654), 1:600.

Biotin-conjugated Ab was subsequently revealed by streptavidin Marina BlueTM-conjugate (Life technologies, S11221), used at 1:400 (30 minutes incubation, followed by 1 wash in 1X PBS).

Microphotography

Immunofluorescences were photographed on a Leica DM 6000 (Fig. S3A), Leica TCS SP2 (Figs S1B and S2) and a Nikon C1 (the remaining figures) apparatuses, the first and the third one equipped with an EXi Blue Fluorescence Microscopy Camera and a Hamamatsu C4742-95 camera, respectively. The following objectives were used: 20x in air (Figs S3, S4, S6, S7, S8, S9 and S13); 40x in oil (Figs 20, 24, S1 and S2); 60x in oil (Fig. S11). Images were acquired in confocal modality in case of Figures 20, 24, S1, S2 and S11, in ordinary modality in the remaining cases. Z-stacks of 5 and 10–20 2µm-spaced layers were merged in AVERAGE- and MAX-modality, in case of Figures 20, 24 and S1, S2, and S11, respectively. For each independent biological replicate, at least 6 distinct fields, each corresponding to one single neuron (case morphometry) and 10 fields (case pCreb1 densitometry), were acquired by an operator blind of cells “genotype” and analyzed after a randomization of images.

Neurite morphometry

After image acquisition and randomization, neuronal silhouettes, including somas and neurites, were generated with the Pencil Tool of Adobe Photoshop CS2 software, by an operator blind of sample genotype. These silhouettes were analyzed by the NeurphologyJ (Ho et al. 2011) interactive plug-in, in ImageJ software. Four parameters were measured: number of somas, total neurite length, number of attachment points, number of end points. Primary parameters were subsequently used for calculations of three derived indexes, “total number of exit points”, “average neurite length” and “branching index”, subject of subsequent analysis as detailed in Figure 17A. Numerical calculations and statistical assessments were performed by Excel software.

Postsynaptic element density evaluation

After images acquisition and randomization, Psd95$^+$, Cherry$^+$ and Gephyrin$^+$ spots adjacent to the Egfp$^+$ neuritic shaft were counted by an operator blind of sample identity. Counting was restricted to the proximal segment of the apical dendrite, as detailed in Figure S12A. Then, the linear density of spots along the main dendrite axis was calculated, averaged and statistically evaluated by parametric and non-parametric tests, as detailed in Figure S12 legend.

pCreb1 densitometry

Creb1 [pSer133] levels were quantified by ImageJ software. Neuronal cells were circled and, for each of them, the total corrected cellular fluorescence (TCCF, i.e., the difference between the “integrated density” and the “area of selected cell” × “mean fluorescence of background readings” product) was calculated. Control-normalized values were averaged and statistical significance of results was evaluated by Excel software, as detailed in figure legends. Graphs were generated by GraphPad Prism 6.01.

Luciferase reporter assay

For luciferase assays, cells were transfected at DIV8 with a firefly luciferase reporter (pTal-Luc, 1 µg/2 cm^2 well, Clontech) and a NanoLuc luciferase vector (pNL1.1.PGK, 10 ng/2 cm^2 well, Promega), to normalize transfection efficiency. The transfection was performed using Lipofectamine 3000 reagent, according to manufacturer’s instructions. Cells were harvested 48h after transfection and processed using the Nano-Glo Dual-Luciferase Reporter Assay (Promega). Luciferase activity was measured by a Thermo Scientific Multiskan FC device. Assays were run in biological multiplicate as detailed in Figure 22D.

Pharmacological treatments

All drugs were diluted in sterile water or DMSO where required. Seven days after plating, engineered neurons were treated with H-89 (10 µM, Sigma) protein kinase A (PKA) inhibitor, or KN-93 (2 µM, Sigma) CaM kinase II and IV inhibitor, or A6730 (5µM, Sigma) protein kinase B (PKB/AKT) inhibitor, or GF109203X (1 µM, Selleckchem) protein kinase C (PKC) inhibitor, or DMSO as a control. Cells were fixed 5 days after drug administration, for immunoprofiling and pCreb1 quantification.

Phosphatase assay

PP1 and PP2A phosphate activities were evaluated by RediPlateTM 96 EnzChekTM Serine/Threonine Phosphatase Assay Kit (ThermoFisher), according to the manufacturer instructions, with minor modifications. Briefly, DIV12 engineered neural cells were washed by 1X PBS and lysed with lysis buffer for phosphatase assays (5 M NaCl, 0.5 M EDTA pH 8.0, 1 M Tris pH 8.0, 1% NP-40, 1X "cOmpleteTM, Mini, EDTA-free Protease Inhibitor Cocktail (Roche)"). Cell lysates were centrifuged at 9300g for 15 min and supernatants were stored at -80 °C. Thawed samples were evaluated for protein concentration by the BCA method (Pierce). Different amounts of proteins, dissolved in 100 µL of 1X reaction buffer containing 1 mM $NiCl_2$ (PP-2A assay) or 2 mM DTT plus 200 µM $MnCl_2$ (PP-1 assay), were added to each well of a 96-well plate containing reconstituted 6,9-difluoro-4-methyl-umbellifery (DiFMUP) Serine/threonine phosphatase substrate [upon removal of the phospho-group, this substrate gives rise to DiFMU, which exhibits fluorescence at 358/452 nm]. After incubation at 30 °C for 30 min, multiwell plates were evaluated for fluorescence on an EnSpire® Multimode Plate Reader. Wells devoid of lysate served as background measurements. Phosphatase activities were inferred on the basis of fluorescence readings, collected in the previously determined zone of linear relationship between protein amount and fluorescence.

RESULTS

Foxg1 promotes dendrite elongation and neurite branching

To investigate the impact of *Foxg1* overexpression on the architecture of pyramidal neocortical neurons, dorsal telencephalic precursors obtained from E12.5 *Mtapt*$^{EGFP/+}$ donors (able to generate homogeneously EGFP-stained neurons, suitable for morphometric analysis) were employed. They were acutely made conditional gain-of-function (GOF) for *Foxg1*, by lentiviral vectors and TetON/OFF technology. Two days later, these cells and an equal number of mCherry-labeled controls were mixed and co-injected into the parietal parenchyma (Fig. 17D) or into the intraventricular cavity (Fig. 17B) of P0 wild type mice. Two transgene activation schedules were followed. *Foxg1* transgene was turned on upon cells transplantation, by TetOFF technology (Fig. 17B). Alternatively, it was switched on earlier, *in vitro*, by TetON technology, and then let fade *in vivo* (Hayashi et al. 2005) (Fig. 17D). Ten and seven days after engineered cell transplantation, respectively, brains were fixed and profiled by immunofluorescence and NeurphologyJ analysis (Ho et al. 2011) (Fig. 17B,D). Three key parameters describing neuronal architecture were evaluated: number of neurite exitpoints, average neurite length and neurite branching index (Fig. 17A). Regardless of the transgene activation schedule, the first two parameters were upregulated, the third one downregulated (Figs 17C,E and S1A,B). Similar results were achieved when *Foxg1* transgene was kept on 7 days *in vitro* prior to transplantation, by TetON technology, and the engrafted neurons allowed to mature over 7 days *in vivo* (Fig. S2A–C).

To better define neurite anomalies evoked by *Foxg1* overexpression and dissect the underlying molecular mechanisms, we repeated the morphometric analysis *in vitro*, staining neurites by antibodies able to label axons (anti-Smi312 and anti-NF), dendrites (anti-Map2) and whole *Mtapt*$^{EGFP/+}$ neurons (anti-EGFP), in different, appropriate combinations. We overexpressed *Foxg1* over 7 days, we allowed engineered neurons to differentiate over 2 weeks (Fig. 18A) and we specifically profiled axons and dendrites. We found an increase of dendrite exit point number and dendrite length as well as a decrease of the dendrite branching index. Axonal parameters were not affected (Figs 18B and S3A). To rule out a possible dominant negative effect caused by exaggerated *Foxg1* upregulation (Fig. S5A,B), we adopted two complementary strategies. First, we run an additional *in vitro* GOF assay, where doxycycline concentration was lowered to 100 ng/mL (Fig. 18C), so limiting *Foxg1* expression gain to about 3-folds (Fig. S5A,B). Second, we set up a complementary *Foxg1*-LOF assay, halving *Foxg1*-mRNA levels by RNAi (Figs 18E and S5C,D). Interestingly, in the former case only the average dendrite length was upregulated. The other two dendritic parameters and the axonal ones were

unaffected (Figs 18D and S3B). Conversely, when *Foxg1* was knocked-down, the average dendrite length was reduced compared to wild type controls, as expected.

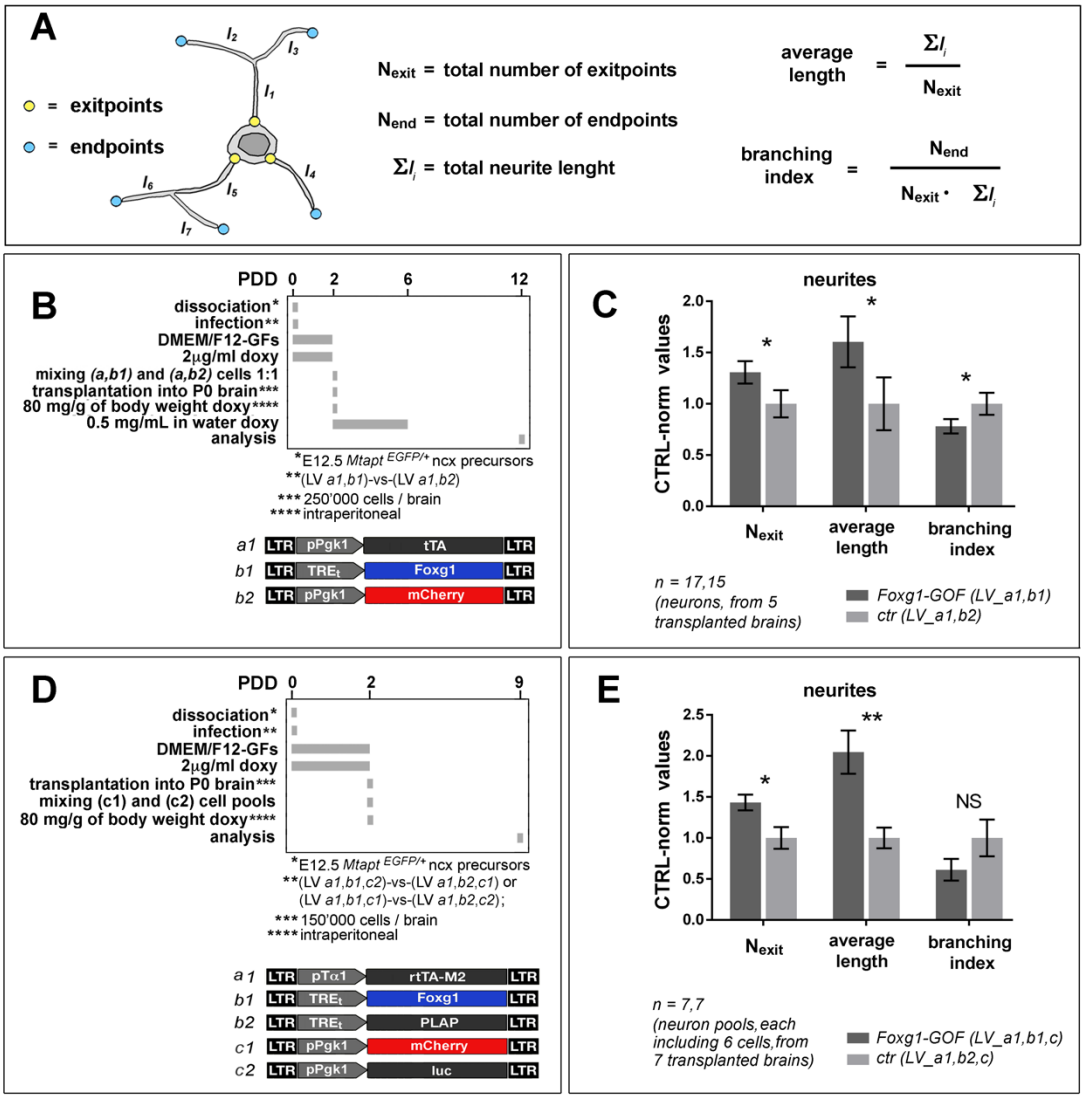

Figure 17. *In vivo* regulation of neurite morphology by *Foxg1*. (*A*) Definition of landmarks and parameters employed for neuronal morphometry. (*B*,*C*) Functional assessment of *Foxg1* impact on neurite morphology, upon co-transplantation of conditionally engineered neocortical precursors in wild type neonatal brains: gain-of-function (GOF), TetOFF assays, late transgene activation. In (*B*), protocol and materials, and in (*C*), control-normalized results. Absolute control values of exitpoints number, average neurite length and arborization index were 5.26, 35.40, µm and 5.9 x 10^{-2} μm^{-1}, respectively. (*D*,*E*) As in (*B*,*C*): GOF, TetON assays, early transgene activation. In (*D*) protocol and material, and in (*E*) control-normalized results. Absolute control values of exitpoints number, average neurite length and arborization index were 1.98, 24.20 µm and 2.60 μm^{-1}, respectively. Statistical significance of results evaluated by t-test (one-way, paired): *P < 0.05, **P < 0.01, ***P < 0.001. *n* is the number of statistical replicates, i.e., single unpaired neurons (*C*) and paired neuronal pools (*E*), evenly and randomly pooled from the indicated cotransplanted brains. PDD, post-dissociation days.

However, in such case, the branching indices, both dendritic and axonal, were reduced as well (Figs 18F and S3C). All these data suggest that, over a wide expression range surrounding the baseline, increasing *Foxg1* levels promote dendrite elongation. It also suggests that a branching-promoting activity exerted by *Foxg1* in physiological conditions may be artifactually reversed in dendrites by dominant negative mechanisms, upon pronounced gene upregulation.

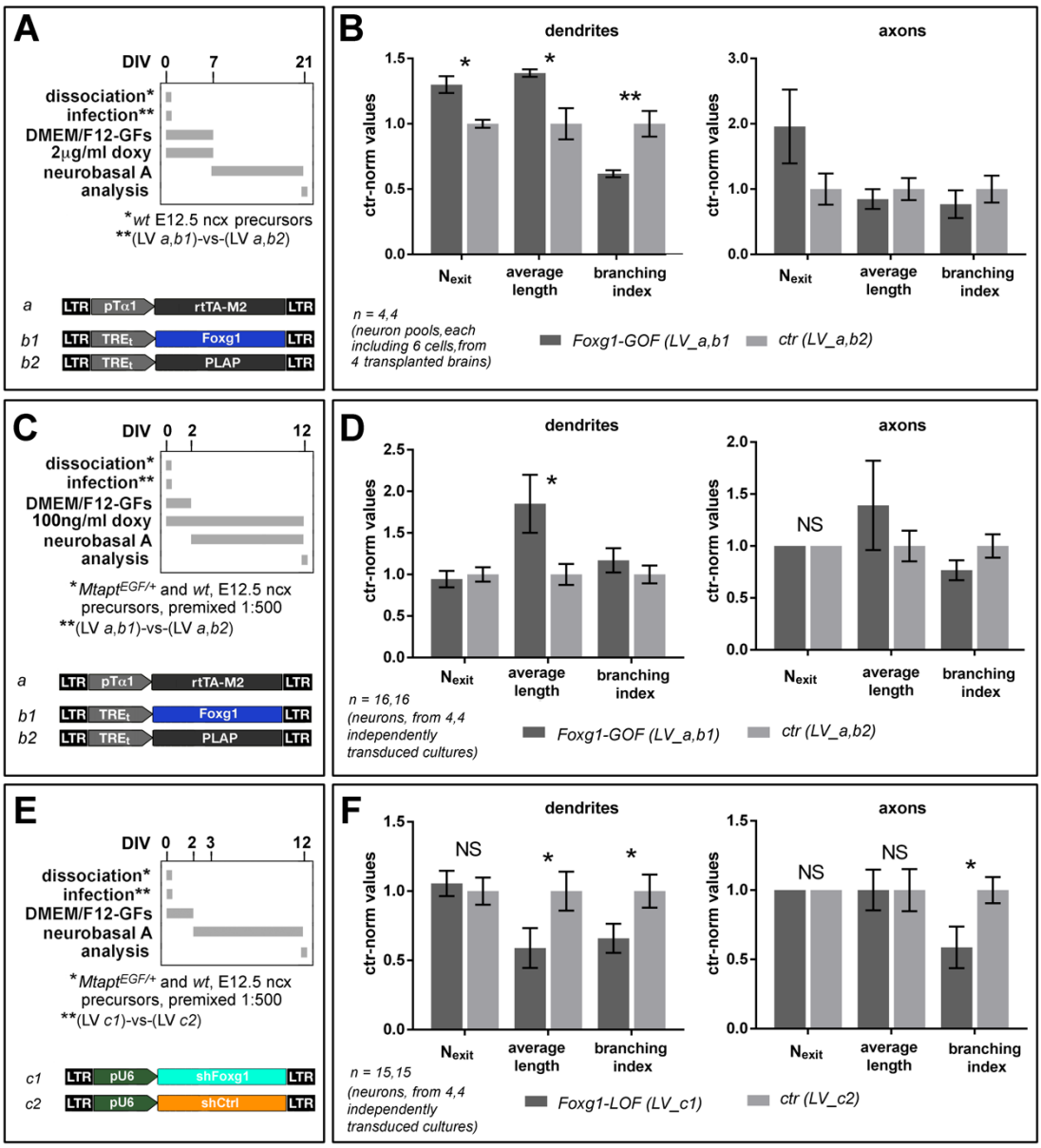

Figure 18. *In vitro* regulation of dendrite and axon morphology by *Foxg1*. Functional assessment of Foxg1 impact on dendrite and axon morphology, in cultured, engineered neocortical precursors. Landmarks and parameters employed for neuronal morphometry defined as in Figure 1A. (*A–D*) GOF, TetON assays: (*A*,*B*) high-level/early and (*C*,*D*) low-level/chronic transgene activation; (*A*,*C*) protocols and materials, (*B*,*D*) control-normalized results. As for (*B*) data, absolute control values of dendrite exitpoints number, average dendrite length and dendrite arborization index were 1.62, 38.55 μm and 0.93 × 10^{-2} $μm^{-1}$, respectively, absolute control values of axon exitpoints number, average axon length and axon arborization index were 1, 24.40 μm and 2.90 × 10^{-2} $μm^{-1}$, respectively. As for (*D*) data, absolute control values of dendrite exitpoints number, average dendrite length and dendrite arborization index were 6.75, 149.12 μm and 0.61 × 10^{-2} $μm^{-1}$, respectively, absolute control values of axon exitpoints number, average axon length and axon arborization index were 1, 639.40 μm and 3.14 × 10^{-2} $μm^{-1}$, respectively. (*E*,*F*) Loss of function (LOF), constitutive RNAi assays. (*E*) protocols and materials, (*F*) control-normalized data. As for (*F*) data, absolute control values of dendrite exitpoints number, average dendrite length and dendrite arborization index were 7.2, 275.32 μm and 0.89 × 10^{-2} $μm^{-1}$, respectively, absolute control values of axon exitpoints number, average axon length and axon arborization index were 1, 1404.13 μm and 3.02 × 10^{-2} $μm^{-1}$, respectively. Statistical significance of results evaluated by t-test (one-way, unpaired): *P < 0.05, **P < 0.01, ***P < 0.001. *n* is the number of statistical replicates, i.e., independently transduced cultures (*B*) or single neurons, evenly and randomly pooled from the indicated, independently transduced cultures (*D*,*F*).

Foxg1 dendritogenic activity does not subtend a neuronal identity shift

We wondered if the neuroarchitectural phenotype evoked by *Foxg1* could simply originate from a neuron identity change triggered by its overexpression.

It was previously shown that *FOXG1* overexpression is responsible for the overproduction of GABAergic neurons in human cerebral organoids originating from autistic patient iPSCs (Mariani et al. 2015). Based on previous unpublished data from our lab (Do DM PhD Thesis, Fig. 26), first we ruled out that *Foxg1* overexpression in murine neocortical precursors, according to the time schedule followed in our morphometric assays, could change the neurotransmitter phenotype of their derivatives, from glutamatergic to GABAergic.

Next, it was shown that decreased *Foxg1* levels in neocortical progenitors may reduce their UL neuron outputs (Siegenthaler et al. 2008) and it has been suggested that sustained *Foxg1* expression in newborn neurons may ease the activation of UL differentiation programs (Miyoshi and Fishell 2012). To rule out that the dendritic phenotype observed did not simply reflect an unbalanced laminar output of the engineered precursors, but it was due to a genuine pro-dendritogenic activity, as a proof-of-principle, we restricted dendrite morphometry to distinct neuronal populations, expressing the DL marker Ctip2 or not expressing it. Interestingly, both Ctip2^{+} and Ctip2^{-} *Foxg1*-GOF neurons showed an upregulation of their average dendrite length compared to their control counterparts (Figs 19A,B and S4), suggesting that *Foxg1* really promotes dendrite elongation, in both DL and UL neurons.

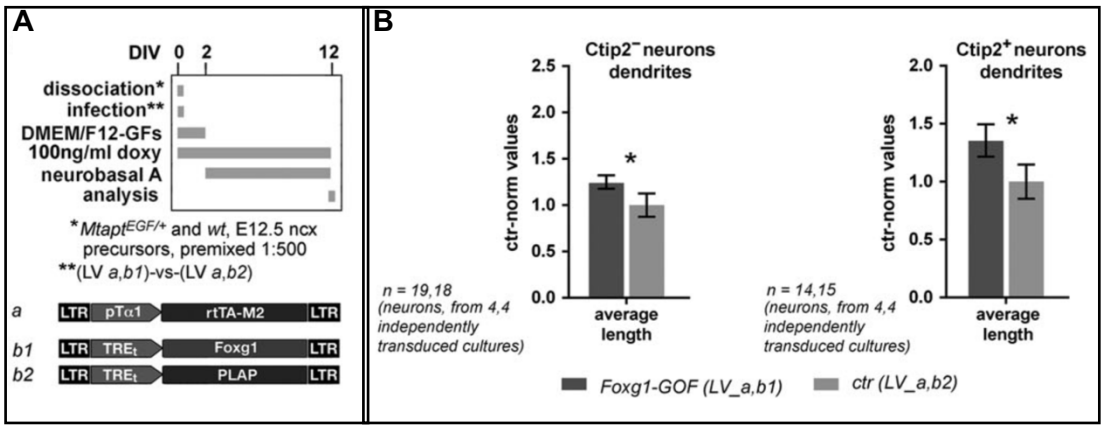

Figure 19. (*A*,*B*) Evaluation of average dendrite length restricted to Ctip2^{+} and Ctip2^{-} neurons. GOF, TetON assays, low-level/chronic transgene activation; (*A*) protocols and materials, (*B*) control-normalized results. As for (*H*) data, absolute control values of dendrite length were 86.48 µm and 137.79 µm, in case of Ctip2^{+} and Ctip2^{-} neurons, respectively. Statistical significance of results evaluated by t-test (one-way, unpaired): *P < 0.05, **P < 0.01, ***P < 0.001. *n* is the number of statistical replicates, i.e., independently single neurons, evenly and randomly pooled from the indicated, independently transduced cultures.

Potential mediators of *Foxg1* dendritogenic activity

To cast light on molecular mechanisms mediating the impact of *Foxg1* on neurite morphology, we selected a set of genes involved in neuritogenesis control and we evaluated their expression levels by qRT-PCR, in *Foxg1*-GOF and -LOF neocortical neurons (Fig. 20A,C). One of them, *Hes1*, promoting dendrite elongation (Salama-Cohen et al. 2005; Chacón and Rodríguez-Tébar 2012), was upregulated and downregulated in *Foxg1*-GOF and -LOF neurons, respectively (Fig. 20B,D). Two other genes, *Syt* and *Ndr1*, encoding for two inhibitors of dendrite elongation (Ultanir et al. 2012; Staahl et al. 2013), were downregulated in *Foxg1*-GOF neurons (Fig. 20B). Within *Foxg1*-LOF neurons, *Syt* displayed an opposite change and *Ndr1* was unaffected (Fig. 20D). All that suggests that: (1) *Hes1*, *Syt* and *Ndr1* modulation occurring in *Foxg1*-GOF cells genuinely reflects physiological regulation of these three genes by *Foxg1* and (2) such modulation may be instrumental in the dendritic overgrowth evoked by *Foxg1* overexpression.

Next, *NeuroD1*, a known promoter of dendritic outgrowth (Gaudillière et al. 2004; Gao et al. 2009), was downregulated in *Foxg1*-GOF cultures (Fig. 20B) and upregulated in *Foxg1*-LOF cultures (Fig. 20D), *Rnd2*, a key antagonizer of dendritic overgrowth (Heng et al. 2008), was conversely upregulated in both *Foxg1*-GOF and -LOF cells (Fig. 20B,D). That points to *Foxg1* as a natural inhibitor of *NeuroD1* and *Rnd2* expression, with a possible dominant negative suppression of *Rnd2* inhibition occurring in *Foxg1*-GOF cells. Obviously, as such, the modulation of *NeuroD1* and *Rnd2* mRNA levels taking place in *Foxg1*-GOF cultures could not contribute to the dendritic overgrowth evoked by *Foxg1* overexpression, which-rather-occurred despite it. Finally, *Ccd1*, previously linked to axonal morphology (Ikeuchi et al. 2009), was downregulated in *Foxg1*-GOF neurons (Fig. 20B,D). Collectively, these data suggest that the dendritic overgrowth we observed in *Foxg1*-GOF cultures could have arisen from *Hes1* upregulation and *Syt* and *Ndr1* downregulation, overwhelming functional consequences of depressed *NeuroD1* and increased *Rnd2* expression. Finally, we monitored nuclear levels of phospho-(S133)-Creb1 (pCreb1), a pleiotropic effector known to promote dendrite overgrowth (Redmond et al. 2002; Chen et al. 2005; Landeira et al. 2018) (Fig. 20E). For sake of specificity, this analysis was restricted to *Mtapt*$^{EGFP/+}$-positive neurons randomly chosen from cultures previously profiled for dendrite length (Fig. S6A–C). Nuclear pCreb1 levels turned out to be increased by about +70% ($P < 0.001$) in *Foxg1*-GOF neurons compared to controls (Fig. 20F). This points to pCreb1 as a further putative mediator of *Foxg1*-driven dendrite overgrowth.

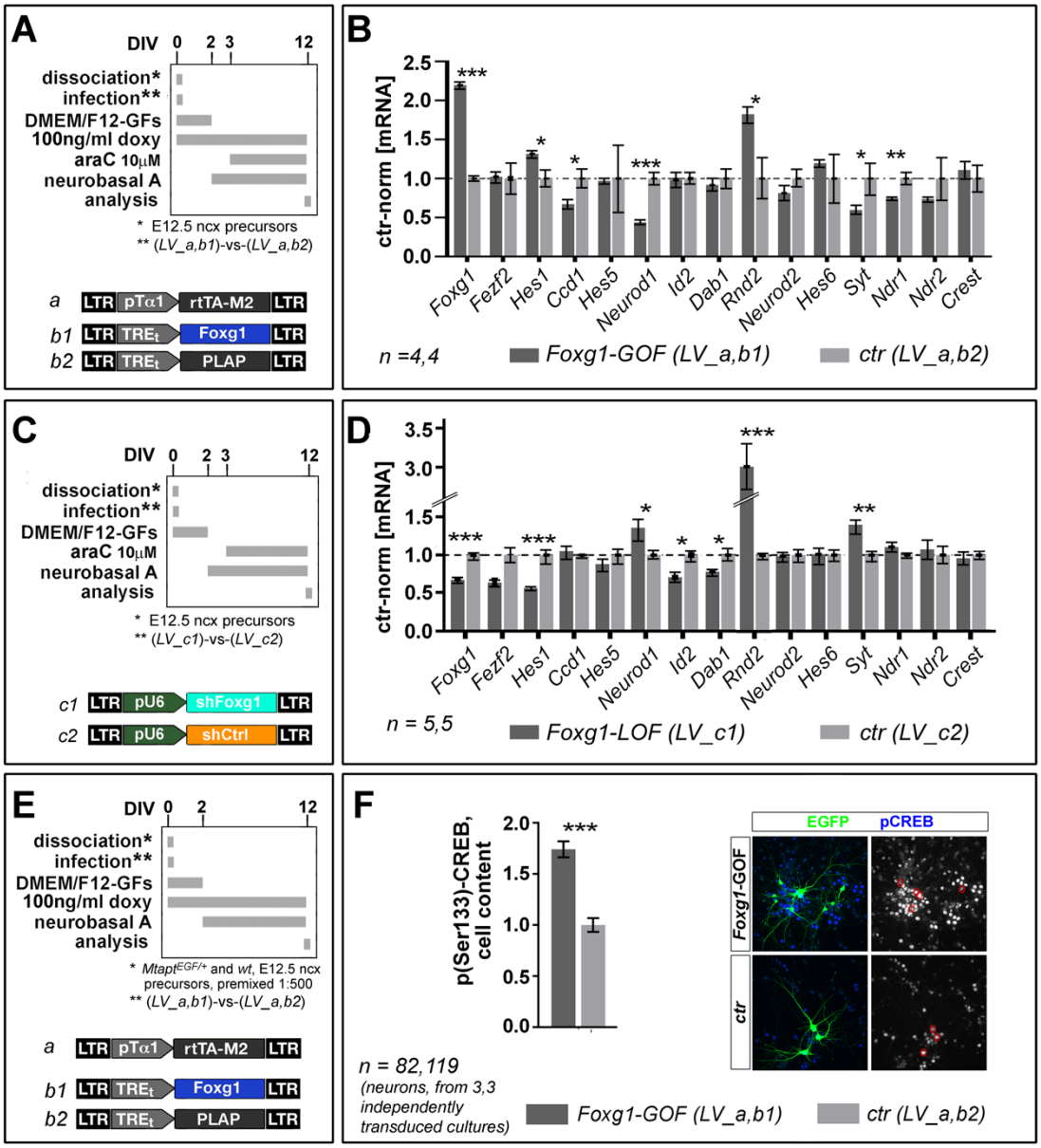

Figure 20. Hypothesis-driven, transcriptional profiling and pCreb1 immuno-scoring of necortical neurons with altered *Foxg1* expression levels. (*A*–*D*) qRT-PCR profiling of *Foxg1*-GOF (*A*,*B*) and *Foxg1*-LOF (*C*,*D*) neuronal cultures, for selected genes, putatively mediating *Foxg1* impact on neuronal morphology. (*E*,*F*) Immunofluorimetric evaluation of p(Ser133)-Creb1 levels in *Foxg1*-GOF neurons, randomly chosen from cultures previously profiled for dendritic morphometry (as shown in Fig. S6). In (*A*,*C*,*E*) protocols and materials, and in (*B*,*D*,*F*) results, respectively. Statistical significance of results evaluated by t-test (one-way, unpaired): *P < 0.05, **P < 0.01, ***P < 0.001. *n* is the number of statistical replicates. These replicates are: independently transduced neuronal cultures in case of (*A*–*D*), and single neurons, evenly taken from independently transduced cultures in case of (*E*,*F*).

Upregulation of *Hes1* and pCreb1 and downregulation of *Syt* and *Ndr1* mediate *Foxg1* dendritogenic activity

To assess the relevance of *Hes1* arousal to *Foxg1*-dependent dendrite elongation, we counteracted *Hes1* upregulation evoked by *Foxg1* via RNAi and assayed cytoarchitectonic consequences of that (Fig. 21A). Interestingly, *Hes1* RNAi fully abolished dendrite overgrowth promoted by *Foxg1*, while not affecting dendrite length in control neurons (Figs 21B and S8A). Consistently, a suppression of *Foxg1*-dependent dendrite overgrowth was also observed upon overexpression of *Hes6*, a natural dominant negative antagonist of *Hes1* function (Fig. S7A,B,D). Finally, *Hes1* upregulation phenocopied *Foxg1* overexpression (Figs 21A,C and S8B). All that suggests that *Hes1* knock-down abolishes a key molecular event linking *Foxg1* upregulation to dendrite overgrowth.

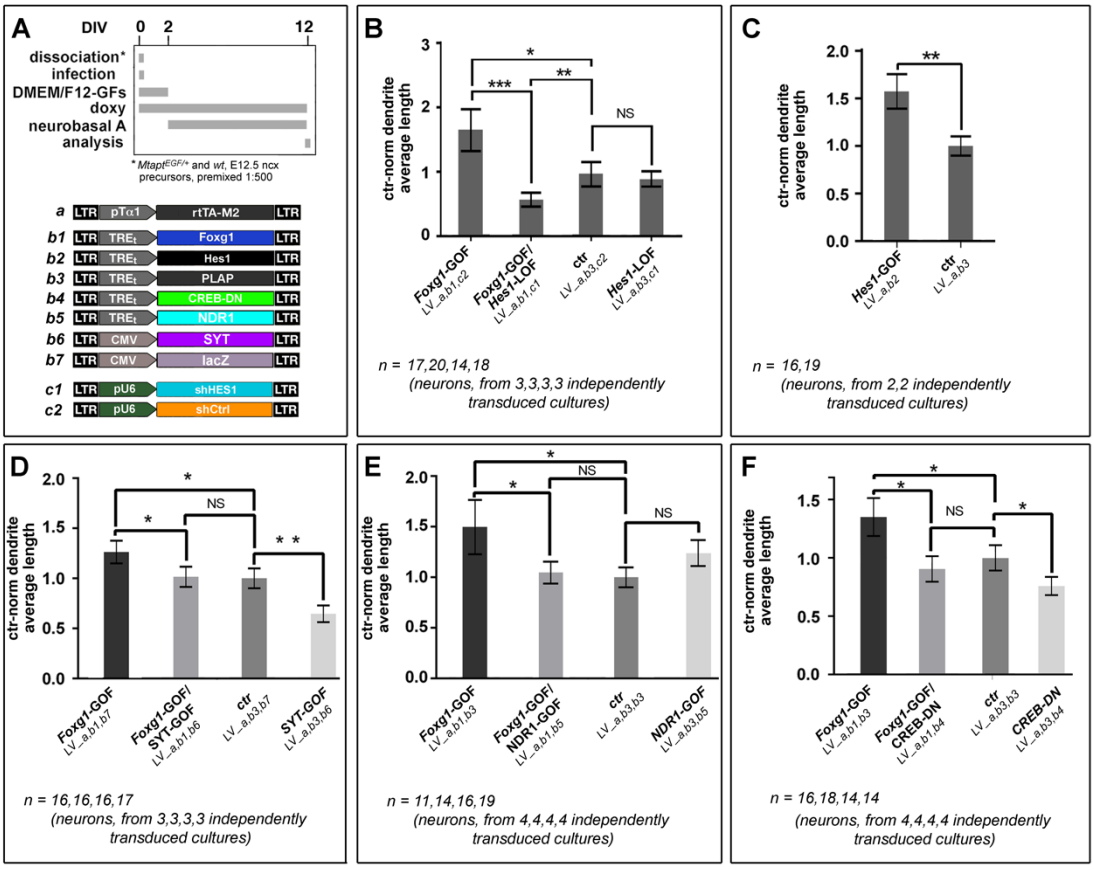

Figure 21. *Foxg1* stimulates dendrite elongation via *Hes1* and pCreb1 upregulation as well as *Ndr1* and *Syt* downregulation. (*A*) Experimental protocols and materials employed for functional validation of *Hes1*, *Ndr1*, *Syt*, and pCreb1 as mediators of pro-dendritogentic activity of *Foxg1*. These include, lentiviral sets "a" and "b1–b5", for neuron-restricted overexpression of *Foxg1*, *Hes1*, Creb-DN, and *NDR1*, "b6,7", for constitutive overexpression of *SYT*, and "c1,2" for constitutive *Hes1* RNAi. Landmarks and parameters employed for neuronal morphometry defined as in Figure 1A. TetON transgene activation was generally elicited by 100 ng/mL doxycycline; only in case of Creb-DN, doxycycline concentration was lowered to 60 ng/mL. (*B*,*C*) Assessment of *Hes1* requirement for *Foxg1*-dependent dendrite elongation (*B*) and intrinsic *Hes1* ability to elicit this effect (*C*). (*D*,*E*) Assessment of *Syt* and *Ndr1* requirement for *Foxg1*-dependent dendrite elongation. (*F*) Assessment of pCreb1 requirement for *Foxg1*-dependent dendrite elongation. Thoughout Figure 21, results shown as control-normalized values. Absolute average values of control dendrite length were 166.03 µm (*B*), 178.13 µm (*C*), 139.82 µm (*D*), 125.06 µm (*E*), and 128.65 µm (*F*). Statistical significance of results evaluated by t-test (one-way, unpaired): *P < 0.05, **P < 0.01, ***P < 0.001. *n* is the number of

statistical replicates. These replicates are single neurons evenly taken from independently transduced cultures. Finally, statistical significance of interaction among *Foxg1* and candidate mediators of its activity, evaluated by two-ways ANOVA, was as follows: $p_{(Foxg1,Hes1)} < 0.01$; $p_{(Foxg1,SYT)} < 0.28$; $p_{(Foxg1,NDR1)} < 0.03$; $p_{(Foxg1,pCreb1)} < 0.28$.

Next, we assessed functional relevance of *Syt* and *Ndr1* decrease to *Foxg1*-dependent dendrite elongation. To this aim, we counteracted *Foxg1*-dependent *Syt* and *Ndr1* downregulation by delivering a *Syt* or an *NDR1* transgene to engineered *Foxg1*-GOF neurons (Fig. 21A). Interestingly, these manipulations abolished dendritic elongation elicited by *Foxg1* overexpression (Figs 21A,D,E and S9A,B), pointing to an implication of *Syt* and *Ndr1* in this phenomenon. Finally, to assess pCreb1 implication in *Foxg1* dendritogenic activity, we overexpressed a dominant negative variant of this protein (Creb-DN) in *Foxg1*-GOF cultures, by lentiviral/TetON technology, and monitored the impact of this manipulation on dendrite length. As neuronal cultures hardly tolerated chronic, sustained expression of Creb-DN (not shown), we reduced levels of doxycycline to about 60ng/mL, so limiting the overexpression of both *Foxg1* and Creb-DN (Fig. 21A). Even in these conditions, *Foxg1* caused an appreciable dendritic overgrowth (Fig. 21F, S10A). Interestingly, this effect was fully abolished upon Creb-DN co-expression, pointing to an involvement of pCreb1 in the execution of the dendritogenic program ruled by *Foxg1* (Fig. 21F).

Pleiotropic *Foxg1* impact on *Hes1* and pCreb1 levels

Concerning mechanisms mediating *Foxg1*-dependent *Hes1* upregulation, we first wondered if canonical Notch signaling might be involved. As knock-down of this pathway by a dominant negative variant of Mastermind-like1 (*Maml1*-DN) did not rescue *Foxg1*-dependent dendrite overgrowth (Fig. S7A,C,D), we discarded this hypothesis.

Second, we supposed that *Foxg1* might straightly transactivate *Hes1*. To address this issue, we inspected the *Hes1* locus for putative *Foxg1*-binding sites (BSs), by Jaspar software (Mathelier et al. 2014). We found 8 high-score hits, we named J1 to J8, in the 5′-to-3′ order (Fig. 22A). We monitored *Foxg1* recruitment to genomic regions including these sites, in *Foxg1*-GOF and control neocortical neurons, by Chromatin Immuno-precipitation (ChIP)-qPCR (Fig. 22B). In 4 cases out of 8 (J2, J5, J6, and J8), the ChIP-qPCR signal was upregulated in *Foxg1*-GOF samples versus wild type controls (Fig. 22B,C), so corroborating Jaspar predictions. Two of these elements, J2 and J5, were cloned in a firefly luciferase reporter plasmid (Fig. 22D), and, upon transfection of the resulting construct in *Foxg1*-GOF neurons, one of them, J2, gave rise to a stronger *luc* signal compared to controls (Fig. 22E). This suggests that *Foxg1* can straightly transactivate *Hes1* in postmitotic neurons.

Third, we hypothesized that additional indirect mechanisms could contribute to *Foxg1*-dependent *Hes1* upregulation. Specifically, we suspected that *Nfia* and

Sirt1 could be implicated. In fact, *Nfia* is expressed by postmitotic neocortical neurons (http://developingmouse.brain-map.org) and it was shown to trans-represses *Hes1* in HEK293 cells (Piper et al. 2010). *Sirt1* displaces pCreb1 from the *Hes1* promoter, so dampening *Hes1* transcription (Fusco et al. 2016). As expected, we found that *Nfia* was downregulated and upregulated in *Foxg1*-GOF and *Foxg1*-LOF neurons, respectively (Fig. 22F–H). Moreover, the transduction of an *Nfia* transgene into *Foxg1*-GOF neurons restored normal *Hes1*-mRNA levels (Fig. 22F,I). That suggests that upregulation of *Hes1* occurring upon *Foxg1* overexpression is further enhanced by *Foxg1*-dependent suppression of the *Nfia*-mediated negative feedback, which normally limits *Hes1* expression (Piper et al. 2010). Next, we found that *Sirt1* was downregulated in *Foxg1*-GOF neurons too (Fig. 22G). Together with previously shown *Foxg1*-driven pCreb1 upregulation, this phenomenon may lead to preferential pCreb1 vs Sirt1 recruitment to *Hes1* promoter, further contributing to *Hes1* upregulation and dendrite overgrowth.

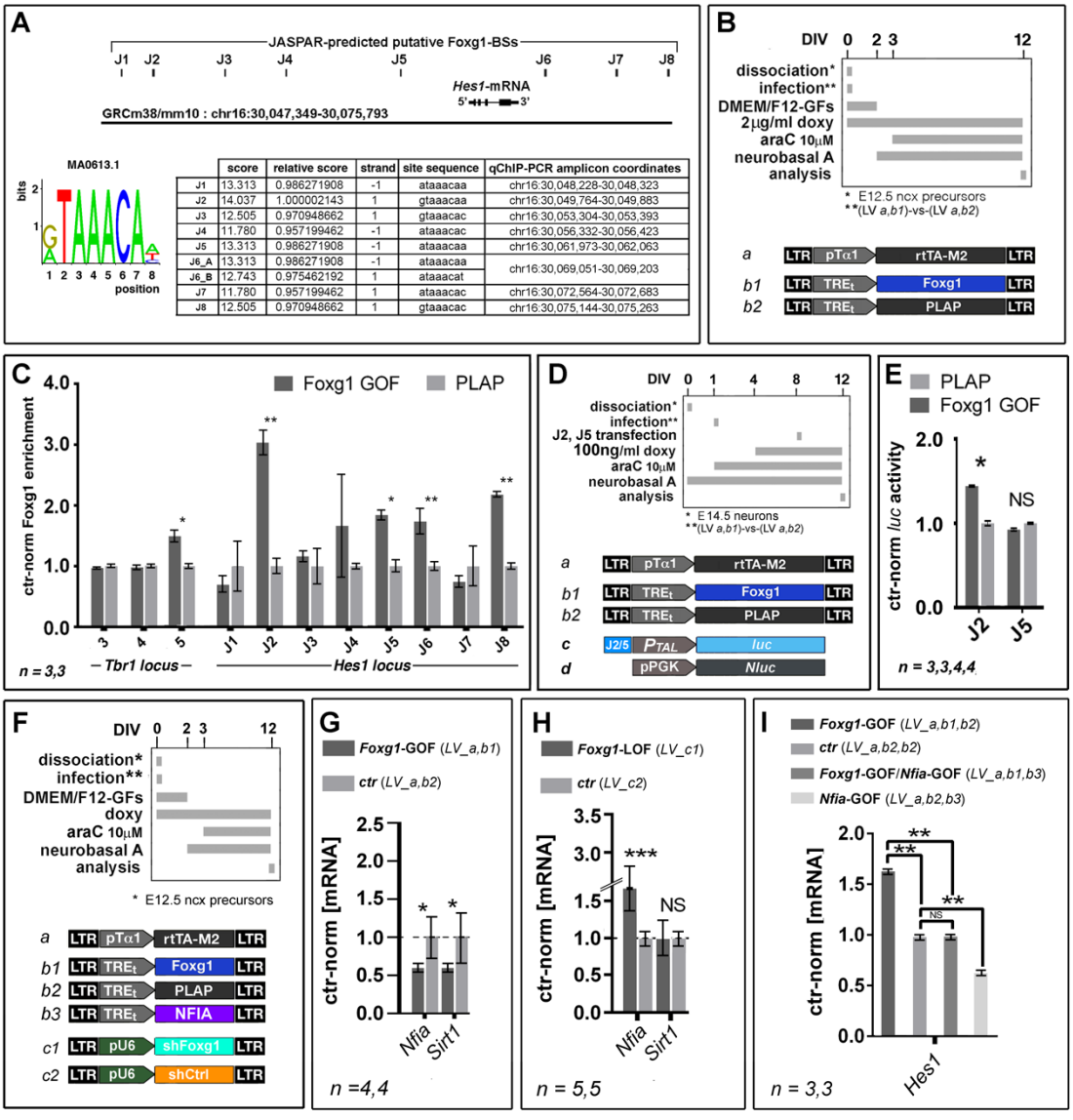

Figure 22. Molecular mechanisms mediating *Foxg1*-dependent *Hes1* control. (*A*) *In silico* scanning of the *Hes1* locus for putative *Foxg1*-binding sites (BSs), by Jaspar software. Top, genomic location of *Hes1*_J1–J8 putative BSs. Bottom

left, MA0613.1 consensus Foxg1-BS. Bottom right, key features of *Hes1*_J1–J8 and genomic coordinates of diagnostic amplicons (including BSs), used for their qChIP-PCR validation. (*B*,*C*) Quantitative Chromatin Immuno Precipitation-PCR (qChIP-PCR) evaluation of *Hes1*_J1–J8 BSs for differential *Foxg1*-enrichment: protocol (*B*) and results (*C*). Here, presumptive Foxg1-BSs of the *Tbr1* locus were also scanned, as positive controls, however only one of them gave a statistically significant signal (*Tbr1*_BS.5). Key features of these Tbr1 locus Foxg1-BSs are listed in Supplementary Table 1. (*D*,*E*) Evaluation of *Foxg1* level-sensitive, cis-activation abilities of *Hes1*_J2 and _J5 by a Dual-Glo® Luciferase Assay in primary neocortical cultures: protocol (*D*) and results (*E*). (*F–I*) *Nfia* and *Sirt1* implication in *Foxg1*-dependent upregulation of *Hes1*: protocol (*F*), *Nfia* and *Sirt1* responsivity to *Foxg1* expression levels (*G*,*H*), and rescue of *Foxg1*-induced *Hes1* upregulation by *Nfia* overexpression (*I*). Thoughout Figure 22, results shown as control-normalized values. Statistical significance of results evaluated by t-test (one- way, unpaired): *P < 0.05, **P < 0.01, ***P < 0.001. *n* is the number of statistical replicates. These replicates are neuronal cultures.

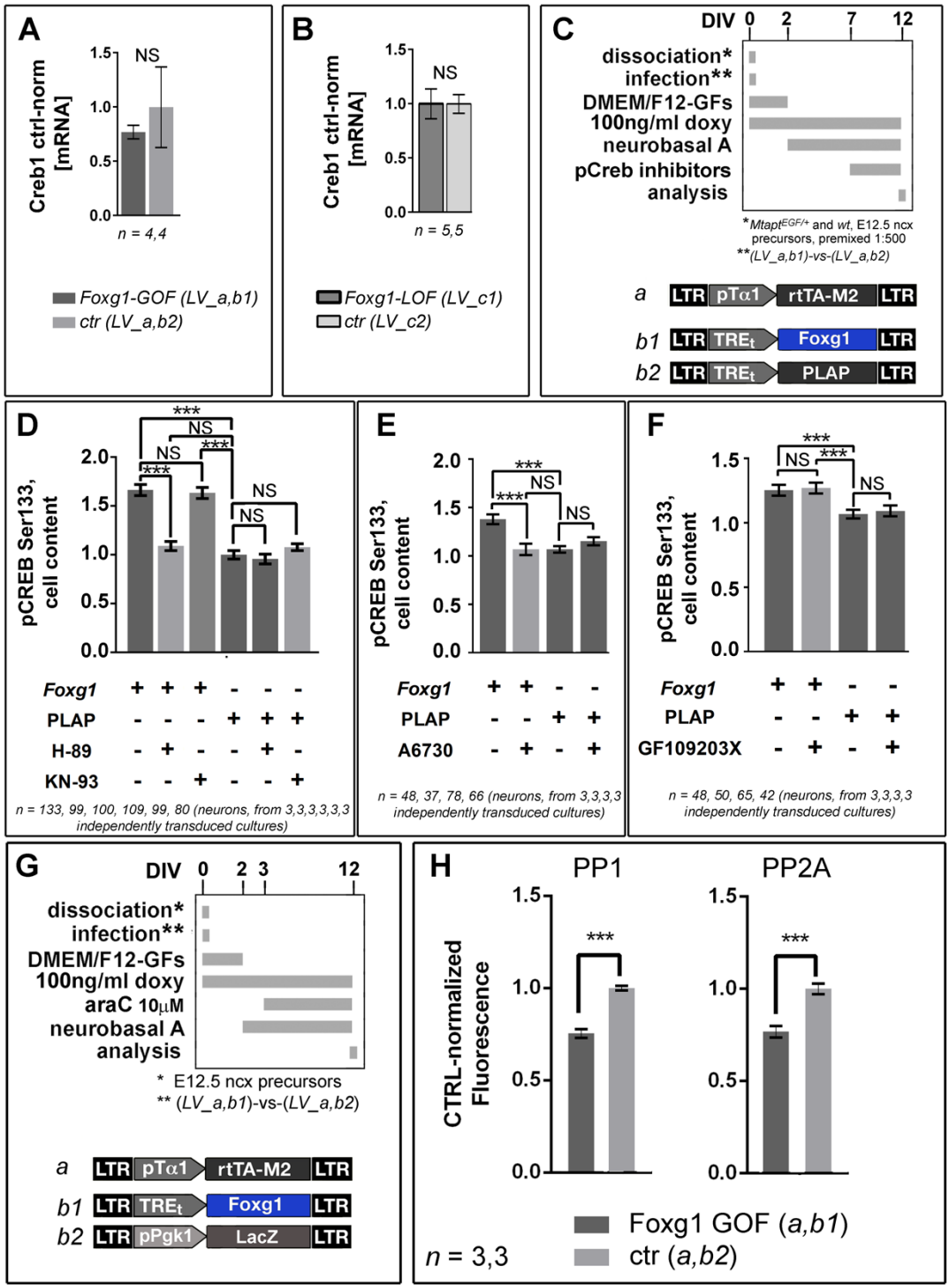

Figure 23. Molecular mechanisms underlying *Foxg1*-dependent pCreb1 control. (*A*,*B*) *Creb1*-mRNA levels in neuronal cultures GOF and LOF for *Foxg1*. Protocols and materials as in Figure 20A,C. (*C–F*) Assessment of PKA, CaMKII&IV, AKT and PKC requirement for *Foxg1*-driven pCreb1 upregulation: protocol (*C*) and results (*D–F*). Here, these kinases

were pharmacologically inhibited by 10 µM H-89, 2 µM KN-93, 5 µM A6730, and 1 µM GF109203X, respectively, and pCreb1 levels were evaluated by quantitative immunofluorescence. (*G*,*H*) *Foxg1*-dependent down-regulation of PP1 and PP2A activities required for pCreb1 dephosphorylation: protocol (*G*) and results (*H*). Here, phosphatase activity was inferred on the basis of DiFMUP fluorescence, as evaluated by RediPlate^{TM} 96 EnzChek^{TM} Serine/Threonine Phosphatase Assay Kit. Throughout Figure 23, results shown as control-normalized values. Statistical significance of results evaluated by t-test (one-way, unpaired): *P < 0.05, **P < 0.01, ***P < 0.001. *n* is the number of statistical replicates. These replicates are: single neurons evenly taken from independently transduced cultures in case of (*D*–*F*); independently transduced neuronal cultures in case of (*A*,*B*,*H*).

Concerning mechanisms mediating *Foxg1*-driven pCreb1 upregulation, we wondered if *Foxg1* might straightly transactivate *Creb1*. This prediction turned out to be wrong (Fig. 23A,B). Therefore, we hypothesized that *Foxg1* might rather impact pCreb1 levels by affecting the S133-phosphorylation rate of Creb1.

Interestingly, we found that pharmacological inhibition of PKA and PKB/AKT, two key mediators of this phosphorylation in postmitotic neurons (Chen et al. 2005; Landeira et al. 2018), by H-89 and A-6730, respectively, abolished *Foxg1*-dependent pCreb1 upregulation, while not affecting pCreb1 levels in control neurons (Fig. 23C–E). No effect was conversely elicited by inhibition of other serine kinases implicated in neuronal Creb1 phosphorylation, CaMKII & IV (Redmond et al. 2002) and PKC (Valerio et al. 2006), by KN-93 and GF209103X, respectively (Fig. 23C,D,F).

Next, we found that *Foxg1* overexpression also reduced the activity of the two major phosphatases involved in pCreb1 dephosphorylation, PP1 and PP2A (Sakamoto et al. 2011) (Fig. 23G,H).

Altogether, these data *prove* that Foxg1 specifically promotes Creb1 phosphorylation via PKA and PKB and *suggest* that a Foxg1-driven decrease of PP1 and PP2A may further contribute to pCreb1 upregulation.

Mutual epistatic relationships among mediators of *Foxg1* dendritogenic activity

To cast light on molecular articulation of the functional cascade triggered by *Foxg1* which promotes dendrite elongation, we upregulated *Hes1* in wild type neocortical neurons and monitored consequences of that on pCreb1, *Foxg1*, *Ndr1*, and *Syt* (Fig. 24A). We detected an increase of pCreb1, consistent with an implication of it in *Hes1* dendritogenic activity (Fig. 24B). We also found a downregulation of *Foxg1*-mRNA and an upregulation of *Syt*-mRNA, possibly limiting such activity. [*Ndr1*-mRNA was unaffected and endogenous *Hes1*-mRNA was dampened, as expected (Takebayashi et al. 1994; Hirata et al. 2002)] (Fig. 24D).

Next, we reduced pCreb1 signaling by Creb-DN delivery and monitored *Syt* and *Ndr1* mRNA levels (Fig. 24E). We found an upregulation of both (Fig. 24F),

suggesting that the pCreb1 impact on dendritogenesis may be mediated to some extent by repression of these two genes.

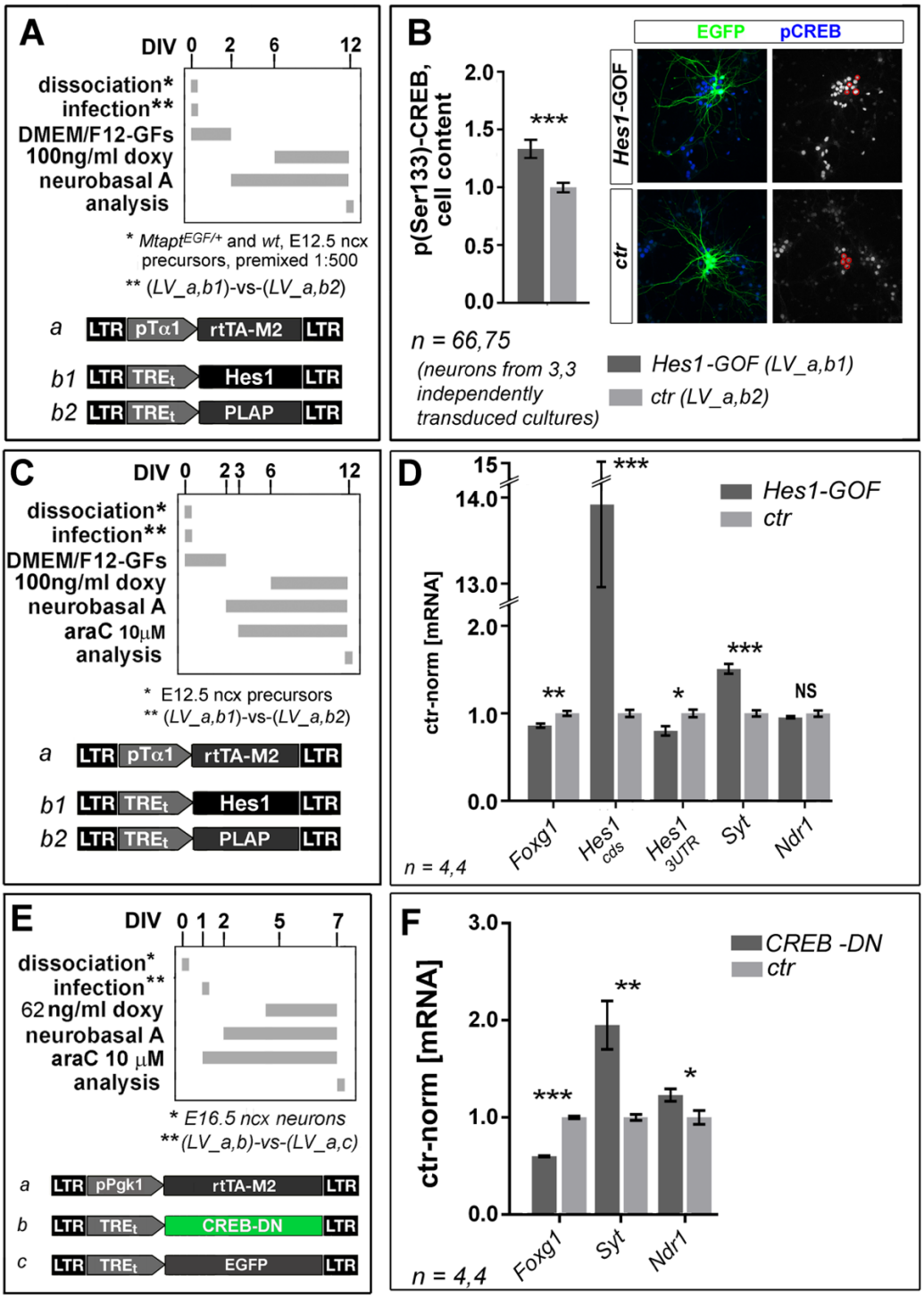

Figure 24. Epistatic relationships among *Foxg1*, *Hes1*, *Syt*, *Ndr1* and pCreb1. (*A*,*B*) Immunofluorimetric evaluation of p(Ser133)-Creb1 levels in randomly chosen, *Hes1*-GOF neurons. (*C*–*F*) qRTPCR evaluation of *Foxg1*, *Hes1*, *Syt* and *Ndr1* mRNA levels upon *Hes1* overexpression (*C*,*D*) and functional inactivation of Creb1 (*E*,*F*). In (*A*,*C*,*E*) protocols and materials. In (*B*,*D*,*F*) control-normalized results. Statistical significance evaluated by t-test (one-way, unpaired): *P < 0.05, **P < 0.01, ***P < 0.001. *n* is the number of statistical replicates. These replicates are: single neurons evenly taken from the indicated, independently transduced cultures in case of (*B*); neuronal cultures in case of (*D*,*F*).

DISCUSSION

Here, by means of lentivector-mediated, gain- and loss-of- function (GOF and LOF) manipulation of *Foxg1* expression levels in neocortical projection neurons, we found that this gene robustly promotes dendrite elongation, *in vitro* as well as *in vivo* (Figs 17 and 18).

We profiled engineered neurons for selected effectors controlling dendrite morphology and we identified four putative mediators of this activity, *Hes1*, *Syt*, *Ndr1*, and pCreb1 (Fig. 20). Counteracting changes of their expression levels elicited by *Foxg1* abolished *Foxg1*-dependent dendritic overgrowth (Fig. 21). Moreover, *Hes1* overexpression recapitulated *per se* the dendritic *Foxg1*-GOF phenotype (Fig. 21). All that confirms functional involvement of these effectors in *Foxg1* control of neurite morphology and points to *Hes1* as a key mediator of it.

We investigated functional relationships among these effectors. We found that:
(a) *Foxg1* promotes expression of *Hes1* by directly transactivating it and downregulating *Nfia* and *Sirt1*, which normally mediate negative feedbacks limiting its expression (Fig. 22 and Fusco et al. 2016);
(b) *Foxg1*-dependent Creb1 phosphorylation requires PKA and AKT kinases and is possibly enhanced by the decline of PP1 and PP2A phosphatase activities occurring in *Foxg1*-GOF neurons (Fig. 23);
(c) *Hes1* overexpression upregulates pCreb1 (Fig. 24A,B);
(d) functional knock-down of pCreb1 leads to an upregulation of *Syt* and *Ndr1* as well as to a decline of *Foxg1* (Fig. 24E,F).
Based on this, we proposed a tentative cascade connecting *Foxg1* to downstream effectors of its dendritogenic activity (Fig. 25A,B). Remarkably, we also found that, in addition to its impact on pCreb1, *Hes1* upregulates *Syt* while dampening *Foxg1* (Fig. 24C,D). This further suggests that dedicated homeostatic mechanisms mediated by *Hes1* limit the impact of *Foxg1* overexpression on dendrite elongation (Fig. 25C).

Hes1 implication in pro-dendritogenic *Foxg1* activity adds to a large body of literature, on dendritogenesis control by Notch signaling machinery, in dentate gyrus, CA fields and neocortex. Contrasting effects of this machinery (Sestan et al. 1999; Redmond et al. 2000; Breunig et al. 2007; Bonini et al. 2011) are elicited by two key effectors of it, Notch1-4 Intra-Cytoplasmic Domains (NICD1-4) and *Hes1*,*5*. Notch proteins prevent neuronogenesis progression through *Hes1* and *Hes5* stimulation (Ohtsuka et al. 1999) and inhibit the pro-dendritogenic Creb1 activity via straight protein–protein interaction (Hallaq et al. 2015). Within neurons, *Hes1* and *Hes5* sustain dendritogenesis, regardless of the pathway stimulating their transcription (Salama-Cohen et al. 2005; Chacón and Rodríguez-Tébar 2012; Osorio et al. 2013).

Here we confirmed *Hes1* capability to stimulate dendrite elongation (Fig. 21C). This capability was particularly prominent, as *Hes1* impact on dendrite elongation largely overwhelmed the effect of other *Foxg1*-induced gene fluctuations exerting an opposite effect on this process (Gaudillière et al. 2004; Heng et al. 2008) (Figs 20B and 21B). Robustly and specifically upregulated by *Foxg1* in intermitotic progenitors (Brancaccio et al. 2010) as in postmitotic neurons (Fig. S13), *Hes1* could prime dendrite elongation prior to neuronal birth and sustain it after neuron exit from cell cycle.

pCreb1, already detectable in periventricular neuronogenic layers of the embryonic cortex (Dworkin et al. 2009), is transiently upregulated in newborn neurons lacking spontaneous electrical activity (Landeira et al. 2018). Later, it is expressed in more mature neurons along a sparse pattern reflecting their activity (Redmond et al. 2002). Among its pleiotropic neuronal functions, pCreb1 robustly stimulates dendrite development (Redmond et al. 2002; Chen et al. 2005; Landeira et al. 2018), acting as a hub which integrates a number of different molecular cues and convey them to dendritogenesis control. Specifically, its levels reflect CaMKIIa, PKA and PKB/AKT activity in newborn neurons (Landeira et al. 2018), CaMKIV and PKA/PKG-Rap1-Mek-Erk signaling in more mature neurons (Redmond et al. 2002; Chen et al. 2005) and are limited by PP1 and PP2A (Sakamoto et al. 2011).

We found *Foxg1* and *Hes1* both upregulate pCreb1 (Figs 20F and 24B) and stimulate dendrite overgrowth (Figs 17, 18 and 21C). Moreover, pCreb1 increase - dependent on PKA and AKT (Fig. 23D,E) and possibly sustained by *Foxg1*-dependent PP1 and PP2A depression (Fig. 23H) - was needed for *Foxg1*-driven dendrite elongation (Fig. 21F). It is tempting to speculate that, promoted by *Foxg1* via a direct and an indirect pathway (Figs 20B,D and 22), Hes1 may act as a functional bridge connecting *Foxg1* to the ultimate dendritogenesis promoter, pCreb1.

In sum, building on previous knowledge of molecular tuning of dendritogenesis, we have found a cascade promoting dendrite elongation, active within neocortical projection neurons, including *Foxg1*, *Hes1* and pCreb1, which is tempered by *Hes1*-to-*Foxg1* negative feedback and *Hes1*-dependent *Syt* upregulation (Fig. 25A,B). Moreover, we showed that *Foxg1* directly inhibits two negative modulators of *Hes1* transcription, *Nfia* and *Sirt1*, possibly exacerbating *Hes1* transcriptional activation controlled by *Foxg1* itself (Fig 25A). This cascade may repress dendritogenesis antagonizers still active in immature neurons, such as *Syt* and *Ndr1* (Fig 25A), and overwhelm the decline of later dendritogenic effectors downregulated by *Foxg1*, such as *NeuroD1*, ultimately resulting in dendrite elongation.

Concerning the biological meaning of Foxg1 regulation of dendritogenesis, three considerations are in order.

First, a positive impact of *Foxg1* on dendrite elongation was detectable regardless of the transgene activation schedule, restricted to immature neural progenitors or including more advanced neuronal precursors (Fig. 17 and 18). This suggests that *Foxg1* may normally prime dendrite elongation in proliferating progenitors and further sustain this process, after its reactivation associated to neuronal exit from the multipolar stage (Miyoshi and Fishell 2012).

Second, the dendritogenic activity of *Foxg1* was evident even after small shifts of its mRNA levels around the baseline (Figs 17 and 18), of a magnitude comparable with fluctuations evoked by neuronal depolarization (Fimiani et al. 2016). This indicates that modulation of *Foxg1* expression associated to neuronal activity can contribute to physiological neuroarchitectural tuning.

Third, as a consequence of such neuroarchitecture sensitivity to Foxg1 levels, an anomalous enlargement of the dendritic tree might take place in West syndrome patients with a supranumerary *FOXG1* allele, concurring to their hypsarrhytmic abnormalities (Korff and Nordli 2006; Striano et al. 2011; Tohyama et al. 2011; Pontrelli et al. 2014). In this respect, the increase of dendritic spine density triggered by *Foxg1* overexpression (as described in Lucy Centrone's Master Thesis and shown in Fig. S12) might further enhance functional consequences of this phenomenon.

In conclusion, *Foxg1*, modulated in both neocortical primordium (Miyoshi and Fishell 2012) and its postnatal derivatives (Fimiani et al. 2016), may act as a key hub, which integrates neurodevelopmental and plasticity-linked cues and conveys them to neurocircuital tuning of pyramidal neurons. Any change of its copy number can dramatically twist molecular computation subtended by this integration, resulting in severe perturbation of neuronal functional regime.

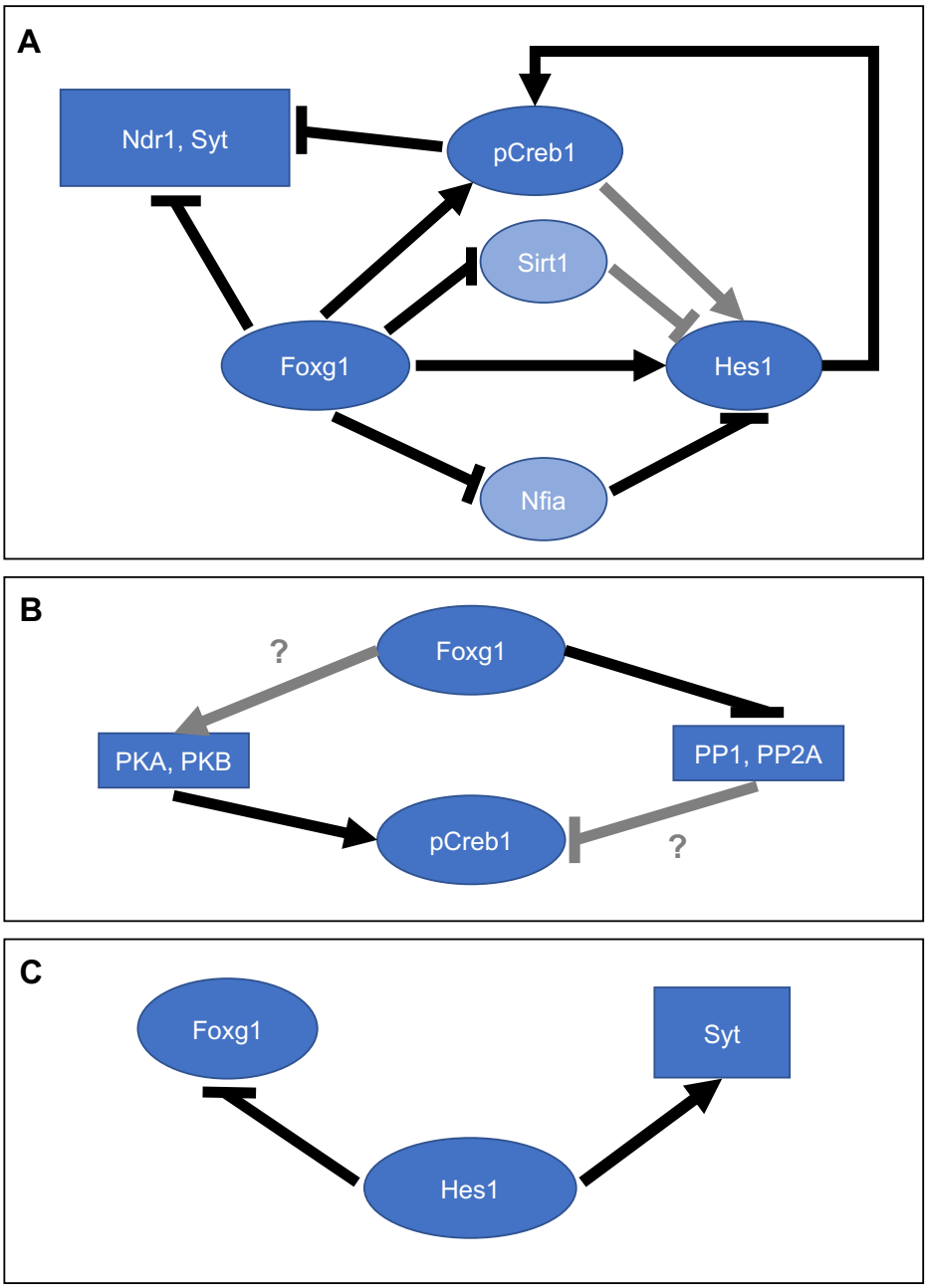

Figure 25. Schematic representation of the pro- and anti-dendritogenic cascades. *(A)* A synopsis of the epistatic relationships involving effectors of the Foxg1-driven cascade promoting dendrite overgrowth, as inferred on the basis of Figures 20–24 primary data. In case of grey arrow, the relationship was not directly tested but it was inferred from literature. *(B)* A synopsis of the epistatic relationships involving *Foxg1* and pCreb1 via kinases and phosphatases differential modulation. In case of grey arrows with question marks, the interactions were not directly tested and are supposed here to be direct rather than indirect. *(C)* A synopsis of the epistatic relationships involving putative effectors of the Hes1-driven cascade antagonizing dendrite overgrowth, as inferred on the basis of Figures 24 primary data.

APPENDIX

Can we employ *Foxg1* upregulation to fix dendritic defects peculiar to *Foxg1*-haploinsufficient neurons?

Upon having assessed the impact of *Foxg1* on dendrite growth in immature neuronal precursors, we wondered if a *Foxg1*-encoding transgene could repair the dendritic deficits peculiar to *Foxg1*$^{+/-}$ murine neocortical tissue (Fig. 26B), as a therapeutic model for Rett-like syndrome occurring in *Foxg1*-haploinsufficient patients. To this aim, we overexpressed *Foxg1* in *Foxg1*$^{+/-}$ (and wild type, as a control) postmitotic neuronal cultures. Similar to Fig. 18, to ease morphometric profiling, these cultures included "green" *Mtapt*$^{EGFP/+}$ and "black" *Mtapt*$^{+/+}$" elements, at 1:500 ratio (Fig. 26B). Unexpectedly, we found a decrease of average dendrite length in both *Foxg1*$^{+/+}$ and *Foxg1*$^{+/-}$ neurons expressing the exogenous *Foxg1* transgene, with a more prominent effect in *Foxg1*$^{+/-}$ neurons (Fig. 26B).

We speculated that this might originate from the inability of *post-mitotic Foxg1*-transgene activation to reproduce key features of the pro-dendritogenic molecular cascade triggered by *intermitotic* transgene activation. We focused our attention on inhibitors of dendrite elongation *Syt* and *Ndr1* (Ultanir et al. 2012; Staahl et al. 2013). We monitored their expression in wild type neurons made *Foxg1*-GOF and -LOF, via postmitotic lentiviral manipulations (Fig. 26 C-F). We found that *Syt* was upregulated in *Foxg1*-GOF neurons and not affected in *Foxg1*-LOF neurons (Fig. 26D). *Ndr1* did not respond to *Foxg1* level manipulations at all (Fig. 25D,F).

Next, we hypothesized that *Syt* upregulation could account for the anti-dendritogenic activity elicited by late *Foxg1* upregulation. To test this hypothesis, first we monitored dendritic length in wild type neurons made *Syt*-LOF by *Syt*-RNAi (Fig 25G,H). We found that this parameter was increased (Fig. 26H), consistently with Staahl et al. 2013 and results of our previous *Syt*-GOF manipulations (Fig. 21D). Then, we downregulated *Syt* via RNAi in *wild-type* neurons made *Foxg1*-GOF by means of postmitotic activation of a *Foxg1*-encoding transgene (Fig 25G). Remarkably, we found that dendritic length was increased in *Syt*-LOF/*Foxg1*-GOF neurons compared to controls (Fig. 26I).

To sum up: (1) *late Foxg1* upregulation in *Foxg1*-haploinsufficient neurons does not correct their dendritic deficits, rather it exacerbates them; (2) a substantial etiological contribution to this scenario originates from the diverse impact of *Foxg1* upregulation on *Syt* expression (inhibitory upon early onset, excitatory upon late onset). The latter phenomenon is puzzling and distinct mechanisms may underlie it (e.g. differential accessibility to Foxg1 of *cis*-active modules impinging on *Syt* regulation, and/or differential availability of specific cofactors

needed for it). Remarkably, it does not preclude late therapy of *Foxg1* haplo-insufficiency. However, to implement such therapy, it has to be considered and properly counteracted (see Fig. 26I).

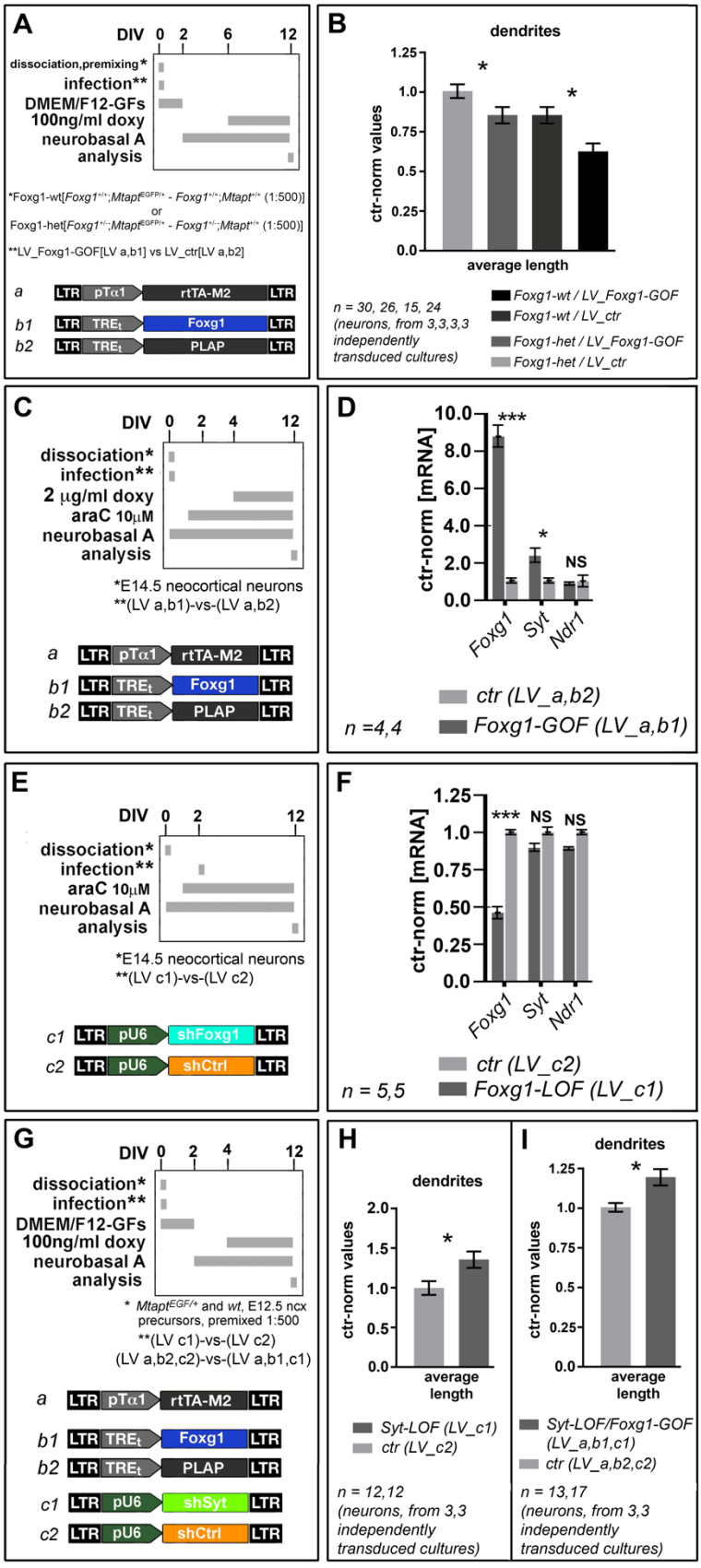

Figure 26. Post-mitotic impact of *Foxg1*-GOF on dendrite elongation. (*A*,*B*) Morphometric assessment of post-mitotic *Foxg1*$^{+/+}$ and *Foxg1*$^{+/-}$ neurons induced to express a *Foxg1*-encoding transgene or a control. (*C*–*F*) qRTPCR evaluation of *Foxg1*, *Syt* and *Ndr1* mRNA levels upon *Foxg1* overexpression (*C*,*D*) and downregulation (*E*,*F*). (G-I) Morphometric assessment of Syt downregulation (G,H) or in combination with Foxg1 overexpression (G,I) in post-mitotic neurons. In (*A*,*C*,*E*,*G*) protocols and materials. In (*B*,*D*,*F*,*H,I*) control-normalized results. Absolute average values of control dendrite length were 149.72 µm (*B*), 110.32 µm (*H*), 107.71 µm (*I*). Statistical significance evaluated by t-test (one-way, unpaired): *P < 0.05, **P < 0.01, ***P < 0.001. *n* is the number of statistical replicates. These replicates are: single neurons evenly taken from the indicated, independently transduced cultures in case of (*B,H,I*); neuronal cultures in case of (*D*,*F*).

Foxg1 stimulation in mouse and human neural cells: a possible therapeutic tool

In order to fix the Foxg1 deficit peculiar to *Foxg1*$^{+/-}$ neurons, we hypothesized to stimulate the spared *Foxg1* allele by artificial small activating RNAs (saRNAs). In fact, these effectors were shown to achieve a gentle and specific upregulation of the gene of interest, not conflicting with its endogenous regulation (reviewed in Mallamaci 2017). As such, they look especially suitable to get the precise correction of gene expression levels required to safely fix consequences of *Foxg1* haploinsufficiency. It was specifically reported that the *Foxg1*-saRNA miR.αFoxg1.1694 selectively activates *Foxg1* in neural precursors originating from neocortex and complies with fine endogenous tuning of this gene by neuronal activity (Fimiani et al. 2016). Given the high similarity occurring between the murine miR.αFoxg1.1694 target sequence and its human counterpart, we hypothesized to employ this miR to correct *human FOXG1* deficits.

As a first step, propaedeutic to its use in human *FOXG1*-defective neural cells, we tested miR.αFoxg1.1694 in: (a) mouse *Foxg1*-haploinsufficient neurons and (b) human wild type differentiated neural cells. In the former case, we delivered miR.αFoxg1.1694 to neuron-enriched, E16.5+DIV2 neocortical *Foxg1*$^{+/-}$ cultures (Fig. 27A,B). In the latter case, we infected mixed, neuronal-astroglial cultures originating from wild type neocortical neural stem cells, 8 days after their plating in prodifferentiative medium (Fig. 26C,D and Fig. S13). We found an upregulation of *Foxg1* mRNA in both mouse (~2x over 10 days) and human (~1.3 over 4 days) cells (Fig. 27B,D).

All this is encouraging, as it suggests that prolonged saRNA-treatment of human *FOXG1*-haploinsufficient neurons might upregulate *FOXG1*-mRNA up to levels close to physiological ones. This has to be experimentally verified.

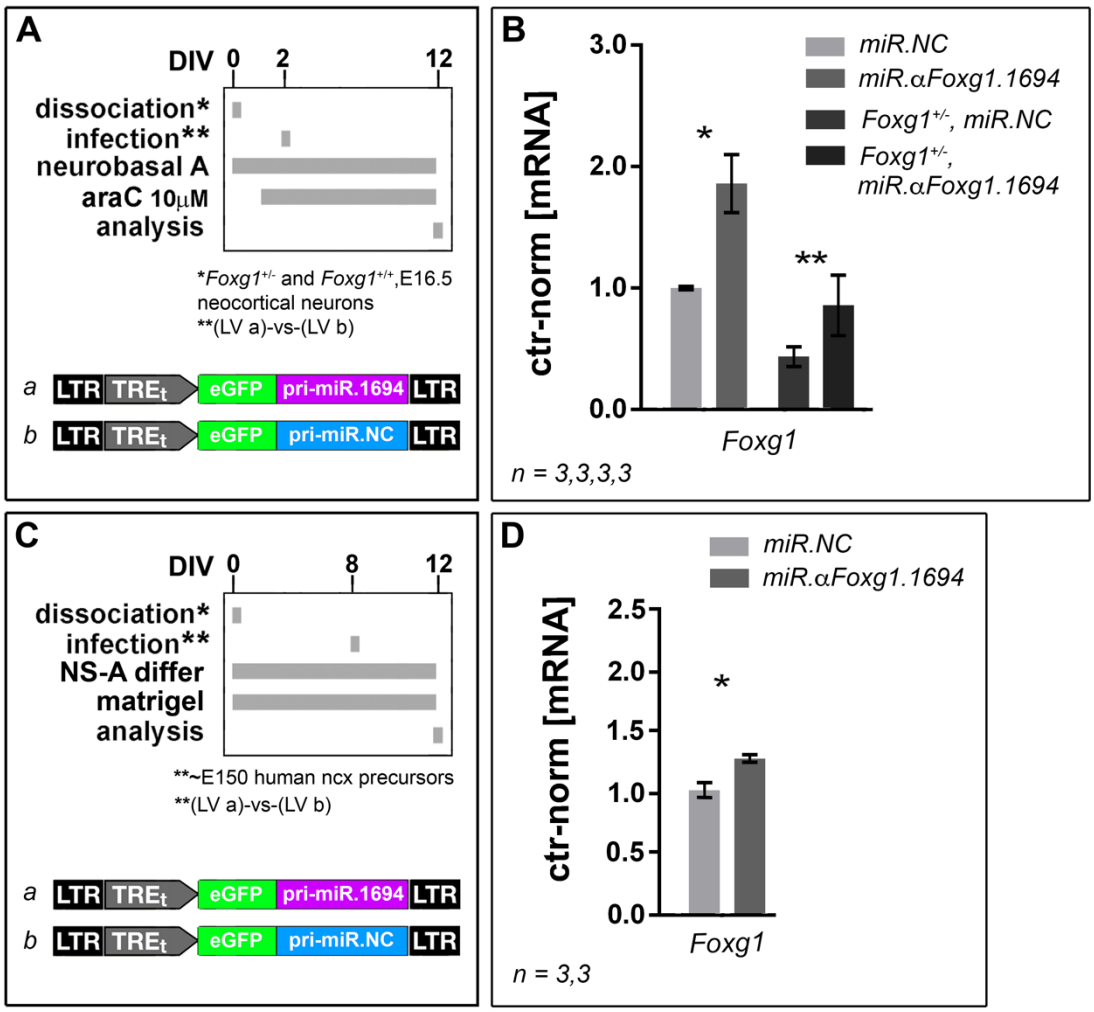

Figure 27. Post-mitotic transcriptional stimulation and *Foxg1* $^{+/-}$ and *FOXG1*$^{+/+}$ neural cells. (*A–D*) qRTPCR evaluation of *Foxg1* levels upon *Foxg1* saRNA transcriptional stimulation. In (*A*,*C*) protocols and materials. In (*B*,*D*) control-normalized results. Statistical significance evaluated by t-test (one-way, unpaired): *P < 0.05, **P < 0.01, ***P < 0.001. *n* is the number of statistical replicates (neuronal cultures).

SUPPLEMENTARY FIGURES AND TABLES

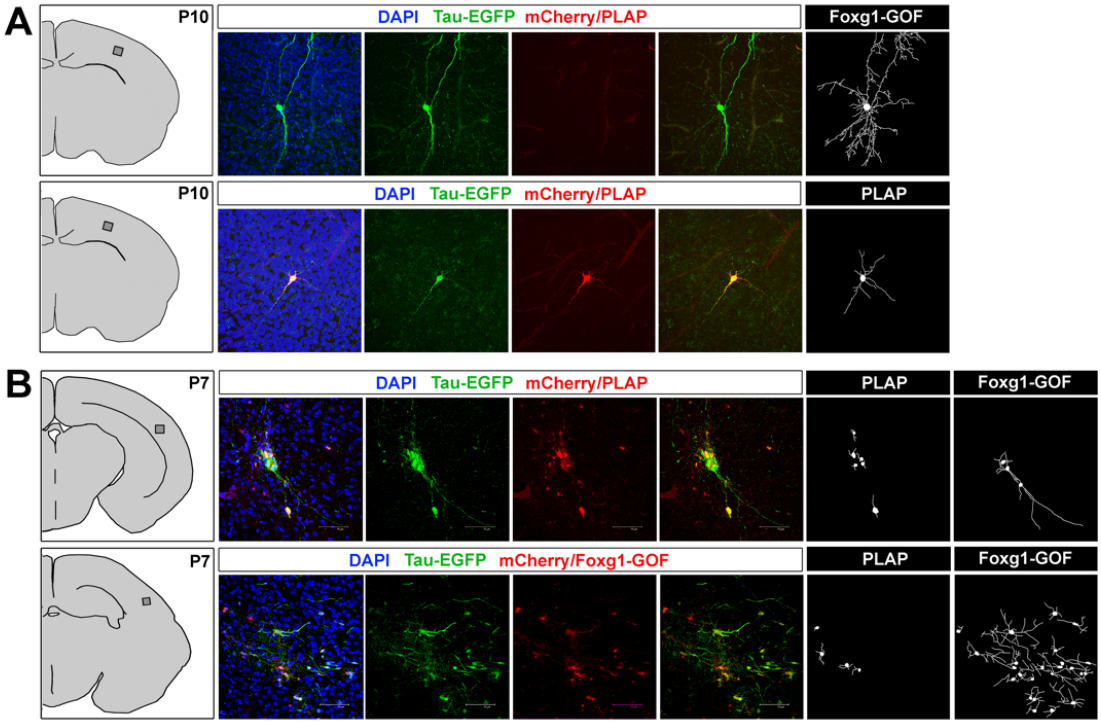

Figure S1. (*A*) Examples of immunostained transplanted cells referred to by Fig. 1B,C, and their locations within the P10 rostral parietal neocortex. (*B*) Examples of immunostained transplanted cells referred to by Fig. 1D,E, and their location within the P7 caudal parietal neocortex. Here, Mtapt$^{EGFP/+}$ cells (shortly Tau-EGFP cells) transplanted into different recipient animals were alternatively labelled according to the two, mCherry/Plap and mCherry/*Foxg1*-GOF patterns (first and second rows, respectively). Neurites were skeletonized for morphometric evaluation.

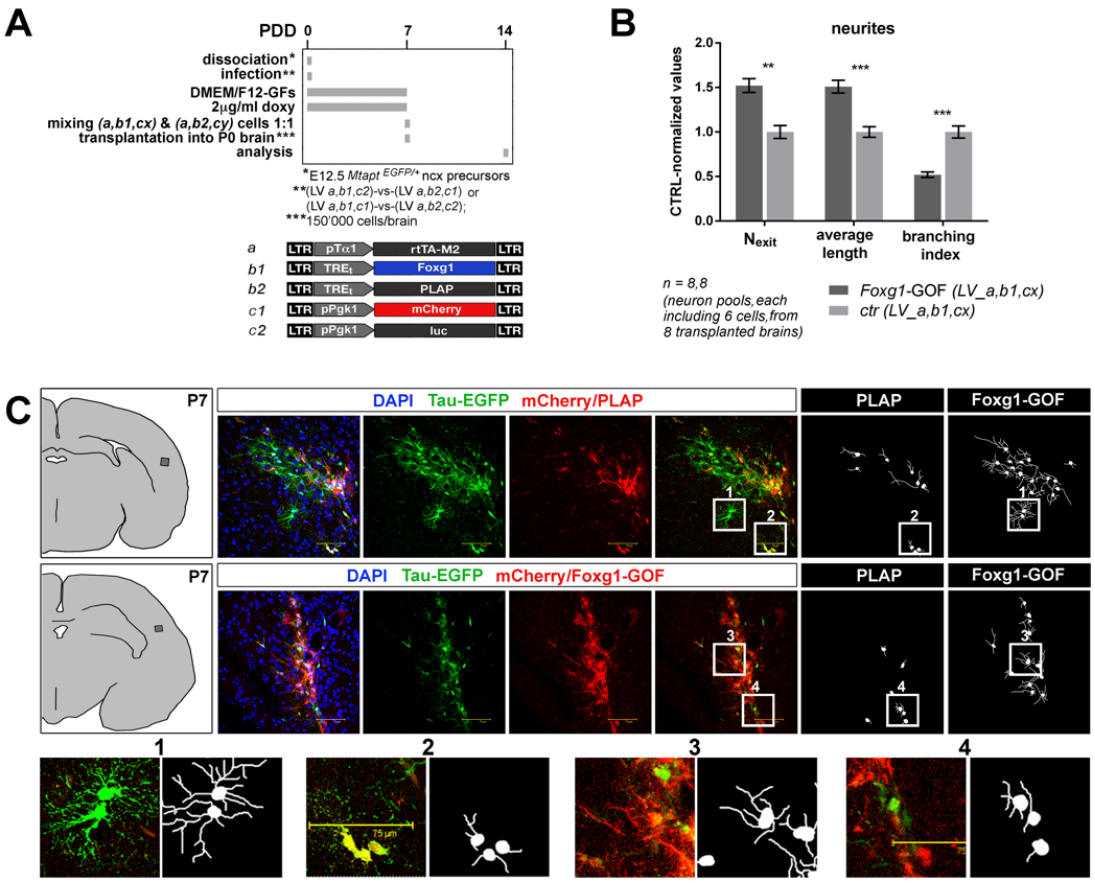

Figure S2. (*A*,*B*) Functional assessment of Foxg1 impact on neurite morphology, upon transplantation of conditionally engineered neocortical precursors in wild type neonatal brains: gain-of-function (GOF), TetON assay, early transgene activation. Landmarks and parameters employed for neuronal morphometry defined as in Fig. 1A. in (*A*), protocol and materials, and in (*B*), control-normalized results. Absolute control values of exitpoints number, average neurite length and arborization index were 2.31, 42.20 μm and 1.42 x 10^{-2} μm^{-1}, respectively. Statistical significance of results evaluated by t-test (one-way, paired): *P < 0.05, **P < 0.01, ***P < 0.001. *n* is the number of paired statistical replicates, i.e. neuron pools cotransplanted into as many recipient brains. (C) Examples of immunostained transplanted cells referred to by panels (*A*,*B*) and their locations within the P7 intermediate parietal neocortex.

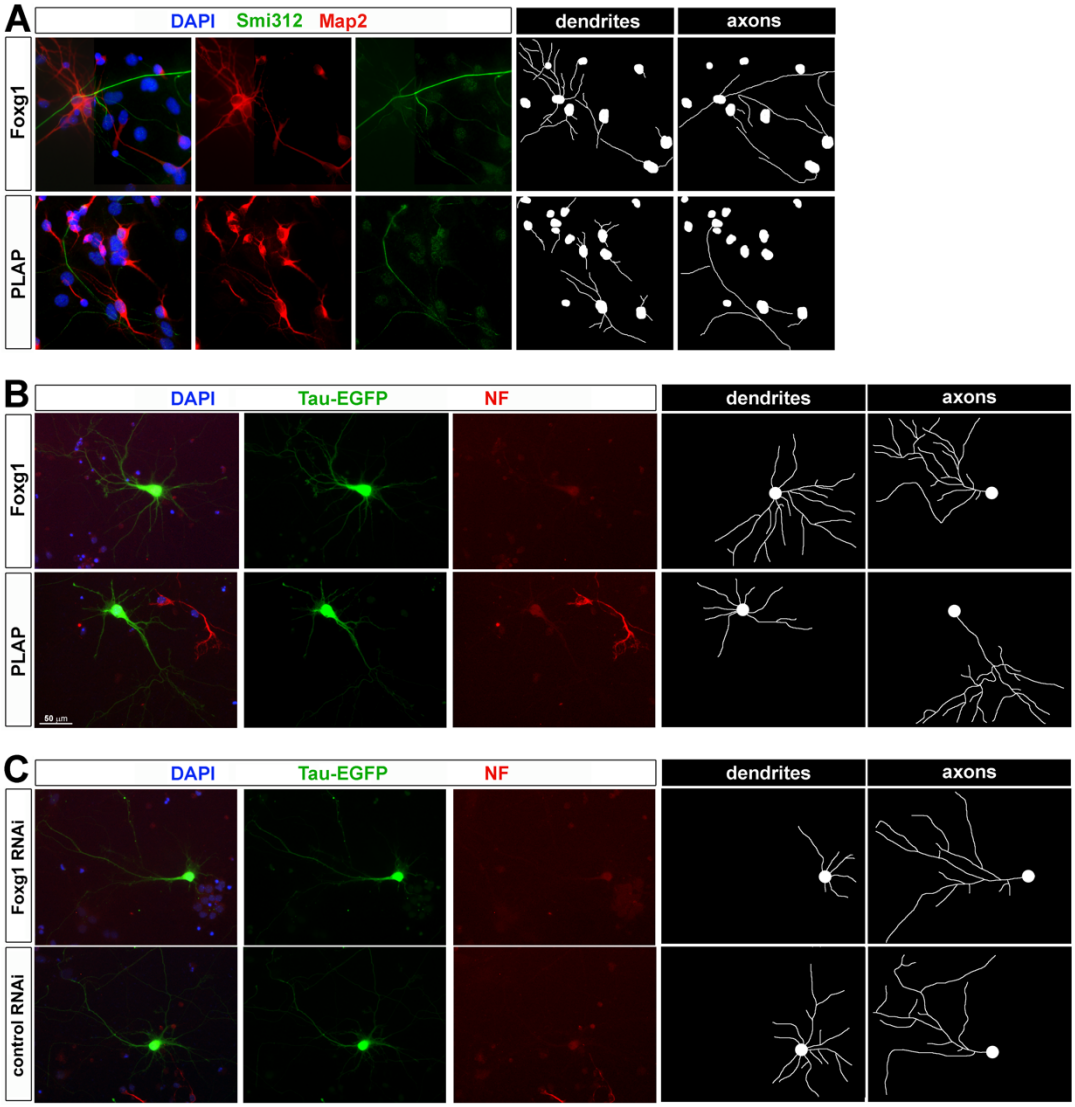

Figure S3. (*A,B,C*) Examples of primary data referred to by Fig. 2A,B, 2C,D and 2E,F, respectively. Axons were stained by anti-Smi312 (*A*) and anti-NF (*B*,*C*) antibodies. Dendrites were stained by anti-Map2 (*A*). Alternatively, they were recognized as not-anti-NF immunoreactive subsets of neurite trees expressing EGFP under the control of the Mtapt-promoter (Tau-EGFP) (*B*,*C*). Both neurites were skeletonized for morphometric evaluation (*A*,*B*,*C*).

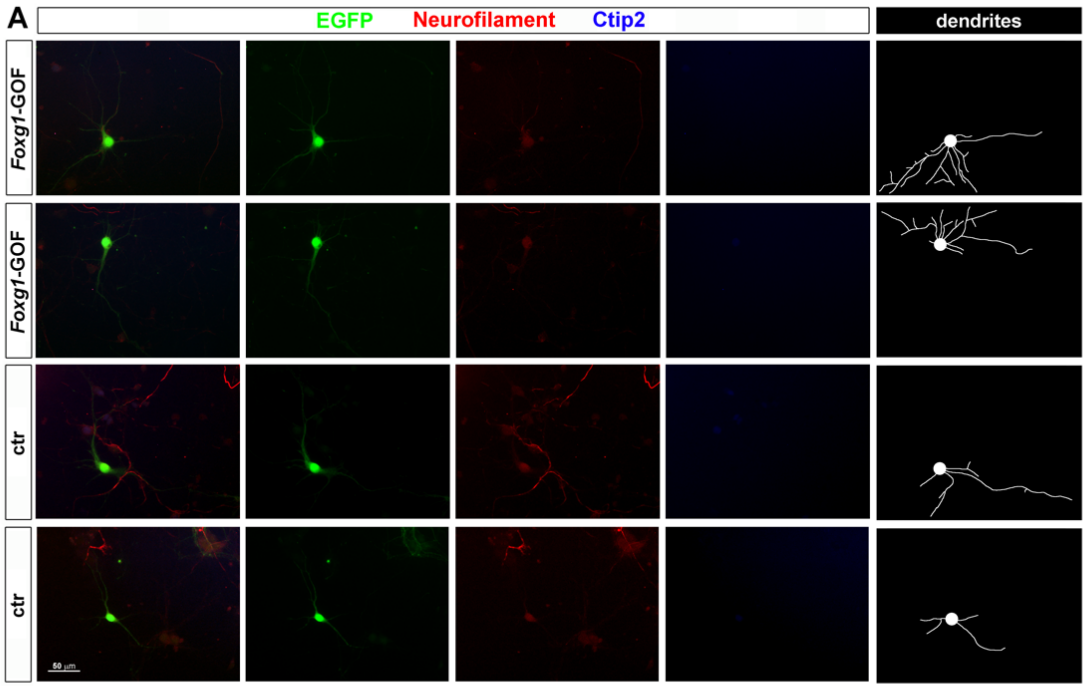

Figure S4. (*A*) Examples of primary data referred to by Fig. 2G,H. Neurons were categorized as Ctip2+ and Ctip2- ones. Dendrites were recognized as not-anti-NF immunoreactive subsets of neuritic trees expressing EGFP under the control of the Mtapt-promoter (Tau-EGFP). Dendrites were skeletonized for the morphometric evaluation.

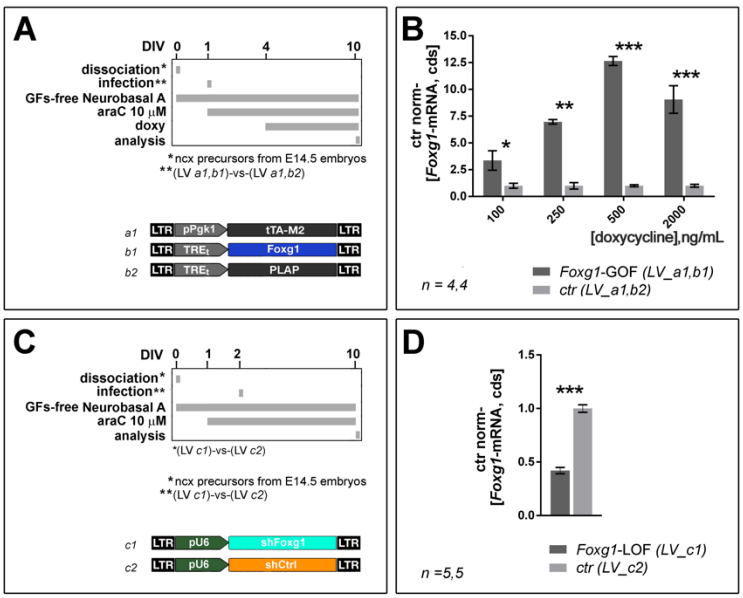

Figure S5. (*A*,*B*) Evaluation of the *Foxg1*-mRNA expression gain, upon lentiviral delivery of a Pgk1-promoter/rtTA-M2-driven *Foxg1* transgene to differentiating neocortical precursors and delayed exposure to their post-mitotic derivatives to doxycycline, in the 100-to-2,000 ng/mL concentration range. In (*A*), protocol and materials, in (*B*) results. (*C*,*D*) Evaluation of the *Foxg1*-mRNA expression decrease elicited upon lentiviral delivery of a constitutive *Foxg1*-RNAi effector to differentiating neocortical precursors. In (*C*), protocol and materials, in (*D*) results. Statistical significance of results evaluated by t-test (one-way, unpaired): *P < 0.05, **P < 0.01, ***P < 0.001. *n* is the number of statistical replicates, i.e. independently transduced neuronal cultures.

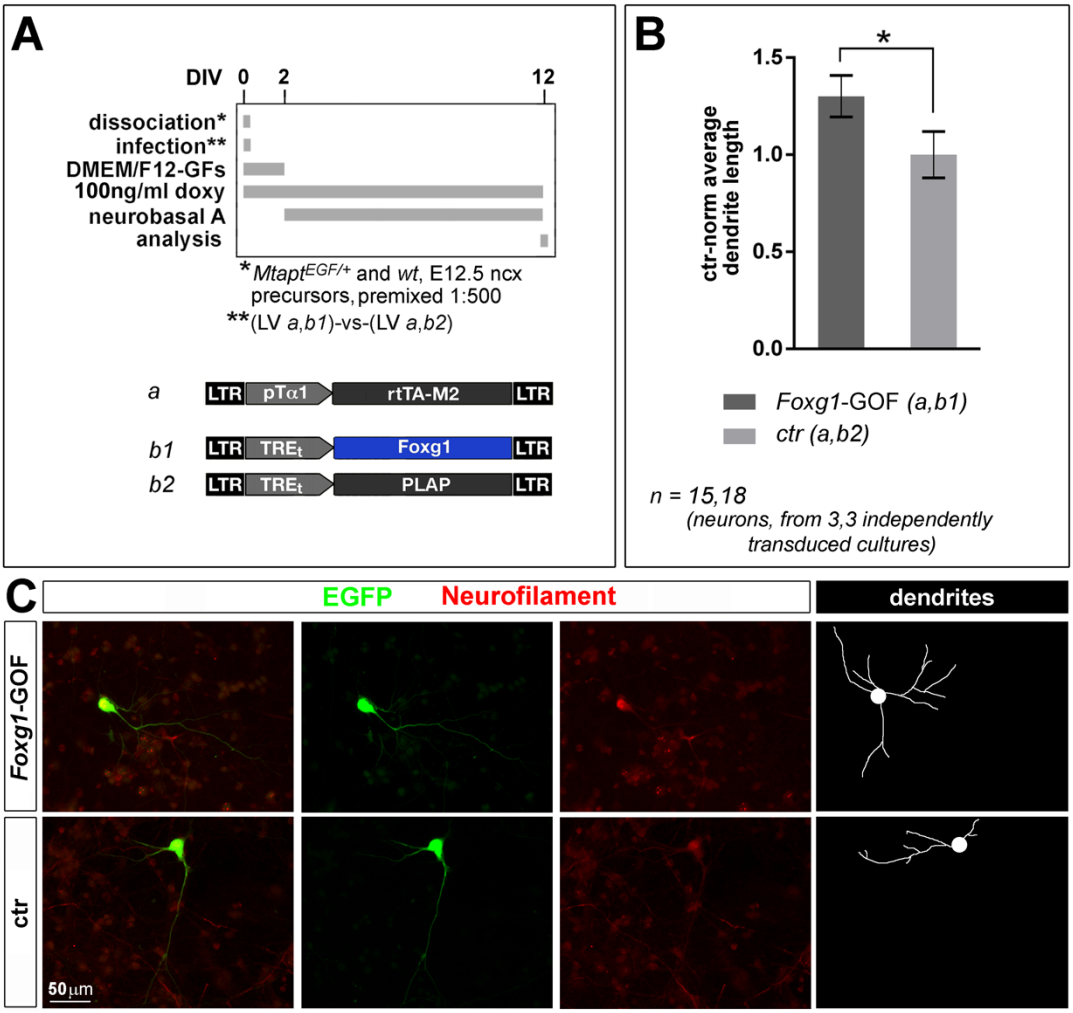

Figure S6. (*A*,*B*) Neural cells to be scored for pCreb1 levels were cultured and profiled for average dendrite length as in Fig. 2C,D. Absolute average neurite length was 175.74 μm. (C) Dendrites were skeletonized for morphometric evaluation. Statistical significance of results evaluated by t-test (one-way, unpaired): *P < 0.05. n is the number of statistical replicates, i.e. single neurons evenly taken from independently transduced cultures.

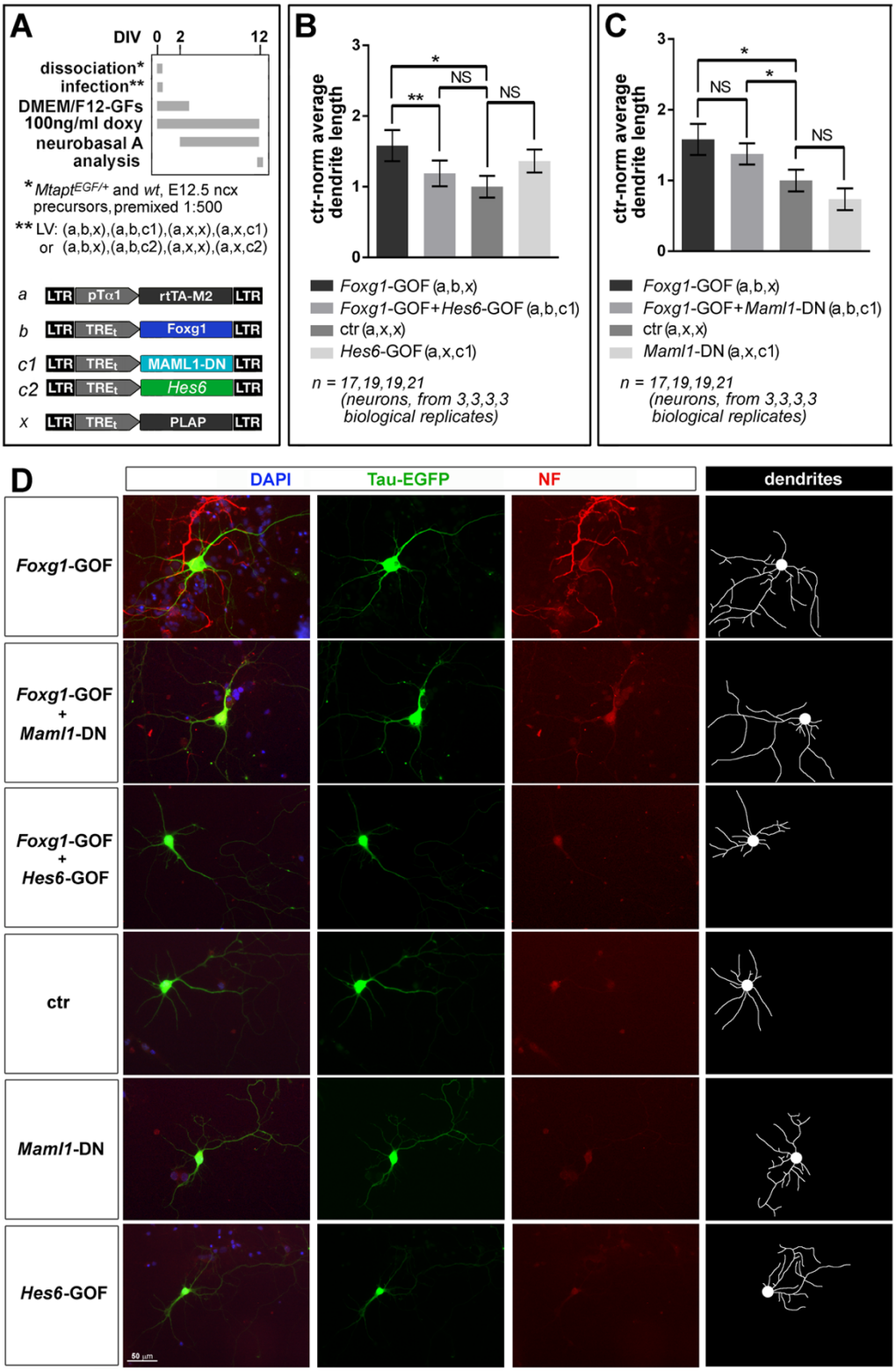

Figure S7. (*A-B*) Trying to rescue Foxg1-dependent dendrite overgrowth, via neuronogenic lineage-restricted overexpression of a dominant-negative inhibitor of Hes1 function (Hes6, A,B) or a dominat-negative effector inhibiting Notch-mediated Hes1 transactivation (Maml1, A,C). Landmarks and parameters employed for neuronal morphometry defined as in Fig. 1A. In (A), protocols and materials, in (B,C), control-normalized results. Here, absolute average, control dendrite length was 129.87 µm. (D) Examples of primary data referred to by panels (B,C). Here, axons were decorated by an anti-NF antibody and dendrites recognized as not-anti-NF immunoreactive neurites expressing EGFP under the control of the Mtapt-promoter (Tau-EGFP). Dendrites were skeletonized for morphometric evaluation. Statistical significance of results evaluated by t-test (one-way, unpaired): *P < 0.05, **P < 0.01, ***P < 0.001. n is the number of statistical replicates, i.e. single neurons evenly taken from the indicated, independently, transduced cultures.

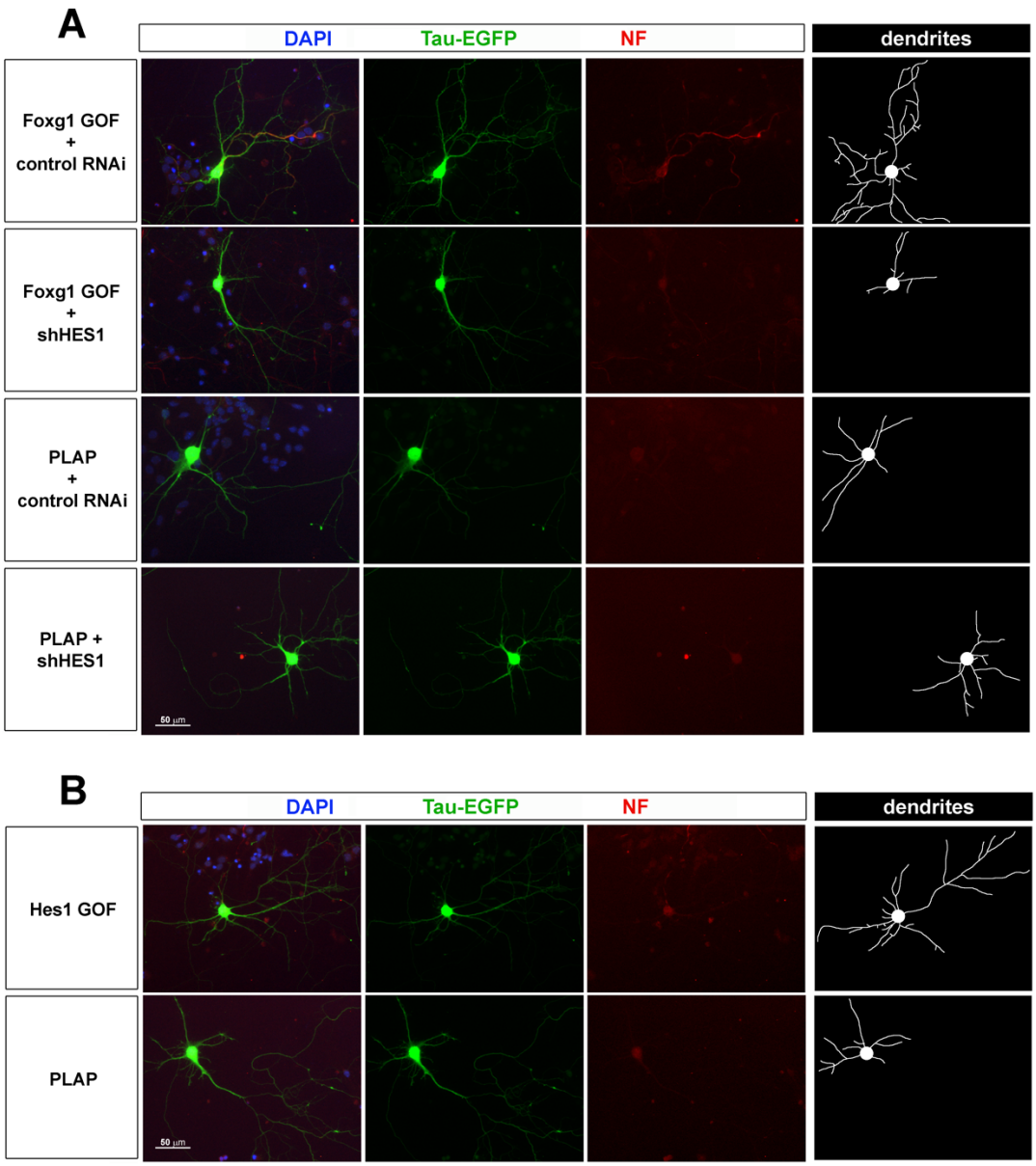

Figure S8. (*A*,*B*) Examples of primary data referred by Fig. 21B and Fig. 21C, respectively. Axons were decorated by anti-NF antibodies, dendrites were recognized as not-anti-NF immonoreactive neurites expressing EGFP under the control of the Mtapt-promoter (Tau-EGFP). Dendrites were skeletonized for morphometric evaluation.

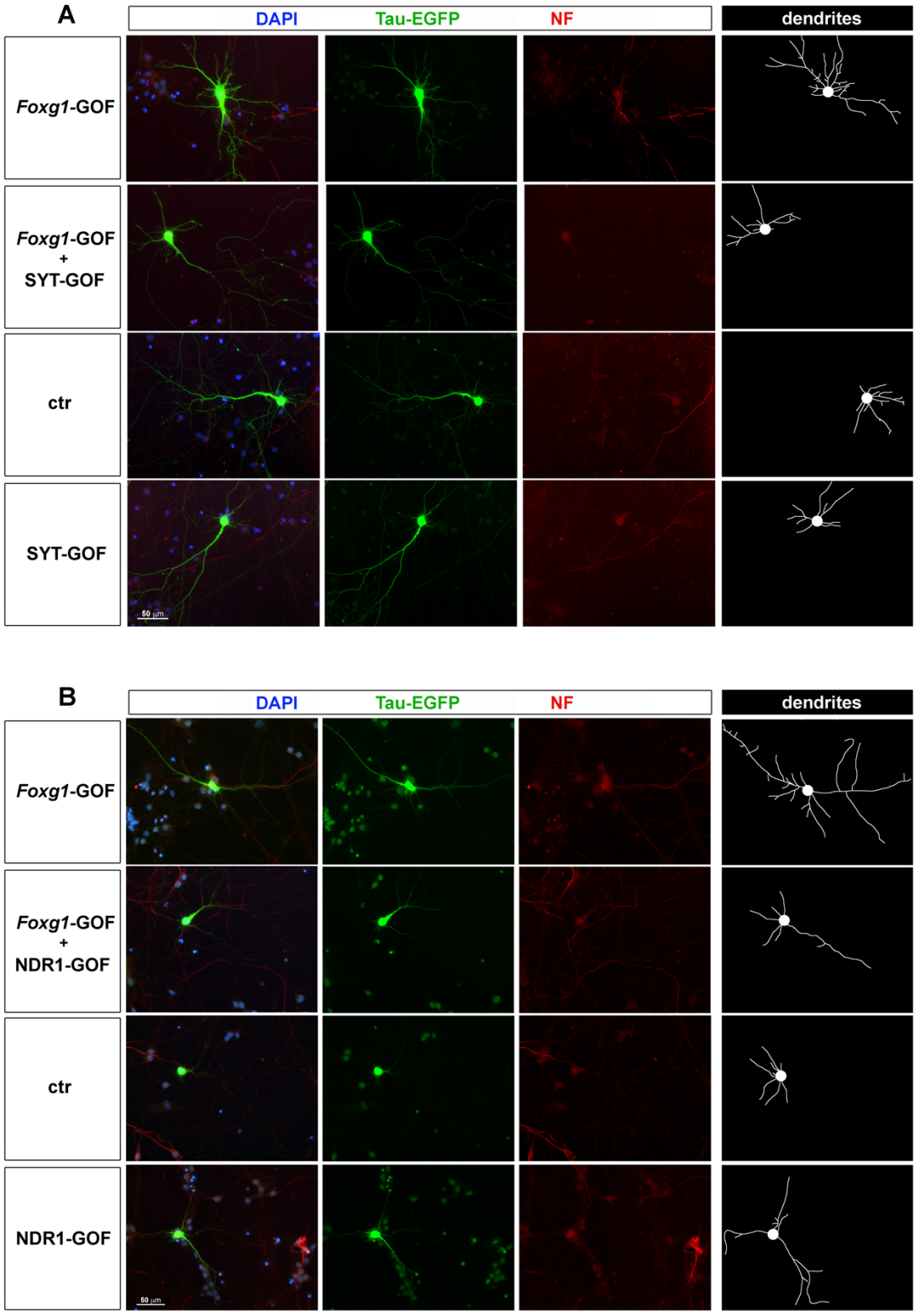

Figure S9. (*A*,*B*) Examples of primary data referred by Fig. 21D and Fig. 21E, respectively. Staining and image processing were as in Figure S8.

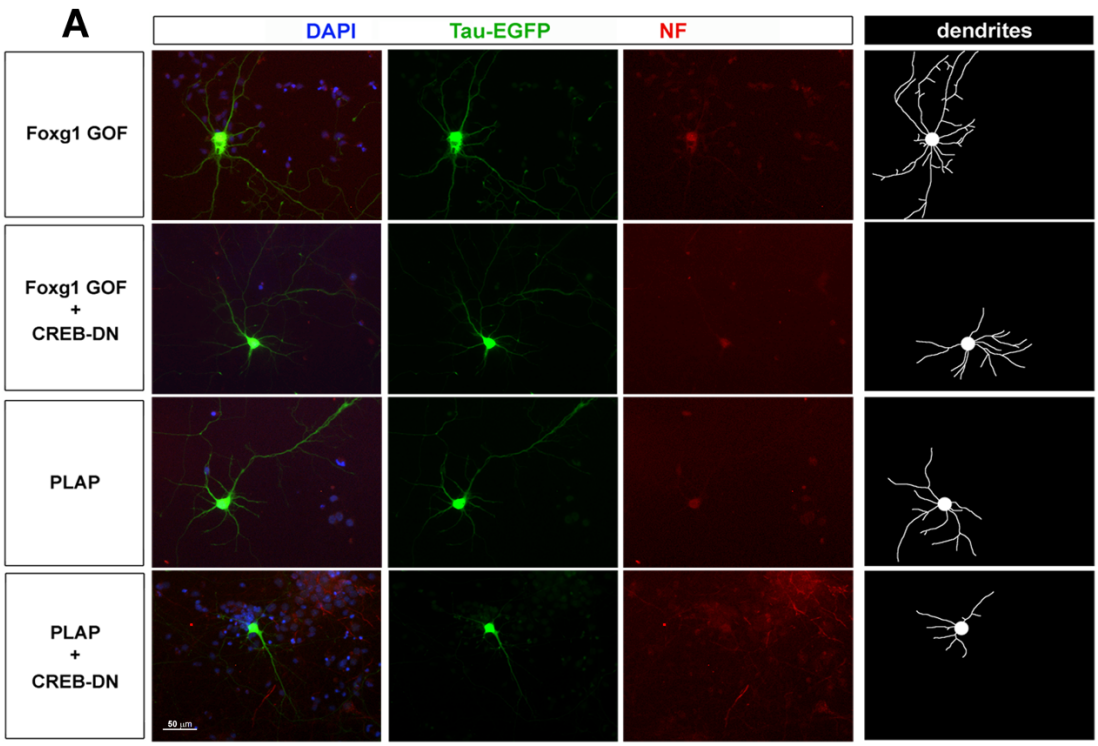

Figure S10. (*A*) Examples of primary data referred by Fig. 21F. Staining and image processing were as in Figure S8.

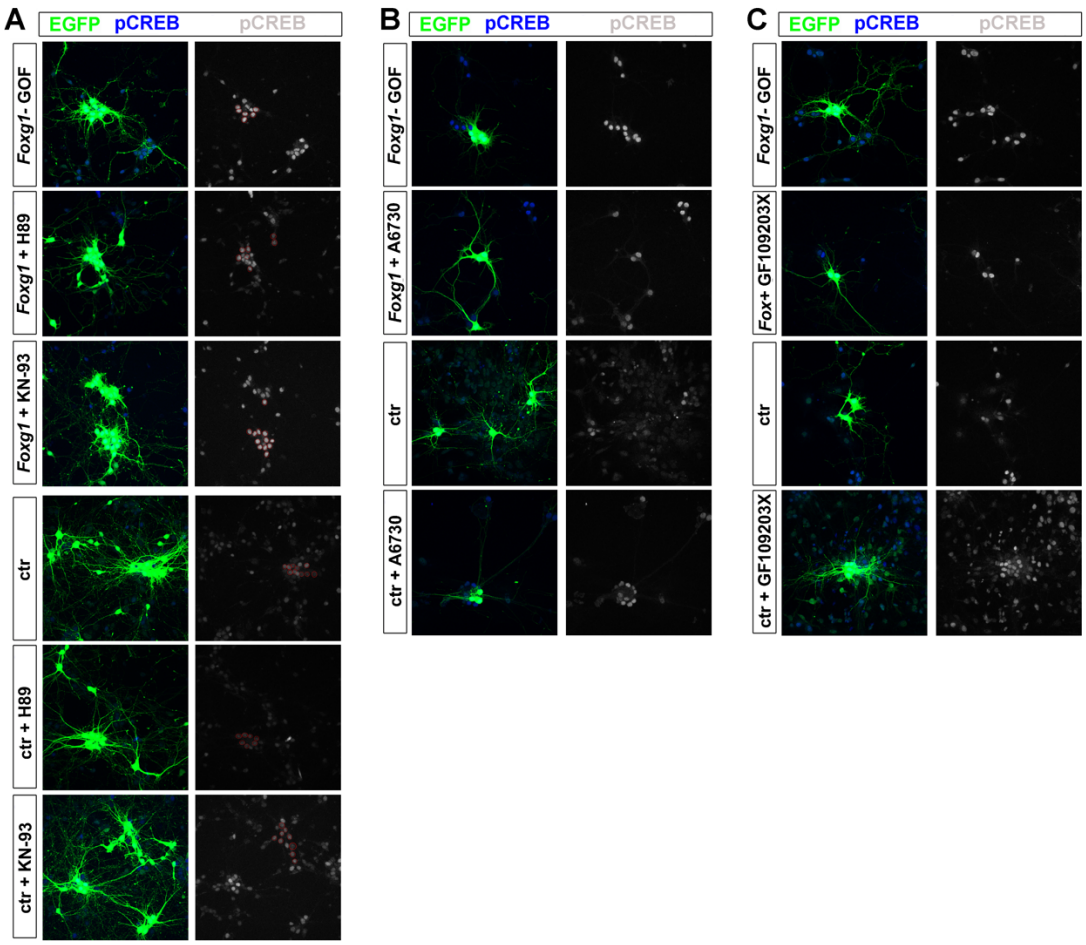

Figure S11. (*A-C*) Examples of neurons subject of quantitative pCreb1 immunofluorimetry, circled in red, upon combined *Foxg1*/kinase manipulation.

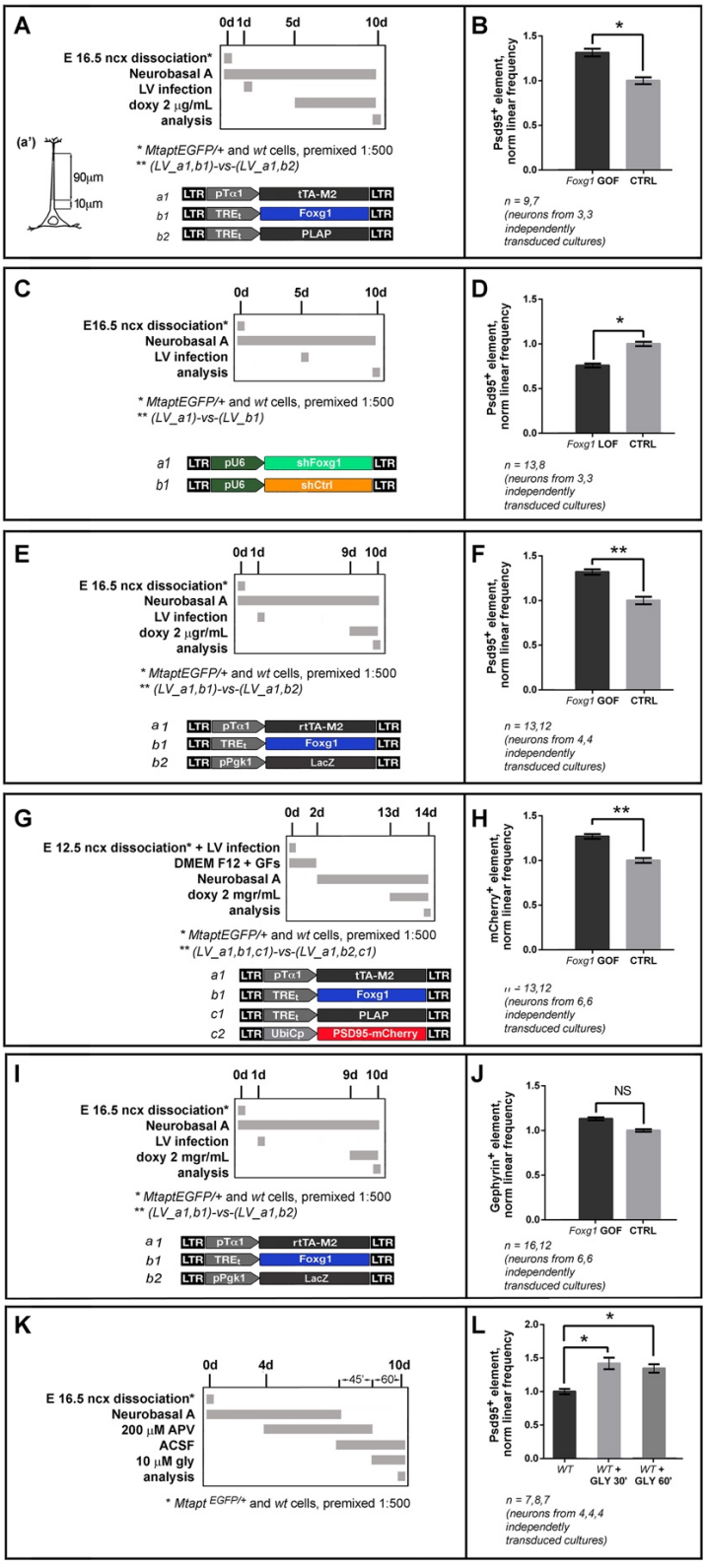

Figure S12. Linear densities of Psd95$^+$ (A-H) and Gephyrin$^+$ (I,J) elements in apical dendrites of Mtapt$^{EGFP/+}$ neocortical neurons (decorated by a lentivirus-delivered Psd95-mCherry chimera in (G,H)), upon Foxg1 overexpression (A,B,E-J) or downregulation (C,D), as revealed by immunofluorescence. Foxg1-GOF (A,B) and (E,F) assays only differ for Foxg1-transgene activation schedule. In (K,L) changes of Psd95$^+$ spines elicited by short-term exposures of wild-type neurons to 10 mM glycine are provided as references (Srivastava et al. 2011). In (A,C,E,G,I,K) protocols and materials, in (B,D,F,H,J,L) results. Throughtout the Figure S12, the analysis was restricted to the apical dendrite segment (grey region in A(a') schematics). Statistical significance of results evaluated by t-test (one-way, unpaired) (D,F,H,J,L), and non-parametric Mann-Whitney test (B): *P< 0.05, **P< 0.01, ***P< 0.001. n is the number of statistical replicates, i.e. single neurons evenly taken from the indicated, independently transduced cultures.

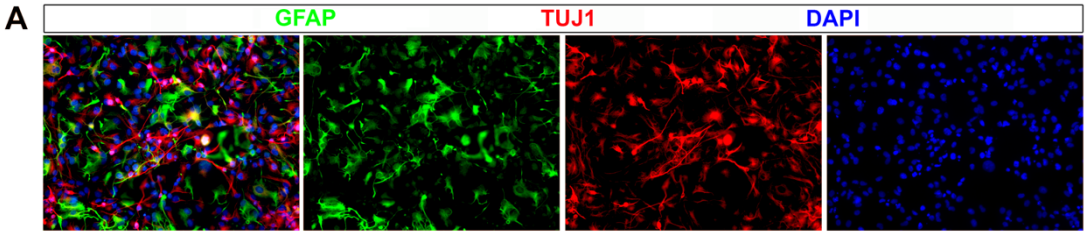

Figure S13. (*A*) Examples of human neuronal-astroglial cultures referred by Fig. 27C,D. Neurons were decorated by anti-Tuj1 antibodies, astroglial cells were stained by anti-GFAP antibodies.

BIBLIOGRAPHY

Aguiar, DP, S Sghari, and S Creuzet. 2014. "The facial neural crest controls fore- and midbrain patterning by regulating Foxg1 expression through Smad1 activity." *Development* 2494-2505.

Ahn, S, M Olive, S Aggarwal, D Krylov, DD Ginty, and C Vinson. 1998. "A dominant-negative inhibitor of CREB reveals that it is a general mediator of stimulus-dependent transcription of c-fos." *Mol Cell Biol* 967-977.

Aizawa, H, SC Hu, K Bobb, K Balakrishnan, G Ince, I Gurevich, M Cowan, and A Ghosh. 2004. "Dendrite development regulated by CREST, a calcium-regulated transcriptional activator." *Science* 197-202.

Alcamo, EA, L Chirivella, M Dautzenberg, G Dobreva, I Farinas, R Grosschedl, and SK McConnell. 2008. "Satb2 regulates callosal projection neuron identity in the developing cerebral cortex." *Neuron* 364-377.

Amor, DJ, T Burgess, TY Tan, and MD Pertile. 2012. "Questionable pathogenicity of FOXG1 duplication." *Eur. J. Hum. Genet.* 596-597.

Ariani, F, G Hayek, D Rondinella, R Artuso, and MA Mencarelli. 2008. "FOXG1 is responsible for the congenital variant of Rett syndrome." *Am. J. Med. Genet.* 89-93.

Arlotta, P, BJ Molyneaux, J Chen, J Inoue, R Jominami, and JD Macklis. 2005. "Neuronal subtype-specific genes that controlo corticospinal motor neuron development in vivo." *Neuron* 207-221.

Armstrong, D, JK Dunn, B Antalffy, and R Trivedy. 1995. "Selective dendritic alterations in the cortex of Rett syndrome." *J. Neuropat. Exp. Neurol.* 195-201.

Baek, ST, B Copeland, EJ Yun, SK Kwon, A Guemez-Gamboa, AE Schaffer, S Kim, et al. 2015. "An AKT3-FOXG1-reelin network underlies defective migration in human focal malformations of cortical development." *Nat. Med.* 1445-1454.

Ballas, N, DT Lioy, C Grunseich, and G Mandel. 2009. "Non-cell autonomous influence of MeCP2-deficient glia on neuronal dendritic morphology." *Nat. Neurosci.* 311-317.

Beddington, RS, and EJ Robertson. 1999. "Axis development and early asymmetry in mammals." *Cell* 195-209.

Bertossi, C, M Cassina, L De Palma, M Vecchi, S Rossato, I Toldo, M Dona', A Murgia, C Boniver, and S Sartori. 2014. "14q12 duplication including FOXG1: is there a common age-dependent epileptic phenotype?" *Brain Dev.* 402-407.

Bisgaard, AM, M Kirchhoff, Z Tumer, B Jepsen, and K Brondum-Nielsen. 2006. "Additional chromosomal abnormalities in patients with a previously detected abnormal karyotype, mental retardation, and dysmorphic features." *Am. J. Med. Genet.* 2180-2187.

Bonini, SA, G Ferrari-Toninelli, D Uberti, M Montinaro, L Buizza, C Lanni, M Grilli, and M Memo. 2011. "Nuclear factor B-dependent neurite remodeling is mediated by notch pathway." *J Neurosci* 11697-11705.

Brancaccio, M, C Pivetta, Granzotto M, C Filippis, and A Mallamaci. 2010. "Emx2 and Foxg1 inhibit gliogenesis and promote neuronogenesis." *Srem Cells Dayt Ohio* 1206-1218.

Bredenkamp, N, C Seoighe, and N Illing. 2007. "Comparative evolutionary analysis of the FoxG1 transcription factor from diverse vertebrates identifies conserved recognition sites for microRNA regulation." *Dev. Genes. Evol.* 227-233.

Breunig, JJ, J Silbereis, Vaccarino FM, N Sestan, and P Rakic. 2007. "Notch regulates cell fate and dendrite morphology of new-born neurons in the postnatal dentate gyrus." *PNAS* 20558-20563.

Britanova, O, C de Juan Romero, A Cheung, KY, Schwark, M Kwan, A Gyorgy, T Vogel, S Akopov, M Mitkovski, and D Agoston. 2008. "Satb2 is a postmitotic determinant for upper-layer neuron specification in the neocortex." *Neuron* 378-392.

Brunetti-Pierri, N, AR Paciorkowski, R Ciccone, E Della Mina, MC Bonaglia, R Borgatti, CP Schaaf, VR Sutton, Z Xia, and N Jelluma. 2011. "Duplications of FOXG1 in 14q12 are associated with developmental epilepsy, mental retardation, and severe speech impairment." *Eur. J. Hum. Genet.* 102-107.

Caiazzo, M, S Giannelli, P Valente, G Lignani, A Carissimo, A Sessa, G Colasante, et al. 2015. "Direct conversion of fibroblasts into functional astrocytes by defined transcription factors." *Stem Cell Rep* 25-36.

Calegari, F. 2003. "An inhibition of cyclin-dependent kinases that lengthens, but does not arrest, neuroepithelial cell cycle induces premature neurogenesis." *J. Cell Sci.* 1433-1443.

Cassady, JP, AC D'Alessio, S Sarkar, VS Dani, ZP Fan, K Ganz, R Roessler, M Sur, RA Young, and R Jaenisch. 2014. "Direct lineage conversion of adult mouse liver cells and B lymphocytes to neural stem cells." *Stem Cell Rep* 948-956.

Chacón, PJ, and A Rodriguez-Tebar. 2012. "Increased expression of the homologue of enhancer-of-split 1 protects neurons from beta amyloid neurotoxicity and hints at an alternative role for transforming growth factor beta1 as a neuroprotector." *Alxheimers Res Ther* 4-31.

Chan, DW, VWS Liu, RMY To, PM Chiu, WYW Lee, KM Yao, ANY Cheung, and HYS Ngan. 2009. "Overexpression of FOXG1 contributes to TGF-B resistance through inhibition of p21WAF1/CIP1 expression in ovarian cancer." *Br. J. Cancer* 1433-1443.

Chen, B, SS Wang, AM Hattox, H Rayburn, SB Nelson, and SK McConnell. 2008. "The Fezf2-Ctip2 genetic pathway regulates the fate choice of subcortical projection neurons in the developing cerebral cortex." *Proc. Natl. Acad. Sci. U.S.A.* 11382-11387.

Chen, JG, MR Rasin, KY Kwan, and N Sestan. 2005. "Zfp312 is required for subcortical axonal projections and dendritic morphology of deep-layer pyramidal neurons of the cerebral cortex." *Proc. Natl. Acad. Sci. USA* 17792-17797.

Cheung, ZH, WH Chin, Y Chen, YP Ng, and NY Ip. 2007. "Cdk5 is involved in BDNF-stimulated dendritic growth in hippocampal neurons." *PLoS Biol.*

Chugani, HT, WD Shields, DA Shewmon, DM Olson, ME Phelps, and WJ Peacock. 1990. "Infantile spasms: I. PET identifies focal cortical dysgenesis in cryptogenic cases of surgical treatment." *Ann. Neurol.* 406-413.

Cline, HT. 2001. "Dendritic arbor development and synaptogenesis." *Curr. Op. in Neurobiol.* 118-126.

Cubelos, B, A Sebastian-Serrano, L Beccari, ME Calcagnotto, E Cisneros, S Kim, A Dopazo, M Alvarez-Dolado, JM Redondo, and P Bovolenta. 2010. "Cux1 and Cux2 regulate dendritic branching, spine morphology, and synapses of the upper layer neurons of the cortex." *Neuron* 523-535.

Danesin, C, and C Houart. 2012. "A Fox stops the Wnt: implications for forebrain development and diseases." *Curr. Opin. Genet. Dev.* 323-330.

Danesin, C, JN Peres, M Johansson, V Snowden, A Cording, N Papalopulu, and C Houart. 2009. "Integration of telencephalic Wnt and Hedgehog signaling center activities by Foxg1." *Dev. Cell.* 576-587.

Dastidar, SG, PMZ Landrieu, and SR D'Mello. 2011. "FoxG1 promotes the survival of postmitotic neurons." *J. Neurosci.* 402-413.

De Felipe, J, and I Farinas. 1992. "The pyramidal neuron of the cerebral cortex: morphological and chemical characteristics of the synaptic inputs." *Prog. in Neurobiol.* 563-607.

de la Torre-Ubieta, L, and A Bonni. 2011. "Transcriptional regulation of neuronal polarity and morphogenesis in the mammalian brain." *Neuron* 22-40.

de la Torre-Ubieta, L, B Gaudilliere, Y Yang, Y Ikeuchi, T Yamada, S DiBacco, J Stegmuller, U Schuller, DA Salih, and D Rowitch. 2010. "A FOXO-Pak1 transcriptional pathway controls neuronal polarity." *Genes Dev* 799-813.

Desai, AR, and SK McConnell. 2000. "Progressive restriction in fate potential by neural progenitors during cerebral cortical development." *Dev. Camb. Engl.* 2863-2872.

Desguerre, I, F Pinton, R Nabbout, ML Moutard, S N'Guyen, C Marsac, G Ponsot, and O Dulac. 2013. "Infantile spasms with basal ganglia MRI hypersignal may reveal mitochondrial disorder due to T8993G MT DNA mutation." *Neuropediatrics* 265-269.

Devroe, E, H Erdjument-Bromage, P Tempst, and PA Silver. 2004. "Human Mob proteins regulate the NDR1 and NDr2 serine-threonine kinases." *J Biol Chem* 24444-24451.

Dijkhuizen, PA, and A Ghosh. 2005. "BDNF regulates primary dendrite formation in cortical neurons via the PI3-kinase and MAP kinase signaling pathways." *J. Neurobiol.* 278-288.

Dijkhuizen, PA, and A Ghosh. 2005. "Regulation of dendritic growth by calcium and neurotrophin signaling." *Prog. Brain Res.* 17-27.

Diodato, A, M Pinzan, M Granzotto, and A Mallamaci. 2013. "Promotion of cortico-cerebral precursors expransion by artificial pri-miRNAs targeted against the Emx2 locusq." *Curr Gene Ther* 152-161.

Du, K, H Asahara, US Jhala, BL Wagner, and M Montminy. 2000. "Characterization of a CREB gain-of-function mutant with constitutive transcriptional activity in vivo." *Mol Cell Biol* 4320-7.

Dulac, O, Chiron, Robain, Plouin, Jambaque, and Pinard. 1994. "Infantile spasms: a pathophysiological hypothesis." *Semin. Pediatr. Neurol.* 83-89.

Dworkin, S, J Malaterre, F Hollande, PK Darcy, RG Ramsay, and T Mantamadiotis. 2009. "cAMP response element binding protein is required for mouse neural progenitor cell survival and expansion." *Stem Cells* 1347-1357.

Ermakova, GV, EA Solovieva, NY Martynova, and AG Zaraisky. 2007. "The homeodomain factor Xanf represses expression of genes in the presumptive rostral forebrain that specify more caudal brain regions." *Dev. Biol.* 483-497.

Falace, A, N Vanni, A Mallamaci, P Striano, and F Zara. 2013. "Do regulatory regions matter in FOXG1 duplications?" *Eur. J. Hum. Genet.* 365-366.

Falcone, C, Daga A, Leanza G, and Mallamaci A. 2016. "Emx2 as a novel tool to suppress glioblastoma." *Oncotarget* 41005-41016.

Fietz, and Huttner. 2011. "Cortical progenitor expansion, self-renewal and neurogenesis-a polarized perspective." *Curr. Opin. Neurobiol.* 23-35.

Fimiani, C, E Goina, Q Su, Gao G, and Mallamaci A. 2016. "RNA activation of haploinsufficient Foxg1 gene in murine neocortex." *Sci Rep.*

Finsterwald, C, H Fiumelli, JR Cardinaux, and JL Martin. 2010. "Regulation of dendritic development by BDNF requires activation of CRTC1 by glutamate." *J. Biol. Chem.* 28587-28595.

Flavell, SW, and ME Greenberg. 2008. "Signaling mechanisms linking neuronal activity to gene expression and plasticity of the nervous system." *Ann. Rev. Neurosci.* 563-590.

Franco, SJ, C Gil-Sanz, I Martinez-Garay, A Espinosa, SR Harkins-Perry, C Ramos, and U Muller. 2012. "Fate-restricted neural progenitors in the mammalian cerebral cortex." *Science* 746-749.

Frantz, GD, and SK McConnell. 1996. "Restriction of late cerebral cortical progenitors to an upper-layer fate." *Neuron* 55-61.

Fusco, S, L Leone, SA Barbati, D Samengo, R Piacentini, G Maulucci, G Toietta, et al. 2016. "A CREB-Sirt1-Hes1 Circuitry Mediates Neural Stem Cell Response to Glucose Availability." *Cell Rep* 1195-1205.

Gao, FB. 1998. "Messenger RNAs in dendrites: localization, stability, and implications for neuronal function." *BioEssays* 70-78.

Gao, P, MP Postiglione, TG Krieger, L Hernandez, C Wang, Z Han, C Streicher, et al. 2014. "Deterministic progenitor behavior and unitary production of neurons in the neocortex." *Cell* 775-788.

Gao, Z, K Ure, JL Ables, DC Lagace, KA Nave, S Goebbels, AJ Eisch, and J Hsieh. 2009. "Neurod1 is essential for the survival and maturation of adult-born neurons." *Nat. Neurosci.* 1090-1092.

Garaffo, G, D Conte, P Provero, D Tomaiuolo, Z Luo, P Pinciroli, C Peano, et al. 2015. "The Dlx5 and Foxg1 transcription factors, linked via miRNA-9 and -200, are required for the development of the olfacotry and GnRH system." *Mol. Cell Neurosci.* 103-119.

Gaudilliere, B, Y Konishi, N de la Iglesia, G Yao, and A Bonni. 2004. "A CaMKII-NeuroD signaling pathway specifies dendritic morphogenesis." *Neuron* 229-241.

Geng, X, S Acosta, O Lagutin, HJ Gil, and G Oliver. 2016. "Six3 dosage mediates the pathogenesis of holoprosencephaly." *Development* 4462-4473.

Glaze, DG, RA Hrachovy, JD Frost, P Kellaway, and TE Zion. 1988. "Prospective study of outcome of infants with infantile spasms treated during controlled studies of ACTH and prednisone." *J. Pediatr.* 389-396.

Goldberg, JL, MP Klassen, Y Hua, and BA Barres. 2002. "Amacrine-signaled loss of intrinsic axon growth ability by retinal ganglion cells." *Science* 1860-1864.

Götz, M, and WB Huttner. 2005. "The cell biology of neurogenesis: developmental cell biology." *Nat. Rev. Mol. Cell Biol.* 777-778.

Gould, E, CS Woolley, M Frankfurt, and BS McEwen. 1990. "Gonadal steroids regulate dendritic spine dendity in hippocampal pyramidal cells in adulthood." *J. of Neurosci.* 1286-1291.

Hallaq, R, Volpicelli F, I Cuchillo-Ibanez, C Hooper, K Mizuno, D Uwanogho, M Causevic, et al. 2015. "The notch intracellular domain represses CRE-dependent transcription." *Cell Signal* 621-629.

Han, W, KY Kwan, S Shim, MMS Lam, Y Shin, X Xu, Y Zhu, M Li, and N Sestan. 2011. "TBR1 directly represses Fezf2 to control the laminar origin and development of the corticospinal tract." *Proc. Natl. Acad. Sci. U.S.A.* 3041-3046.

Hanashima, C, L Shen, SC Li, and E Lai. 2002. "Brain factor-1 controls the proliferation and differentiation of neocortical progenitor cells through independent mechanisms." *J. Neurosci.* 6526-6536.

Hanashima, C, M Fernandes, JM Hebert, and G Fishell. 2007. "The role of Foxg1 and dorsal midline signaling in the generation of cajal-retzius subtypes." *J. Neurosci.* 11103-11111.

Hand, R, D Bortone, P Mattar, L Nguyen, JL Heng, S Guerruer, E Boutt, E Peters, AP Barnes, and C Parras. 2005. "Phosphorylation of Neurogenin2 specifies the migration properties and the dendritic morphology of pyramidal neurons in the neocortex." *Neuron* 45-62.

Hansen, DV, JH Lui, PRL Parker, and AR Kriegstein. 2010. "Neurogenic radial glia in the outer subventricular zone of human neocortex." *Nature* (464): 554-561.

Hayashi, M, Y Hayashi, CY Liu, JW Tichelaar, and WWY Kao. 2005. "Over expression of FGF7 enhances cell proliferation but fails to cause pathology in corneal epithelium of Kerapr-rtTA/FGF7 bitransgenic mice." *Mol Vis* 201-207.

Hebert, JM, and SK McConnell. 2000. "Targeting of Cre to the Foxg1 (BF-1) locus mediates loxP recombination in the telencephalon and other developing head structures." *Dev Biol* 296-306.

Hebert, JM, Y Mishina, and SK McConnell. 2002. "BMP signaling is required locally to pattern the dorsal telencephalic midline." *Neuron* 1029-1041.

Heng, JI-T, L Nguyen, DS Castro, C Zimmer, H Wildner, O Armant, D Skowronska-Krawczyk, F Bedogni, J-M Matter, and R Hevner. 2008. "Neurogenin 2 controls cortical neuron migration through regulation of Rnd2." *Nature* 114-118.

Hevner, RF, L Shi, N Justice, Y Hsueh, M Sheng, S Smiga, A Bulfone, AM Goffinet, AT Campagnoni, and JL Rubenstein. 2001. "Tbr1 regulates differentiation of the preplate and layer 6." *Neuron* 353-366.

Hirata, H, S Yoshiura, T Ohtsuka, Y Bessho, T Harata, K Yoshikawa, and R Kageyama. 2002. "Oscillatory expression of the bHLH factor Hes1 regulated by a negative feedback loop." *Science* 840-843.

Ho, SY, CY Chao, HL Huang, TW Chiu, P Charoenkwan, and E Hwang. 2011. "NeurphologyJ: an automatic neuronal morphology quantification method and its application in pharmacological discovery." *BMC Bioinform* 12:230.

Horch, HW, and LC Katz. 2002. "BDNF release from single cells elicits local dendritic growth in nearby neurons." *Nat. Neurosci.* 1177-1184.

Hrachovy, RA, and JD Frost. 1989. "Infantile spasms." *Pediatr. Clin. Nortn Am.* 311-329.

Hrachovy, RA, JD Frost, and P Kellaway. 1981. "Sleep characteristics in infantile spasms." *Neurology* 688-693.

Hu, S, V Hatini, RC Marcus, SC Li, and E Lai. 1999. "Dorsal-ventral patterning defects in the eye of BF-1-deficient mice associated with a restricted loss of shh expression." *Dev. Biol.* 53-63.

Huber, AB, AL Kolodkin, DD Ginty, and JF Cloutier. 2003. "Signaling at the growth cone: ligand-receptor complexes and the control of axon growth and guidance." *Annu. Rev. Neurosci.* 509-563.

Hudmon, A, and H Schulman. 2002. "Neuronal CA2+/calmodulin-dependent protein kinase II: the role of structure and autoregulation in cellular function." *Ann. Rev. Biochem.* 473-510.

Huppke, P, F Laccone, N Kramer, W Engel, and F Hanefeld. 2000. "Rett syndrome: Analysis of MECP2 and clinical characterization of 31 patients." *Hum. Molec. Genet.* 1369-1375.

Huynh, MA, Y Ikeuchi, S Netherton, L de la Torre-Ubieta, R Kanadia, J Stegmuller, C Cepko, S Bonni, and A Bonni. 2011. "An isoform-specific SnoN-FOXO1 repressor complex controls neuronal morphogenesis and positioning in the mammalian brain." *Neuron* 930-944.

Ikeuchi, Y, J Stegmuller, S Netherton, MA Huynh, M Masu, D Frank, S Bonni, and A Bonni. 2009. "A SnoN-Ccd1 pathway promotes axonal morphogenesis in the mammalian brain." *J Neurosci Off J Soc Neurosci* 4312-4321.

Iwase, S, F Lan, P Bayliss, L de la Torre-Ubieta, M Huarte, HH Qi, JR Whetstine, A Bonni, Tm Roberts, and Y Shi. 2007. "The X-linked mental retardation gene SMCX/JARID1C defines a family of histone H3 lysine 4 demethylases." *Cell* 1077-1088.

Jan, YN, and LY Jan. 2003. "The control of dendrite development." *Neuron* 229-242.

Jeavons, PM, BD Bower, and M Dimitrakoudi. 1973. "Long-term prognosis of 150 cases of "West syndrome"." *Epilepsia* 153-164.

Kang, HJ, YI Kawasawa, F Cheng, Y Zhu, X Xu, M Li, M Sousa, et al. 2011. "Spatio-temporal transcriptome of the human brain." *Nature* 483-489.

Kapsimali, M, WP Kloosterman, E De Bruijn, F Rosa, RH Plasterk, and SW Wilson. 2007. "MicroRNAs show a wide diversity of expression profiles in the developing and mature central nervous system." *Genome Biol.* R173.

Katz, LC, and CJ Shatz. 1996. "Synaptic activity and the construction of cortical circuits." *Science* 1133-1138.

Kaufmann, WE, and HW Moser. 2000. "Dendritic anomalies in disorders associated with mental retardation." *Cereb. Cortex* 981-991.

Kellaway, P, RA Hrachovy, JD Frost, and T Zion. 1979. "Precise characterization and quantification of infantile spasms." *Ann. Neurol.* 214-218.

Kobayashi, D, M Kobayashi, K Matsumoto, and K Shimamura. 2002. "Early subdivisions in the neural plate define distinctive competence for inductive signals." *Development* 83-93.

Konishi, Y, J Stegmuller, T Matsuda, S Bonni, and A Bonni. 2004. "Cdh1-APC controls axonal growth and patterning in the mammalian brain." *Science* 1026-1030.

Korff, CM, and DR Nordli. 2006. "Epilepsy syndromes in infancy." *Pediatr Neurol* 253-263.

Kortum, F, S Das, M Flindt, DJ Morris-Rosendahl, I Stefanova, A Glodstein, D Horn, E Klopocki, G Kluger, and P Martin. 2011. "The core FOXG1 syndrome phenotype consists of postnatal microcephaly, severe mental retardation, absent language, dyskinesia, and corpus callosum hypogenesis." *J. Med. Genet.* 396-406.

Kulkarni, VA, and BL Firestein. 2012. "The dendritic tree and brain disorders." *Mol. and Cell. Neurosci.* 10-20.

Kumamoto, T, and C Hanashima. 2017. "Evolutionary conservation and conversion of Foxg1 function in brain development." *Dev. Growth Differ.* 258-269.

Kumamoto, T, K Toma, and I Gunadi. 2013. "Foxg1 coordinates the switch from nonradially to radially migrating glutamatergic subtypes in the neocortex through spatiotemporal repression." *Cell Rep.* 931-945.

Lagos-Quintana, M, R Rauhut, A Yalcin, J Meyer, W Lendeckel, and T Tuschl. 2002. "Identification of tissue-specific microRNAs from mouse." *Curr. Biol.* 735-739.

Lagutin, OV. 2003. "Six3 repression of Wnt signaling in the anterior neuroectoderm is essential for vertebrate forebrain development." *Genes Dev.* 368-379.

Lai, T, D Jabaudon, BJ Molyneaux, E Azim, P Arlotta, JR Menezes, and JD Macklis. 2008. "SOX5 controls the sequential generation of distinct corticofugal neuron subtypes." *Neuron* 232-247.

Landeira, BS, TT Santana, JA Araujo, EI Tabet, BA Tannous, T Schroeder, and MR Costa. 2018. "Activity-independent effects of CREB on neuronal survival and differentiation during mouse cerebral cortex development." *Cereb Cortex* 538-548.

Lasorella, A, J Stegmuller, D Guardavaccaro, G Liu, MS Carro, G Rothschild, L de la Torre-Ubieta, M Pagano, A Bonni, and A Iavarone. 2006. "Degradation of Id2 by the anaphase-promoting complex couples cell cycle exit and axonal growth." *Nature* 471-474.

Le Guen, T, N Bahi-Buisson, J Nectoux, N Boddaert, and Y Fichou. 2011. "A FOXG1 mutation in a boy with congenital variant of Rett syndrome." *Neurogenetics* 1-8.

Lessard, J, JI Wu, JA Ranish, M Wan, MM Winslow, BT Staahl, H Wu, R Aebersold, IA Graef, and GR Crabtree. 2007. "An essential switch in subunit composition of a chromatin remodeling complex during neural development." *Neuron* 201-215.

Li, N, CT Zhao, Y Wang, and XB Yuan. 2010. "The transcription factor Cux1 regulates dendritic morphology of cortical pyramidal neurons ." *PLoS ONE.*

Liodis, P, M Denaxa, M Grigoriou, C Akufo-Addo, Y Yanagawa, and V Pachnis. 2007. "Lhx6 activity is requirec for the normal migration and specification of cortical interneuron subtypes." *J. Neurosci.* 3078-3089.

Lodato, S, BJ Molyneaux, E Zuccaro, LA Goff, H-H Chen, W Yuan, A Meleski, et al. 2014. "Gene co-regulation by Fezf2 selects neurotransmitter identity and connectivity of corticospinal neurons." *Nat. Neurosci.* 1046-1054.

Lonze, BE, and DD Ginty. 2002. "Function and regulation of CREB family transcription factors in the nervous system." *Neuron* 605-623.

Luo, LY, J Liao, LY Jan, and YN Jan. 1994. "Distinct morphogenetic functions of similar small GTPases: Drosophila Drac1 is involved in axonal outgrowth and myoblast fusion." *Genes and Develop.* 1787-1802.

Magill, ST, XA Cambronne, BW Luikart, DT Lioy, BH Leighton, GL Westbrook, G Mandel, and RH Goodman. 2010. "microRNA-132 regulates dendritic growth and arborization of newborn neurons in the adult hippocampus." *Proc. Natl. Acad. Sci.* 20382-20387.

Mallamaci, A. 2017. "Enhancing neurogenesis and counteracting neuropathogenic gene haploinsufficiencies by RNA gene activation". Adv Exp Med Biol. 23-39.

Mangale, VS, KE Hirokawa, PRV Satyaki, N Gokulchandran, S Chikbire, L Subramanian, AS Shetty, B Martynoga, J Paul, and MV Mai. 2008. "Lhx2 selector activity specifies cortical identity and suppresses hippocampal organizer fate." *Science* 304-309.

Manuel, M, B Martynoga, T Yu, JD West, JO Mason, and DJ Price. 2010. "The transcription factor Foxg1 regulates the competence of telencephalic cells to adopt subpallial fates in mice." *Development* 487-497.

Manuel, MN, B Martynoga, MD Molinek, JC Quinn, C Kroemmer, and JO, Price, DJ Mason. 2011. "The transcription factor Foxg1 regulates telencephalic progenitor proliferation cell autonomously, in part by controlling Pax6 expression levels." *Neural Develop* 6-9.

Mariani, J, G Coppola, P Zhang, A Abyzov, L Provini, L Tomasini, M Amenduni, et al. 2015. "FOXG1-dependent dysregulation of GABA/Glutamate neuron differentiation in autism spectrum disorders." *Cell* 375-390.

Markus, A, Patel TD, and WD Snider. 2002. "Neurotrophic factors and axonal growth." *Curr. Opin. Neurobiol.* 523-531.

Martynoga, B, H Morrison, DJ Price, and JO Mason. 2005. "Foxg1 is required for specification of ventral telencephalon and region-specific regulation of dorsal telencephalic precuros proliferation and apoptosis." *Dev. Biol.* 113-127.

Mathelier, A, X Zhao, AW Zhang, F Parcy, R Worsley-Hunt, DJ Arenillas, S Buchman, C Chen, A Chou, and H Ienasescu. 2014. "JASPAR 2014: an extensively expanded and updated open-access database of transcription factor binding profiles." *Nucleic Acid Res* 142-147.

Matsumoto, A, K Watanabe, T Negoro, M Sugiura, K Iwase, K Hara, and S Miyazaki. 1981. "Long-term prognosis after infantile spasms: a statistical study of prognosis factors in 200 cases." *Dev. Med. Child. Neurol.* 51-65.

McAllister, A Kimberley, CD Lo, and LC Katz. 1995. "Neurotrophins regulate dendritic growth in developing visual cortex." *Neuron* 791-803.

McAllister, A Kimberley, LC Katz, and DC Lo. 1999. "Neurotrophins and synaptic plasticity." *no Hebb* 295-318.

McAllister, AK. 2002. "Neurotrophins and cortical development." *Results Probl. Cell Differ.* 89-112.

McAllister, AK, LC Katz, and DC Lo. 1997. "Opposing roles for endogenous BDNF and NT-3 in regulating cortical dendritic growth." *Neuron* 767-778.

McAllister, and A Kimberley. 2000. "Cellular and molecular mechanisms of dendrite growth." *Cereb. Cortex* 963-973.

McKenna, WL, J Betancourt, KA Larkin, B Abrams, C Guo, JLR Rubenstein, and B. Chen. 2011. "Tbr1 and Fezf2 regulate alternate corticofugal neuronal identities during neocortical development." *J. Neurosci.* 549-564.

Mencarelli, MA, T Kleefstra, E Katzari, FT Papa, and M Cohen. 2009. "Microdeletion syndrome and congenital variant of Rett syndrome." *Eur. J. Med. Genet.* 148-152.

Mironov, VI, AS Romanov, AY Simonov, and MV, Kazantsev, VB Vedunova. 2014. "Oscillations in a neurite growth model with extracellular feedback." *Neurosci. Letters* 16-20.

Miyoshi, G, and G Fishell. 2012. "Dynamic FoxG1 expression coordinates the integration of multipolar pyramidal neuron precursors into the cortical plate." *Neuron* 1045-1058.

Molyneaux, BJ, P Arlotta, JRL Menezes, and JD Macklis. 2007. "Neuronal subtype specification in the cerebral cortex." *Nat. Rev. Neurosci.* 427-437.

Molyneaux, BJ, P Arlotta, RM Fame, JL MacDonald, KL MacQuarrie, and JD Macklis. 2009. "Novel subtype-specific genes identify distinct subpopulations of callosal projection neurons." *J. Neurosci.* 12343-12354.

Monros, E, J Armstrong, E Aibar, P Poo, I Canos, and M Pineda. 2001. "Rett syndrome in Spain: mutation analysis and clinical correlations." *Brain Dev.* 251-253.

Muzio, L, and A Mallamaci. 2005. "Foxg1 confines cajal-retzius neuronogenesis and hippocampla morphogenesis to the dorsomedial pallium." *J. Neurosci.* 4435-4441.

Nguyen, P, T Abel, and E Kandel. 1994. "Requirement of a critical period of transcription for induction of a late phase of LTP." *Science* 1104-1107.

Ohkubo, Y, C Chiang, and JLR Rubenstein. 2002. "Coordinated regulation and synergistic actions of BMP4, SHH and FGF8 in the rostral presencephalon regulate morphogenesis of the telencephalic and optic vesicles." *Neuroscience* 1-17.

Ohtsuka, T, M Ishibashi, G Gradwohl, S Nakanishi, F Guillemot, and R Kageyama. 1999. "Hes1 and Hes5 as notch effectors in mammalian neuronal differentiation." *EMBO J* 2196-2207.

Osorio, C, PJ Chacon, I Kisiswa, M White, S Wyatt, A Rodriguez-Tebar, and AM Davies. 2013. "Growth differentiation factor 5 is a key physiological regulator of dendrite growth during development." *Development* 4751-4762.

Pancrazi, L, G Di Benedetto, L Colombaioni, G Della Sala, G Testa, F Olimpico, A Reyes, M Zeviani, T Pozzan, and M Costa. 2015. "Foxg1 localizes to mitochondria and coordinates cell differentiation and bioenergentics." *Proc. Narl Acad. Sci. USA* 13910-13915.

Papa, FT, MA Mencarelli, R Caselli, E Katzaki, and K Sampieri. 2008. "A 3 Mb deletion in 14q12 causes severe mental retardation, mild facial dysmorphisms and Rett-like features." *Am. J. Med. Genet.* 1994-1998.

Parekh, R, and GA Ascolti. 2013. "Neuronal morphology goes digital: a research hub for cellular and system neuroscience." *Neuron* 1017-1038.

Pfeifer, A, Brandon EP, N Kootstra, FH Gage, and IM Verma. 2001. "Delivery of the Cre recombinase by a self-deleting lentiviral vector: efficient gene targeting in vivo." *Proc Natl Acad Sci USA* 11450-11455.

Philippe, C, D Amsallem, C Francannet, L Lambert, and A Saunier. 2010. "Phenotypic variability in Rett syndrome associated with FOXG1 mutations in females." *J. Med. Genet.* 59-65.

Pilaz, LJ, AL Lennox, JP Rouanet, and DL Silver. 2016. "Dynamic mRNA transport and local translation in radial glial progenitors of the developing brain." *Curr. Biol.* 3383-3392.

Piper, M, G Barry, J Hawkins, S Mason, C Lindwall, E Little, A Sarkar, AG Smith, RX Moldrich, and GM Boyle. 2010. "NFIA controls telencephalic progenitor cell differentiation through repression of the notch effector Hes1." *J Neurosci* 9127-9139.

Polleux, F, and W Snider. 2010. "Initiating and growing an axon." *Cold Spring Harbor Persp. in Biol.* 4.

Pontrelli, G, S Cappelletti, D Claps, P Sirleto, L Ciocca, S Petrocchi, A Terracciano, D Serino, L Fusco, and F Vigevano. 2014. "Epilepsy in patients with duplications of chromosome 14 harboring FOXG1." *Pediatri. Neurol.* 530-535.

Pottin, K, H Hinaux, and S Retaux. 2011. "Restoring eye size in Astyanax mexicanus blind cavefish embryos through modulation of the Shh and Fgf8 forebrain organising centres." *Development* 2467-2476.

Raciti, M, Granzotto M, Duc MD, Fimiani C, Cellot G, Cherubini E, and Mallamaci A. 2013. "Reprogramming fibroblasts to neural-precursor-like cells by structured overexpression of pallial patterning genes." *Mol Cell Neurosci* 42-53.

Rajaei, S, A Erlandson, M Kyllerman, M Albage, and I Lundstrom. 2011. "Early infantile onset 'congenital' Rett syndrome variants: Swedish experience through four decades and mutation analysis." *J. Child Neurol.* 65-71.

Rakic, P. 2002. "Neurogenesis in adult primate neocortex: an evaluation of the evidence." *Nat. Rev. Neurosci.* 65-71.

Ramos, B, A Valin, X Sun, and G Gill. 2009. "Sp4-dependent repression of neurotrophin-3 limits dendritic branching ." *Mol. Cell. Neurosci.* 152-159.

Ramos, B, B Gaudilliere, A Bonni, and G Gill. 2007. "Transcription factor Sp4 regulates dendritic patterning during cerebellar maturation." *Proc. Natl. Acad. Sci.* 9882-9887.

Raymond, GV, ML Bauman, and TL Kemper. 1995. "Hippocampus in autism: a Golgi analysis." *Acta Neuropath.* 117-119.

Redmond, L, AH Kashani, and A Gosh. 2002. "Calcium regulation of dendritic growth via CaM kinase IV and CREB-mediated transcription." *Neuron* 999-1010.

Redmond, L, SR Oh, C Hicks, G Weinmaster, and A Ghosh. 2000. "Nuclear Notch1 signaling and the regulation of dendritic development." *Nat Neurosci* 30-40.

Regad, T, M Roth, N Bredenkamp, N Illing, and N Papalopulu. 2007. "The neural progenitor-specifying activity of FoxG1 is antagonistically regulated by CKI and FGF." *Nat. Cell Biol.* 531-540.

Riikonen, R. 1982. "A long-term follow-up study of 214 children with the syndrome of infantile spasms." *Neuropediatrics* 14-23.

Rolando, S. 1985. "Rett syndrome: report of eight cases." *Brain Dev.* 290-296.

Roy, A, M Gonzalez-Gomez, A Pierani, G Meyer, and S Tole. 2014. "Lhx2 regulates the development of the forebrain hem system." *Cereb. Cortex* 1361-1372.

Rubinson, DA, Dillon CP, AV Kwiatkowski, C Sievers, L Yang, J Kopinja, DL Rooney, et al. 2003. "A lentivirus-based system to functionally silence genes in primary mammalian cells, stem cells and transgenic mice by RNA interference." *Nat Genet* 401-406.

Sakamoto, K, K Karelina, and K Obrietan. 2011. "CREB: a multifaceted regulator of neuronal plasticity and protection: CREB in synaptic plasticity and cell survival." *J Neurochem* 1-9.

Salama-Cohen, P, MA Arevalo, J Meier, R Grantyn, and A Rodriguez-Tebar. 2005. "NGF controls dendrite evelopment in hippocampal neurons by binding to p75NTR and modulating the cellular targets of Notch." *Mol Biol Cell* 339-347.

Sato, M, K Suzuki, H Yamazaki, and S Nakanishi. 2005. "A pivotal role of calcineurin signaling in development and maturation of postnatal cerebellar granule cells." *Proc. Natl. Acad. Sci.* 5874-5879.

Seoane, J, HV Le, L Shen, SA Anderson, and J Massague. 2004. "Integration of smad and forkhead pathways in the control of neuroepithelial and glioblastoma cell proliferation." *Cell* 211-223.

Sestan, N, S Artavanis-Tsakonas, and P Rakic. 1999. "Contact-dependent inhibition of cortical neurite growth mediated by notch signaling." *Science* 741-746.

Shaikh, TH, X Gai, JC Perin, JT Glessner, H Xie, K Murphy, R O'Hara, T Casalunovo, LK Conlin, and M D'Arcy. 2009. "High-resolution mapping and analysis of copy number variations in the human genome: a data resurce for clinical and research applications." *Genome Res.* 1682-1690.

Shalizi, A, B Gaudilliere, Z Yuan, J Stegmuller, T Shirogane, Q Ge, Y Tan, B Schulman, JW Harper, and A Bonni. 2006. "A calcium-regulated MEF2 sumoylation switch controls postsynaptic differentiation." *Science* 1012-1017.

Shalizi, A, PM Bilimoria, J Stegmuller, B Gaudilliere, Y Yang, K Shuai, and A Bonni. 2007. "PIASx is a MEF2 SUMO E3 ligase that promotes postsynaptic dendritic morphogenesis." *J. Neurosci.* 10037-10046.

Shaywitz, AJ, and ME Greenberg. 1999. "CREB: a stimulus-induced transcription factor activated by a diverse array of extracellular signals." *Annu. Rev. Biochem.* 821-861.

Shen, Q, Y Wang, JT Dimos, CA Fasano, TN Phoenix, IR Lemischka, NB, Stifani, S Ivanova, EE Morrisey, and S Temple. 2006. "The timing of cortical neurogenesis is encoded within lineages of individual progenitor cells." *Nat. Neurosci.* 743-751.

Shibata, M, D Kurokawa, H Nakao, T Ohmura, and S Aizawa. 2008. "MicroRNA-9 modulates cajal-retzius cell differentiation by suppressing Foxg1 expression in mouse medial pallium." *J. Neurosci.* 10415-10421.

Shibata, M, H Nakao, H Kiyonari, T Abe, and S Aizawa. 2011. "MicroRNA-9 regulates neurogenesis in mouse telencepahlon by targeting multiple transcription factors." *J. Neurosci.* 3407-3422.

Shoichet, SA, SA Kunde, P Viertel, C Schell-Apacik, and H von Voss. 2005. "Haploinsufficiency of novel FOXG1B variants in a patient with severe mental retardation, brain malformations and microcephaly." *Hum. Genet.* 536-544.

Siegenthaler, JA, BA Tremper-Wells, and MW Miller. 2008. "Foxg1 haploinsufficiency reduces the population of cortical intermediate progenitor cells: effect of increased p21 expression." *Cereb. Cortex* 1865-1875.

Smeets, E, E Schollen, U Moog, G Matthijs, and J Herbergs. 2003. "Rett syndrome in adolescent and adult females: clinical and molecular genetic findings." *Am. J. Med. Genet.* 227-233.

Spruston, N. 2008. "Pyramidal neurons: dendritic structure and synaptic integration." *Nat. Rev. Neurosci.* 206-221.

Srinivasan, K, DP Leone, RK Bateson, G Dobreva, Y Kohwi, T Shigematsu, R Grosschedl, and SK McConnell. 2012. "A network of genetic repression and derepression specifies projection fates in the developing neocortex." *Proc. Natl. Acad. Sci. U.S.A.* 19071-19078.

Srivastava, DP, KM Woolfrey, and P Penzes. 2011. "Analysis of dendritic spine morphology in cultured CNS neurons." *J Vis Exp.*

Staahl, BT, J Tang, W Wu, A Sun, AD Gitler, AS Yoo, and GR Crabtree. 2013. "Kinetic analysis of npBAF to nBAF switching reveals exchange of SS18 with CREST and integration with neural developmental pathways." *J Neurosci* 10348-10361.

Stegmüller, J, Y Konishi, MA Huynh, Z Yuan, S Dibacco, and A Bonni. 2008. "FGFbeta-Smad2 signaling regulates the Cdh1-APC/SnoN pathway of axonal morphogenesis." *J. Neurosci.* 1961-1969.

Striano, P, R Paravidino, F Sicca, P Chiurazzi, S Gimelli, A Coppola, A Robbiano, et al. 2011. "West Syndrome associated with 14q12 duplications harboring FOXG1." *Neurology* 1600-1602.

Sugahara, F, J Pascual-Anaya, Y Oisi, S Kuraku, S Aota, N Adachi, W Takagi, T Hirai, N Sato, and Y Murakami. 2016. "Evidence from cyclostomes for complex regionalization of the ancestral vertebrate brain." *Nature* 97-100.

Takahashi, T, FS Nowakowski, and VS Caviness. 1995. "The cell cycle of the pseudostratified ventricular epithelium of the embryonic murine cerebral wall." *J. Neurosci.* 6046-6057.

Takahashi, T, T Goto, S Miyama, RS Nowakowski, and VSJ Caviness. 1999. "Sequence of neuron origin and neocortical laminar fate: realtion to cell cycle of origin in the developing murine cerebral wall." *J. Neurosci.* 10357-10371.

Takebayashi, K, Y Sasai, Y Sakai, T Watanabe, S Nakanishi, and R Kageyama. 1994. "Structure, chromosomal locus, and promoter analysis of the gene encoding the mouse helix-loop-helix factor HES-1. Negative autoregulation through the multiple N box elements." *J Biol Chem* 5150-5156.

Tao, X, S Finkbeiner, DB Arnold, AJ Shaywitz, and ME Greenberg. 1998. "Ca2+ influx regulates BDNF transcription by a CREB family transcription factor-dependent mechanism." *Neuron* 709-726.

Tessier-Lavigne, M, and CS Goodman. 1996. "The molecular biology of axon guidance." *Science* 1123-1133.

Tohyama, J, T Yamamoto, K Hosoki, K Nagasaki, N Akasaka, T Ohashi, Y Kobayashi, and S Saitoh. 2011. "West syndrome associated with mosaic duplication of FOXG1 in a patient with maternal uniparental disomy of chromosome 14." *Am. J. Med. Genet.* 2584-2588.

Toma, K, T Kumamoto, and C Hanashima. 2014. "The timing of upper-layer neurogenesis is conferred by sequential derepression and negative feedback from deep-layer neurons." *J. Neurosci.* 13259-13276.

Tucker, KL, M Meyer, and YA Barde. 2001. "Neurotrophins are required for nerve growth during development." *Nat Neurosci* 29-37.

Tyler, WA, and TF Haydar. 2010. "A new contribution to brain convolution: progenitor cell logistics during cortex development." *Nat. Neurosci.* 656-657.

Ultanir, SK, NT Hertz, G Li, W-P Ge, AL Burlingame, SJ Pleasure, KM Shokat, LY Jan, and Y-N Jan. 2012. "Chemical genetic identification of NDR1/2 kinase substrates AAK1 and Rabin8 uncovers their roles in dendrite arborization and spine development." *Neuron* 1127-1142.

Valerio, A, V Ghisi, M Dossena, C Tonello, A Giordano, A Frontini, Ferrario M, M Pizzi, P Spano, and MO Carruba. 2006. "Leptini increases axonal growth cone size in developing mouse cortical neurons by convergent signals inactivating glycogen synthase kinase-3beta." *J Biol Chem* 12950-12958.

Vezzali, R, SC Weise, N Hellbach, V Machado, S Heidrich, and T Vogel. 2016. "The FOXG1/FOXO/SMAD network balances proliferation and differentiation of cortical progenitors and activates Kcnh3 expression in mature neurons." *Oncotarget* 7.

Villa, KL, KP Berry, J Subramaniam, JW Cha, WC Oh, HB Kwon, Y Kubota, PTC So, and E Nedivi. 2016. "Inhibitory synapses are repeatedly assembled and removed at persistent sites in vivo." *Neuron* 756-769.

Watanabe, K, T Negoro, K Aso, and A Matsumoto. 1993. "Reappraisal of interictal electroencephalograms in infantile spasms." *Epilepsia* 679-685.

Wayman, GA, S Impey, D Marks, T Saneyoshi, WF Grant, V Derkach, and TR Soderling. 2006. "Activity-dependent dendritic arborization mediated by CaM-kinase I activation and enhanced CREB-dependent transcription of Wnt-2." *Neuron* 897-909.

Wayman, GA, YS Lee, H Tokumitsu, AJ Silva, and TR Soderling. 2008. "Calmodulin-kinase: modulators of neuronal development and plasticity ." *Neuron* 914-931.

Weng, Ap, Y Nam, MS Wolfe, WS Pear, JD Griffin, SC Blacklow, and JC Aster. 2003. "Growth suppression of pre-T acute lymphoblastic leukemia cells by inhibition of notch signaling." *Mol Cell Biol* 655-664.

Wijchers, PJEC, JPH Burbach, and MP Smidt. 2006. "In control of biology: of mice, men and Foxes." *Biochemical Journal* 233-246.

Wu, GY, and HT Cline. 1998. "Stabilization of dendritic arbor structure in vivo by caMKII." *Science* 222-226.

Wu, JI, J Lessard, IA Olave, Z Qiu, A Ghosh, IA Graef, and GR Crabtree. 2007. "Regulation of dendritic development by neuron-specific chromatin remodeling complexes." *Neuron* 94-108.

Xuan, S, CA Baptista, G Balas, W Tao, Soares. VC, and E Lai. 1995. "Winged helix transcription factor BF-1 is essential for the development of the cerebral hemispheres." *Neuron* 1141-1152.

Yamagishi, S, F Hampel, K Hata, D Del Toro, M Schwark, E Kvachnina, M Bastmeyer, et al. 2011. "FLRT2 and FLRT3 act as repulsive guidance cues for Unc5-positive neurons." *EMBO J.* 2920-2933.

Yang, Y, AH Kim, T Yamada, B Wu, PM Billimora, Y Ikeuchi, N de la Iglesia, J Shen, and A Bonni. 2009. "A Cdc20-APC ubiquitin signaling pathway regulates presynaptic differentiation." *Science* 575-578.

Yang, Y, W Shen, Y Ni, Y Su, Z Yang, and C Zhao. 2017. "Impaired interneuron development after Foxg1 disruption." *Cereb. Cortex* 793-808.

Yip, Dj, CP Corcoran, M Alvarez-Saavedra, A DeMaria, S Rennick, AJ Mears, MA Rudnicki, C Messier, and DJ Picketts. 2012. "Snf2l regulates Foxg1-dependent progenitor cell expansion in the developing brain." *Dev. Cell* 871-878.

Zhou, FQ, and WD Snider. 2006. "Intracellular control of developmental and regenerative axon growth." *Philos. Trans. R. Soc. Lond. B Biol. Sci.* 1575-1592.